



HAL
open science

Set-membership state observers design based on explicit characterizations of the estimation-error bounds

Nassim Loukkas

► **To cite this version:**

Nassim Loukkas. Set-membership state observers design based on explicit characterizations of the estimation-error bounds. Automatic. Université Grenoble Alpes, 2018. English. NNT: 2018GREAT040 . tel-01898259

HAL Id: tel-01898259

<https://theses.hal.science/tel-01898259>

Submitted on 18 Oct 2018

HAL is a multi-disciplinary open access archive for the deposit and dissemination of scientific research documents, whether they are published or not. The documents may come from teaching and research institutions in France or abroad, or from public or private research centers.

L'archive ouverte pluridisciplinaire **HAL**, est destinée au dépôt et à la diffusion de documents scientifiques de niveau recherche, publiés ou non, émanant des établissements d'enseignement et de recherche français ou étrangers, des laboratoires publics ou privés.



THÈSE

Pour obtenir le grade de

DOCTEUR DE LA COMMUNAUTÉ UNIVERSITÉ GRENOBLE ALPES

Spécialité : AUTOMATIQUE - PRODUCTIQUE

Arrêté ministériel : 25 mai 2016

Présentée par

Nassim LOUKKAS

Thèse dirigée par **John Jairo MARTINEZ-MOLINA**

et codirigée par **Nacim MESLEM**

préparée au sein du **Laboratoire Grenoble Images Parole Signal
Automatique**

dans l'**École Doctorale Electronique, Electrotechnique,
Automatique, Traitement du Signal (EEATS)**

**Synthèse d'observateurs ensemblistes pour
l'estimation d'état basées sur la
caractérisation explicite des bornes d'erreur
d'estimation**

**Set-membership state observers design
based on explicit characterizations of the
estimation-error bounds**

Thèse soutenue publiquement le **6 juin 2018**,
devant le jury composé de :

Monsieur JOHN-JAIRO MARTINEZ-MOLINA

MAITRE DE CONFERENCES, GRENOBLE INP, Directeur de thèse

Monsieur NACIM RAMDANI

PROFESSEUR, UNIVERSITE D'ORLEANS, Rapporteur

Monsieur LUC JAULIN

PROFESSEUR, ENSTA BRETAGNE, Rapporteur

Monsieur NACIM MESLEM

MAITRE DE CONFERENCES, GRENOBLE INP, Co-directeur de thèse

Monsieur GILDAS BESANÇON

PROFESSEUR, GRENOBLE INP, Président

Monsieur SORIN OLARU

PROFESSEUR, CENTRALE SUPELEC, Examinateur

UNIVERSITÉ DE GRENOBLE ALPES
ÉCOLE DOCTORALE Electronique,
Electrotechnique, Automatique, Traitement du Signal
(EEATS)

T H È S E

pour obtenir le titre de

docteur

de l'Université GRENOBLE ALPES
Mention : **AUTOMATIQUE-PRODUCTIQUE**

Présentée et soutenue par
Nassim LOUKKAS

**Set-membership state observers design based
on explicit characterizations of the
estimation-error bounds**

Thèse dirigée par John Jairo MARTINEZ MOLINA et Nacim MESLEM
préparée au laboratoire (GIPSA-lab)
soutenue le 06 Juin 2018

Jury :

<i>Rapporteurs :</i>	Nacim RAMDANI	- PRISME, , Université d'Orléans
	Luc JAULIN	- Lab-STICC, ENSTA-Bretagne
<i>Examineurs :</i>	Gildas BESANÇON	- GIPSA-lab, Grenoble INP
	Sorin OLARU	- L2S, Centrale Supélec
<i>Directeur :</i>	John Jairo MARTINEZ MOLINA	- GIPSA-lab, Grenoble INP
<i>Encadrant :</i>	Nacim MESLEM	- GIPSA-lab, Grenoble INP

Contents

Table of Acronyms and notations	ix
Résumé en français	1
Introduction	7
0.1 Context and motivations	7
0.2 Contributions of the thesis	10
0.3 Organization of the thesis	10
0.4 Publications	11
1 Notions about interval analysis and invariant sets computation	13
1.1 Introduction	13
1.2 Interval analysis	14
1.3 Invariant sets	28
1.4 Conclusion	37
2 Observers based on ellipsoidal invariant sets for linear systems	39
2.1 Introduction	39
2.2 Problem statement	41
2.3 Set-membership observer design	42
2.4 The set-membership observer implementation	51
2.5 A numerical example	52
2.6 Conclusion	54
3 Observers based on ellipsoidal invariant sets for LPV systems	57
3.1 Introduction	57

3.2	Problem statement	61
3.3	Set-membership design for LPV systems	62
3.4	Set-membership observer design algorithm for LPV systems	68
3.5	Set-membership observer implementation for LPV systems	70
3.6	A numerical examples	72
3.7	Conclusion	76
4	Observers based on interval characterization of the estimation error	79
4.1	Introduction	79
4.2	Problem statement	80
4.3	Observers design based on interval analysis	81
4.4	Observers design based on intervals and invariant sets	86
4.5	Illustrative examples	89
4.6	Extension to a class of nonlinear systems	97
4.7	Conclusion	100
	Conclusion	103
4.8	Main conclusions	103
4.9	Future works	104
	Bibliographie	109

List of Figures

1.1	Graphical representation of boxes $[\mathbf{x}]$ (in blue) and $[\mathbf{y}]$ (in red)	17
1.2	Intersection of two interval vectors: $[\mathbf{x}]$ in yellow, $[\mathbf{y}]$ in red, $[\mathbf{x}] \cap [\mathbf{y}]$ in blue	20
1.3	Union of two interval vectors: $[\mathbf{x}]$ in yellow, $[\mathbf{y}]$ in red, $[\mathbf{x}] \cup [\mathbf{y}]$ in green	21
1.4	Wrapping effect ($\theta = \frac{\pi}{4}$)	24
1.5	Inclusion function	25
1.6	Ellipsoidal set	29
1.7	Projection of an ellipsoidal set.	30
1.8	Half space representation of a polytope	31
1.9	Vertex representation of a polytope.	31
1.10	Computation of polyhedral RPI set from ellipsoidal ones	34
1.11	Shrinking an initial polyhedral RPI set Φ_0 to get an RPI outer-approximation Φ_{k^*} of the mRPI	37
1.12	Shrinking index with respect to the number of iterations k	38
2.1	Principle of the proposed approach	42
2.2	The hypercube Ω (in dashed black lines) including the ellipsoidal RPI set Φ (in red) in steady-state regime	46
2.3	Set-membership estimation. The dashed lines correspond to the bounds obtained from the set-membership state observer. For comparison, the solid lines corresponds to the real system state.	53
2.4	Evolution of the scalar μ_k . This scalar characterizes the contraction of the initial RPI set. The value of μ_k converges to 1 as $k \rightarrow \infty$.	54
2.5	Invariant set and states covariances. The solid line corresponds to the obtained RPI set used for computing <i>deterministic</i> bounds of the estimation error. The dashed line corresponds to the stochastic ellipsoidal defined by (2.41) with $t = 3$.	55
3.1	Relation between the different classes of systems	59

3.2	Example of a polytope Ω_ρ for polytopic representation of an LPV system with 2 varying parameters.	61
3.3	Set-membership estimation. The dashed lines correspond to the bounds obtained from the set-membership state observer. For comparison, the solid lines corresponds to the real system state.	73
3.4	The scheduling parameter ρ_k	73
3.5	Evolution of the scalar μ_k . This scalar characterizes the contraction of the initial RPI set. The value of μ_k converges to 1 as $k \rightarrow \infty$	74
3.6	Minimal ellipsoidal RPI set and steady-state covariance for the estimation error dynamics. The solid line corresponds to the obtained RPI set used for computing <i>deterministic</i> bounds of the estimation error. The dashed line corresponds to the stochastic ellipsoidal defined by (3.58) with a number of standard deviation t equal to 3.6374.	74
3.7	Estimated bounds for system state $x_k(1)$	76
3.8	Estimated bounds for system state $x_k(2)$	77
3.9	Estimated bounds for system state $x_k(3)$	77
3.10	Evolution of the scalar μ_k for the second example. This scalar characterizes the contraction of the initial RPI set. The initial value of μ_k guarantee the inclusion of the initial estimation-error set. The value of μ_k converges to 1 as $k \rightarrow \infty$. Remark the fast convergence.	78
3.11	Steady state ellipsoidal RPI set, for the estimation error dynamics, which includes an stochastic set with a scalar $t = 2.478$	78
4.1	Over-estimation linked to the wrapping effect. Usually, framing at each iteration the set of the solutions by an axis-aligned box led to too pessimistic enclosures of the solutions for the large values of k	83
4.2	Minimal inclusion function, at each time instant k , of the estimation error. No wrapping effect nor the dependency phenomenon in the proposed numerical scheme (4.10).	84
4.3	Thanks to interval and invariant set computations all the possible estimation errors, for all $k \geq 0$, are characterized by a small finite number k^* of boxes.	86
4.4	The inflation and shrinking procedures used to get the time instant k^* and an outer-approximation $[\Phi_{k^*}]$ of the theoretical mRPI set Ω_∞ of the estimation error at the steady state.	87
4.5	The supposed behaviors of the state disturbance and the output noise.	89

4.6	Shrinking procedure to get an outer-approximation of the mRPI set of the estimation error at the steady state.	90
4.7	(a) and (b) show the time evolution of the estimated and the real state trajectories. (c) and (d) plot the guaranteed enclosure of the estimation error. (e) and (f) represent the outer-approximation of all the possible state trajectories .	91
4.8	Profiles of state disturbances and the measurement noise.	93
4.9	Punctual state estimations	94
4.10	Enclosure of the estimation errors	95
4.11	The enclosure of all the possible state trajectories of the system	96
4.12	The estimated states enclosure	100
4.13	The enclosures of the estimation errors	100

List of Tables

4.1	A finite interval sequence of the time evolution of the estimation error.	92
-----	---	----

Table of Acronyms and notations

Table of Acronyms

BRL	<i>Bounded Real Lemma</i>
CPU	<i>Central Processing Unit</i>
LMI	<i>Linear Matrix Inequality</i>
LTI	<i>Linear Time Invariant</i>
LTV	<i>Linear Time Varying</i>
LPV	<i>Linear Parameter Varying</i>
mRPI	<i>minimal Robustly Positive Invariant</i>
NL	<i>Non Linear</i>
PI	<i>Positive Invariant</i>
qLPV	<i>quasi Linear Parameter Varying</i>
RPI	<i>Robustly Positive Invariant</i>

Table of notations

\mathbb{R}	Set of real numbers
\mathbb{R}_+	Set of positive real numbers
\mathbb{R}_+^*	Set of strictly positive real numbers
\mathbb{R}^n	Set of n-dimensional real vector
\mathbf{B}^n	Unitary box in \mathbb{R}^n
A	General notation for a matrix
I_n	Identity matrix in $\mathbb{R}^{n \times n}$
$[x]$	General notation for an interval
\underline{x}	Lower bound
\bar{x}	Upper bound
$m([x])$	Center of an interval x
$w([x])$	Width of an interval x
$rad([x])$	Radius of an interval x
$ [x] $	Amplitude of an interval x
$[\mathbf{x}]$	General notation for an interval vector (or interval matrix)
$\mathbb{W}([\mathbf{x}])$	Element-wise width of an interval vector
$vol([\mathbf{x}])$	Volume of an interval vector
A^T	Transpose of matrix A
A^{-1}	Inverse of matrix A
$det(A)$	Determinant of matrix A
$diag(\sigma_1, \dots, \sigma_n)$	Diagonal matrix of dimension n
$A \succ 0$	General notation for strictly positive definite matrix A
$A \succeq 0$	General notation for positive definite matrix A
$A \prec 0$	General notation for strictly negative definite matrix A
$A \preceq 0$	General notation for negative definite matrix A
$\mathbb{O}_{n,m}$	Zeros matrix of dimensions $n \times m$
$\mathbb{K}_{n,m}$	Matrix of dimensions $n \times m$ having all elements equal to 1
\mathcal{X}	General notation for a set
$Vol(\mathcal{X})$	Volume of the set \mathcal{X}
$\mathcal{V}_{\mathcal{X}}$	Vertices of the set \mathcal{X}
\in	It belongs to
\subset	Subset
\cap	Intersection
$conv(\cdot)$	Convex hull
\oplus	Minkowski sum
$rs(H)$	Round-sum of matrix H
$\mathcal{E}(P, \bar{x}, \rho)$	General notation of an ellipsoid
$\binom{n}{m}$	n combination of m elements
$ \cdot $	Absolute value
$\ \cdot\ _{\infty}$	Infinity norm
$\ \cdot\ _2$	2-norm
$:=$	equal by definition
\star	Term required for the matrix symmetry
\emptyset	Empty set

Résumé en français

Remark: The thesis is written in english, this part is dedicated for a small summary in french.

Remarque: La thèse est rédigée en anglais, cette partie est dédiée à un petit résumé en français.

Nous allons présenter brièvement le contexte, la motivation, l'état de l'art et les contributions de cette thèse. L'organisation de cette thèse est également présentée, qui introduit le contenu et les contributions de chaque chapitre.

Contexte et motivations

L'estimation d'état joue un rôle très important dans le contrôle, le diagnostic et la supervision des systèmes dynamiques. Dans de nombreux cas, l'état n'est pas complètement mesurable et / ou les capteurs sont très coûteux. Nous devons donc l'estimer en utilisant des observateurs d'état. Le rôle de l'observateur est de fournir une estimation de l'état en utilisant les mesures disponibles (mesures de sortie et d'entrée) et de fournir un modèle mathématique du système.

L'observateur d'état des systèmes linéaires a été introduit pour la première fois par [Kal60]. On peut distinguer deux types d'approches d'estimation:

1. **Les approches stochastiques** [Kal60], [Lue71] Ces approches supposent que les perturbations et les bruits de mesure ont une distribution explicite (distribution généralement gaussienne), le problème de l'estimation est résolu en minimisant la variance de l'erreur d'estimation. Pour les systèmes linéaires, des bornes stochastiques raisonnables pour l'erreur d'estimation peuvent être obtenues si l'observateur fonctionne correctement, c'est-à-dire en fournissant des erreurs d'estimation moyenne et blanche et en fournissant des covariances d'innovation compatibles avec les innovations. Sinon, pour les systèmes non linéaires et / ou dans les cas où les observateurs ne respectent pas la cohérence de la covariance d'innovation, les bornes ne sont pas utiles dans la pratique.

Les approches stochastiques sont utilisées dans divers domaines (contrôle [Bat08], économie et environnement [May82], biologie [UW11] ... etc).

2. **Les approches déterministes** [Sch68] Dans plusieurs applications, il est plus naturel de supposer que les perturbations et les bruits de mesure sont inconnus mais bornés, qu'aucune information statistique sur des variables incertaines n'est requise, la seule hypothèse est que le bruit de perturbation et de mesure est inconnu mais appartient à un ensemble connu. Dans ce contexte, les approches d'estimation ensemblistes ont été introduites [Sch68], [Wis68], [DPBO03], [Fog79]. Dans ces approches, l'idée est de

construire un ensemble compact comprenant de manière garantie tous les états possibles compatibles avec le modèle, les incertitudes, les mesures et les perturbations bornées et les bruits de mesure [MMW96], [AGV99].

Dans cette thèse, nous nous intéressons au second type d'approches qui sont les approches déterministes. Nous proposons ici de nouvelles approches ensemblistes pour l'estimation d'état, dans lesquelles des ensembles invariants et l'analyse d'intervalle sont utilisés pour calculer les bornes de l'erreur d'estimation et prendre en compte les bornes des incertitudes.

Dans la littérature, nous pouvons trouver plusieurs approches pour résoudre le problème d'encadrement d'état. D'une part, i) les techniques d'observateur intervalle basées sur la théorie du système coopératif. D'autre part, ii) les observateurs basés sur la théorie des ensembles. Pour implémenter des approches d'estimation d'état ensemblistes, différentes formes d'ensembles sont utilisées: les ellipsoïdes [DWP01], [KV96], [Pol+04], les parallélotopes [CGZ96], les zonotopes [Com03], [Le+13], [Le+12], les intervalles [Moo66], [Jau+01] ... etc.

L'encadrement d'état à l'aide d'ellipsoïdes a été proposé à la fin des années 1960 [Sch68], [DPBO03], [Wis68]. L'application des ensembles ellipsoïdaux aux problèmes d'estimation de l'état a été étudiée dans [KV96], [DWP01], [Pol+04], [DKV06] [DK12]. Ces approches sont basées sur la prédiction / correction des ensembles. L'idée de base ici est de calculer des ensembles ellipsoïdaux garantis contenant le vecteur à estimer en fonction des bornes sur les perturbations et le bruit, le but est de minimiser, à chaque itération, la taille de l'ensemble ellipsoïdal d'estimation. Il existe dans la littérature différents critères de minimisation: le premier critère est la minimisation du déterminant de la matrice de forme de l'ellipsoïde [DWP01] ce qui équivaut à la minimisation du volume de l'ensemble ellipsoïdal, le second critère est la minimisation de la trace de la matrice de forme de l'ellipsoïde [DWP01] qui équivaut à la minimisation de la somme des carrés des demi-longueurs des axes de l'ellipsoïde. Troisièmement, dans [Ben+14a] les auteurs ont proposé une approche basée sur la minimisation du rayon de l'estimation ellipsoïdale en considérant une matrice de gain constant obtenue en résolvant un problème d'inégalité linéaire matriciel (textbf LMI), alors ce gain est mis à jour en ligne à chaque itération en résolvant un problème d'optimisation LMI à chaque itération. La résolution de la LMI à chaque itération conduit à augmenter le temps de calcul en ligne, les auteurs ont également proposé une technique de mise à l'échelle afin de réduire le temps de calcul en ligne tout en conservant une précision acceptable de l'estimation d'état. Les ensembles ellipsoïdaux sont souvent utilisés car, mathématiquement parlant, ils sont faciles à manipuler donc la simplicité de la formulation. Pour obtenir des ellipsoïdes contenant l'état de manière précise, il faut minimiser la taille des ellipsoïdes. Le processus de minimisation peut conduire à de très gros ellipsoïdes correspondant à de très grandes incertitudes dans certains états, ce qui conduit à une perte de précision.

L'utilisation des parallélotopes a été proposée par [CGZ96] et [CAGZ98], les auteurs ont abordé ici le problème de l'estimation récursif de l'état basé sur les parallélotopes en minimisant le volume.

Les zonotopes ont été introduits par [She74], [Mon89]. L'estimation d'état à l'aide de

zonotopes a été proposée par [PQE02] et [Com03]. Dans la littérature, il existe différentes méthodes pour minimiser la taille de l'estimation zonotopique: dans [Com03] une décomposition en valeur singulière est utilisée pour ajouter une étape de correction afin d'obtenir une approximation externe zonotopique cohérente avec la trajectoire incertaine et mesurée. Alors que [ABC05] présentait une autre méthode basée sur la minimisation des segments et du volume du zonotope, cette méthode est plus rapide mais conduit à une perte de précision par rapport à la minimisation du volume de zonotope. dans cite Le: 13, les auteurs ont proposé une estimation d'état zonotopique basée sur la minimisation d'un critère basé sur le rayon P afin de diminuer la taille du zonotope à chaque temps d'échantillon. Récemment, ont proposé un filtre de Kalman zonotopique (ZKF) qui calcule des ensembles zonotopiques minimaux renfermant tous les états admissibles en minimisant une norme de matrice servant de critère de taille de zonotope appelé F-rayon. Les liens explicites entre l'appartenance à l'ensemble et les paradigmes stochastiques pour le filtrage de Kalman sont donnés.

Dans [Ben+14b], les auteurs ont présenté une méthode d'estimation d'appartenance à un ensemble (prédiction / correction) combinant des zonotopes et des ellipsoïdes. L'approche proposée commence par une approximation zonotopique et se poursuit avec une approximation ellipsoïdale; cela permet de gérer le compromis entre la précision de l'estimation zonotopique et la complexité réduite de l'estimation ellipsoïdale, un critère basé sur le P-rayon d'un zonotope est proposé pour effectuer la transition de l'estimation zonotopique à l'estimation ellipsoïdale.

L'analyse par intervalles est également utilisée dans les travaux de **Jaulin02** et [KW02] pour synthétiser un intervalle d'observateurs d'état. Un certain nombre de résultats ont été présentés dans [RRC04], [JLGHS00], [MR11], [Com], [MDN13], pour améliorer la précision de la méthode, des techniques de consistance ont été considérées (approche prédiction / correction) en étudiant la consistance entre le domaine atteignable de la sortie réelle et celui de la sortie du modèle [KW02], [RRC04], [MRC10]. Dans [TRZ12], les auteurs ont proposé une approche intéressante pour concevoir des observateurs intervalles pour des systèmes linéaires discrets où le gain de l'observateur est calculé de telle sorte que la matrice d'état de l'observateur intervalle proposé soit stable et non négative. est restrictive dans la pratique, en ce sens que l'observabilité du système ne garantit pas l'existence d'un tel gain d'observateur. dans [Che+13], les auteurs ont proposé un observateur intervalle basé sur la transformation de similarité qui relie une matrice à sa représentation non négative assurant la positivité de l'erreur d'estimation, le gain correspondant pouvant être une solution d'une LMI formulée. Un inconvénient des observateurs basés sur l'intervalle est le conservatisme dû aux phénomènes de dépendance et à l'effet d'enveloppement.

Les méthodes mentionnées ci-dessus sont des approches en-ligne et traitent le problème d'estimation ensembliste d'état en présence de perturbations inconnues mais bornées et de bruit de mesure borné. Dans ce type d'approches, on caractérise à chaque instant l'ensemble garanti contenant tous les états compatibles avec les incertitudes du modèle, la mesure et les perturbations bornées et les bruits de mesure. La plupart de ces approches sont basées sur la prédiction / correction, c'est-à-dire à chaque itération, on calcule l'ensemble prédit et on prend en compte la mise à jour de la mesure. tous les états possibles consistantes avec le modèle, les incertitudes, la mesure et les perturbations bornées et les bruits de mesure,

cela peut conduire à une augmentation significative du temps de calcul, d'où la nécessité de plus en plus de supports de stockage mémoire et il y a certains critères (volume, segments ... etc) à minimiser en ligne à chaque itération, cette minimisation nécessite la résolution des problèmes d'optimisation et des inégalités matricielles, ceci peut augmenter la complexité de ces approches.

Contributions de la thèse

Dans ce travail, nous proposons deux nouvelles approches ensemblistes pour l'estimation d'état basées sur la caractérisation explicite des bornes d'erreur d'estimation. Ces approches peuvent être vues comme la combinaison entre un observateur ponctuel et une caractérisation ensembliste de l'erreur d'estimation. L'objectif est de réduire la complexité de leur implémentation, de réduire le temps de calcul en temps réel et d'améliorer la précision et des encadrements des vecteurs d'état.

La première approche propose un observateur ensembliste basé sur des ensembles invariants ellipsoïdaux pour des systèmes linéaires à temps-discret et aussi des systèmes à paramètres variables. L'approche proposée fournit un intervalle d'état déterministe qui est construit comme une somme entre le vecteur état estimé du système et les bornes de l'erreur d'estimation. L'avantage de cette approche est qu'elle ne nécessite pas la propagation des ensemble d'état dans le temps.

La deuxième approche est une version intervalle de l'observateur d'état de Luenberger, pour les systèmes linéaires incertains à temps-discret, basés sur le calcul d'intervalle et les ensembles invariants. Ici, le problème d'estimation ensembliste est considéré comme un problème d'estimation d'état ponctuel couplé à une caractérisation intervalle de l'erreur d'estimation.

Organisation de la thèse

Dans cette section, une brève description des principaux chapitres de la thèse est donnée avec les points importants sur les principales contributions:

- Le premier chapitre présente les notions de base et les principes de l'analyse par intervalles et des ensembles invariants et leur importance dans la description des incertitudes. Il commence par quelques définitions et propriétés relatives aux intervalles. Après cela, les opérations sur des intervalles sont expliquées afin de se familiariser avec l'arithmétique d'intervalles. Une section est dédiée à l'explication du pessimisme que l'on peut rencontrer lors de la manipulation des intervalles dus aux phénomènes de dépendance et à l'effet d'enveloppement. La dernière partie du premier chapitre est consacrée à l'introduction de la notion d'ensemble invariant minimale et fournit un algorithme permettant de calculer les approximations de minimal invariant Robuste Positive Invariant (textbf mRPI) pour le système linéaire. L'algorithme est basé sur le calcul d'ensembles invariants en utilisant le lemme réel borné (textbf BRL) et une nouvelle procédure de réduction.

- Dans le deuxième chapitre, la première contribution est présentée, qui est une nouvelle méthode pour concevoir des observateurs ensembliste pour des systèmes linéaires discrets basés sur des ensembles ellipsoïdaux robuste positive invariants (textbf RPI). L'observateur proposé fournit les bornes de toutes les trajectoires d'état possibles. La conception de l'observateur est basée sur le calcul d'un observateur H_∞ à l'aide d'LMI et d'une formulation BRL modifiée.
- Dans le troisième chapitre, nous présenterons l'extension de l'observateur ensembliste invariant ellipsoïdale, présentés dans le deuxième chapitre, dans le cas des systèmes linéaires a paramètres variant (LPV). Des exemples numériques de systèmes LPV seront présentés pour montrer les performances de l'approche proposée.
- Dans le quatrième chapitre, nous présenterons la deuxième contribution principale qui est un observateur intervalle pour les systèmes linéaires à temps discret, considéré comme un problème d'estimation d'état ponctuel couplé à une caractérisation intervalle de l'erreur d'estimation avec un schéma numérique non pessimiste pour calculer les bornes de l'erreur d'estimation est proposée.

Nous finirons ce rapport par une conclusion générale qui résume les contributions de ce travail. Certaines perspectives seront présentées pour étendre l'approche proposée à un système de grande taille et ses applications possibles pour la détection de défauts, les problèmes de commandes tolérants aux défauts et les problèmes de commande prédictif.

Introduction

This chapter addresses the context, motivation, state of the art of the research area and contributions of this thesis. The organization of this thesis is also presented, which introduces the contents and contributions of each chapter.

0.1 Context and motivations

The state estimation plays a very important role in control, diagnosis and supervision of dynamical systems. In many cases, state is not completely measurable and/or the sensors are very expensive, so we need to estimate it using state observers. The role of observer is to provide an estimation of the state using the available measurements (output and input measurements) and given a mathematical model of the system.

The state observer for linear systems was first introduced by [Kal60]. We can distinguish two types of estimation approaches:

1. **The stochastic approaches** [Kal60], [Lue71] These approaches assume that the perturbations and the measurement noises have an explicit distribution (commonly Gaussian distribution), the estimation problem is solved by minimizing the variance of the estimation error. For linear systems, reasonable stochastic bounds for the estimation error can be obtained if the observer is working correctly, i.e. providing zero mean and white estimation errors and providing innovation covariances that are consistent with the innovations. Otherwise, for non-linear systems and/or in cases where the observers do not respect the consistency of the innovation covariance, the bounds are not useful in practice. The stochastic approaches are used in various domains (control [Bat08], economy and environment [May82], biology [UW11]...etc).
2. **The deterministic approaches** [Sch68] In several applications it is more natural to assume that the perturbations and measurement noises are unknown but bounded, no statistical information on uncertain variables is required, the only assumption we have is that the perturbation and measurement noise are unknown but belong to a known set. In this context, set-membership estimation approaches were introduced [Sch68], [Wis68], [DPBO03], [Fog79]. In these approaches, the idea is to construct a compact set that includes, in guaranteed way, all possible states consistent with the model, uncertainties, the measurements and the bounded perturbations and measurement noises [MMW96], [AGV99].

In this thesis, we are interested to the second type of approaches which are the deterministic approaches. Here we propose new set-membership state estimation approaches, where

invariant sets and interval analysis are used for solving the estimation-error bounds and dealing with bounded uncertainties.

In the literature, we can find several approaches for solving the state bounding problem. On one hand, i) interval observer techniques based on the cooperative system theory. On the other hand, ii) set-membership observers based on set theory. In order to implement set membership state estimation approaches, different shape of sets are used: ellipsoids [DWP01], [KV96], [Pol+04], parallelotopes [CGZ96], zonotopes [Com03], [Le+13], [Le+12], intervals [Moo66], [Jau+01] ...etc.

State bounding using ellipsoidal sets was proposed at the end of 1960s [Sch68], [DPBO03], [Wis68]. The application of ellipsoidal sets to the state estimation problems has been studied in [KV96], [DWP01], [Pol+04], [DKV06] [DK12]. Those approaches are based on set prediction / correction. The basic idea here is to compute ellipsoidal sets guaranteed to contain the vector to be estimated given bounds on the perturbations and noise, the aim is to minimize, at each iteration, the size of the estimation ellipsoidal set, to do that, different criteria are considered in the literature: first criterion is the minimization of the determinant of the shape matrix of the ellipsoid [DWP01] which is equivalent to the minimization of the volume of the ellipsoidal set, second criterion is the minimization of the trace of the shape matrix of the ellipsoid [DWP01] which is equivalent to the minimization of the sum of squares of the half lengths of the axes of the ellipsoid. Third, in [Ben+14a] the authors proposed an approach based on the minimization of the radius of the ellipsoidal estimation by considering a constant gain matrix which is obtained by solving an Linear Matrix Inequality (**LMI**) problem, then this gain is updated on-line at each iteration by solving an LMI optimization problem at each iteration. Solving LMIs at each iteration leads to increasing the online computation time, the authors also proposed a scaling technique in order to reduce the online computation time while keeping an acceptable accuracy of the state estimation. The ellipsoidal sets are often used because, mathematically speaking, they are easy to manipulate therefore simplicity of formulation. In order to obtain ellipsoids containing the state in a precise manner, we need to minimize the size of the ellipsoids. The minimization process can lead to very large ellipsoids corresponding to very large uncertainties in some states which leads to a loss of accuracy.

The use of parallelotopes was proposed by [CGZ96] and [CAGZ98], the authors here addressed the problem of recursive state estimation based on minimum-volume bounding parallelotopes.

The zonotopes were introduced by [She74], [Mon89]. The state estimation using zonotopes was proposed by [PQE02] and [Com03]. In literature there exist different methods to minimize the size of the zonotopic estimation: in [Com03] a singular-value decomposition is used to add a correction step to obtain a zonotopic outer approximation consistent with the uncertain trajectory and the measured output. While, [ABC05] presented another method based on the minimization of the segments and the volume of the zonotope, this method is faster but leads to loss of accuracy than the minimization of the volume of zonotope. In [Le+13], the authors proposed a zonotopic state estimation based on minimizing a P-radius-based criterion in order to decrease the size of the zonotope at each sample time. Recently, [10] proposed a Zonotopic Kalman Filter (ZKF) which computes minimal zonotopic sets enclosing all the

admissible states by minimizing a matrix norm serving as a zonotope size criterion named F-radius. Explicit links between the set-membership and the stochastic paradigms for Kalman filtering are given.

In [Ben+14b], the authors presented a set membership estimation (prediction / correction) approach combining zonotopes and ellipsoids. The proposed approach starts with a zonotopic approximation and continues with an ellipsoidal approximation; this allows to manage the trade-off between the accuracy of the zonotopic estimation and the reduced complexity of the ellipsoidal estimation, a criterion based on the P-radius of a zonotope is proposed to make the transition from the zonotopic estimation to the ellipsoidal estimation.

Interval analysis is also used in the works of citeJaulin02 and [KW02] to synthesize an interval state observers. A number of results have been presented in [RRC04], [JLGHS00], [MR11], [Com], [MDN13], to improve the accuracy of the method, consistency techniques were considered (prediction/correction approach) by studying the consistency between the feasible domain for actual output and the feasible one for model output [KW02], [RRC04], [MRC10]. In [TRZ12], the authors proposed an interesting approach to design interval observers for linear discrete-time systems where the observer gain is tuned such that the state matrix of the proposed interval observer is both Schur stable and nonnegative, this condition is restrictive in practice, in the sense that the observability of the system does not guarantee the existence of such observer gain. In [Che+13], the authors proposed an interval observer based on similarity transformation synthesis which connects a matrix to its non negative representation ensuring the positivity of the estimation error, the corresponding gain can be found as a solution of a formulated LMI. One drawback of the interval based observers is the conservatism due to the dependence phenomena and the wrapping effect.

The methods mentioned above are on-line approaches and deal with set-membership state estimation problem in presence of unknown but bounded perturbation and measurement noise, in these methods we characterize at each instant the set guaranteed to contain all possible states consistent with the model, uncertainties, the measurement and the bounded perturbations and measurement noises. Most of those approaches are based on the prediction/correction i.e at each iteration, we calculate the predicted set and take into account the update of measurement, after that in the correction step a consistency test is made in order to obtain the set guaranteed to contain all possible states consistent with the model, uncertainties, the measurement and the bounded perturbations and measurement noises, this lead to a significant increase of the computation time, hence the necessity of more and more memory storage media and cost increasing, and in some approaches, there is some criterions (volume,segments...etc) are minimized on-line at each iteration, this minimization requires resolution of optimization problems and Linear Matrix inequalities, this can increase the complexity of these approaches.

0.2 Contributions of the thesis

In this work, we propose two new approaches for set membership state estimation based on the explicit characterization of the estimation error bounds. These approaches can be seen as the combination between a punctual observer and a set-membership characterization of the observation error. The objective is to reduce the complexity, reduce the computation time ameliorate the precision and deals with the trade-off between complexity, time and precision.

The first approach is a set-membership observer based on ellipsoidal invariant sets for discrete-time linear systems and also Linear Parameter Varying (**LPV**) systems, the proposed approach provides a guaranteed interval that is build as the sum of the estimated system states and its corresponding estimation errors bounds. The important feature of the proposed approach is that does not require propagation of sets.

The second approach is an interval version of the Luenberger state observer for uncertain discrete-time linear systems based on both intervals and invariant sets computation. The set-membership state estimation problem is considered as a punctual state estimation issue coupled with an interval characterization of the estimation error.

0.3 Organization of the thesis

In this section, a short description of the main chapters is given with highlights on the main contributions:

- The first chapter presents the basic notions and principles of interval analysis and invariant sets and their importance in describing uncertainties. It starts with some definitions and properties related to intervals. After that operations on intervals are explained in order to be familiar with interval arithmetic. A section is dedicated to explain the pessimism that can be encountered when manipulating intervals due to dependency phenomena and wrapping effect. The last part of the first chapter is dedicated to introduce the notion of invariant set and gives an algorithm for computing approximations of the minimal Robustly Positive Invariant (**mRPI**) set for linear system. The algorithm is based on the computation of invariant sets using the Bounded Real Lemma (**BRL**) and a novel shrinking procedure.
- In the second chapter, the first contribution is presented which is a new method for designing state set-membership observers for linear discrete-time systems based on Ellipsoidal Robustly Invariant (**RPI**) sets. The proposed observer provides the bounds of the all possible state trajectories. The observer design is based on the computation of an H_∞ observer using LMIs and including a modified BRL formulation.
- In the third chapter, we will present the extension of the set-membership observer based on ellipsoidal invariant sets, presented in the second chapter, in the case of Linear Pa-

parameter Varying systems. Numerical examples of LPV systems will be presented to show the performance of the proposed approach.

- In the fourth chapter, we will present the second main contribution which is an interval observer for discrete-time linear systems which considered as a punctual state estimation issue coupled with an interval characterization of the estimation error with a non pessimistic numerical scheme to compute a rigorous enclosure of the estimation error is proposed.

We conclude this thesis with a general conclusion which summarizes the contributions of this work. Some perspectives will be presented such that extending the proposed approach to a large systems and its possible applications for fault detection, fault tolerant control issues and model predictive control problems.

0.4 Publications

The work in this thesis has resulted in several accepted/submitted publications to international conferences and journals:

Conference papers:

- **N. Loukkas, N. Meslem and JJ. Martinez.** Set-membership tests to evaluate the performance of nominal feedback control laws. *IEEE Conference on Control Applications (CCA). Part of 2016 IEEE Multi-Conference on Systems and Control*, Buenos Aires, Argentina, pp. 1300—1305, September 2016.
- **N. Loukkas, N. Meslem and JJ. Martinez.** Set-membership observer design based on ellipsoidal invariant sets. *IFAC World Congress*, Toulouse, France, July 2017.
- **N. Meslem, N. Loukkas and JJ. Martinez.** A Luenberger-like Interval Observer for a Class of Nonlinear Discrete-time Systems. *Asian control conference*, Gold coast, Australia, 2017.

Journal papers:

- **N. Loukkas, N. Meslem and JJ. Martinez.** Using set invariance to design robust interval observers for discrete-time linear systems. *International Journal of Robust and Nonlinear Control* 2018;1–17. <https://doi.org/10.1002/rnc.4103> . (Accepted)
- **JJ. Martinez, N. Loukkas and N. Meslem.** H_∞ set-membership observer design for LPV Systems. *International Journal of Control*. (Second submission)

Oral presentation:

- **N. Loukkas, N. Meslem and JJ. Martinez.** An Interval Technique to Check the Performance of Control Laws Applied to Wind Turbines. *9th Summer Workshop on Interval Methods*, Lyon, France, June 2016.

Notions about interval analysis and invariant sets computation

Contents

1.1	Introduction	13
1.2	Interval analysis	14
1.2.1	Definitions	15
1.2.2	Interval vector	15
1.2.3	Interval matrix	17
1.2.4	Interval arithmetic	18
1.2.5	Intervals and operations on sets	19
1.2.6	Interval norm	21
1.2.7	Conservatism	22
1.2.8	Inclusion function	23
1.3	Invariant sets	28
1.3.1	Ellipsoidal sets	28
1.3.2	Polyhedral sets	30
1.3.3	Polyhedral mRPI set computation	31
1.4	Conclusion	37

1.1 Introduction

In general, physical systems are frequently described by mathematical models. These mathematical models allow us to analyze the behavior of the system and to design controllers. Thus, it is very important to obtain a mathematical model that describes as much as possible the behavior of the system to be controlled.

Commonly, the mathematical models developed using only theoretical physical principles can not represent accurately the real behavior of the system, this can be due to the lack of information, complexity of the system or the presence of unknown phenomena that have not be considered into the mathematical model. In order to build a more realistic model, a

description of the uncertainties can be added to the original mathematical model. This kind of models are called uncertain models, where the domain of the uncertainties is assumed to be known *a priori*. The concept of uncertain models is very important in system design, control and supervision, see for instance [AP06] [AK06].

There exist two ways to model uncertainties:

1. **The stochastic approaches:** [Kal60], [Lue71] where the uncertainties are represented by a random variables with known probability distribution and co-variance, the stochastic approach is used in various domains (control design, economy and environment [May82] , biology [UW11] ... etc). But in many applications, the probability distribution and co-variance of the uncertain parameters and perturbations are not known, only bounds of these uncertainties can be fixed.
2. **The deterministic approaches:** [Sch68] where the uncertainties are supposed unknown but bounded and no statistical information on uncertain variables is required. In general, these uncertainties are supposed belonging to a convex sets. There exists different shape of sets used to represent the uncertainties. The choice of the shape of sets depends on their accuracy and their complexity for solving a given problem.

There exists a various set shapes to represent the uncertainties: intervals, ellipsoids, polytopes, zonotopes, parallelotopes ... etc. In the context of this thesis, we are mainly interested in ellipsoidal sets and intervals. We also explore a very important concept which is the set invariance.

To be self-contained, this chapter introduces the basic notions and definitions on which the contributions of this thesis are based on. Section 1.2 addresses several basic definitions and properties about interval analysis. In the Section 1.3, we present definitions and properties of ellipsoids. In the same section we also present the concept of set invariance and an efficient method to characterize the minimal robustly positive invariant set for discrete-time linear systems [Mar15].

1.2 Interval analysis

Interval analysis initially developed to quantify numerical errors due to the finite representation of real numbers on a computer. The idea is to manipulate intervals of reals numbers rather than point values. After that, several algorithms based on interval analysis have been developed in several domains [Sun58] [Moo66] [Jau+01] with the aim of solving, in a rigorous way, some mathematical problems and to evaluate the impact of uncertainties.

1.2.1 Definitions

A real interval, denoted by $[x]$, is a bounded convex set of \mathbb{R} defined by:

$$[x] = [\underline{x}, \bar{x}] = \{x \in \mathbb{R} : \underline{x} \leq x \leq \bar{x}\} \quad (1.1)$$

where the real numbers \underline{x} and \bar{x} are respectively the lower and the upper bounds of $[x]$. The set of real intervals is noted by \mathbb{IR} . An interval is said degenerate if $\bar{x} = \underline{x}$.

Example 1.1

According to the definition above, $[-1, 2]$, $[5, 8]$, 3 , $[-\infty, 2]$, $[0, +\infty]$ and \mathbb{R} , are intervals because they satisfy the required properties of intervals.

On another hand, $[4, 1]$, $] -1, 6]$, $] \pi, 4[$ and $[0, +\infty[$ are not intervals because they don't satisfy the required properties of intervals.

For a given interval $[x] \in \mathbb{IR}$, one can associate the following definitions:

- **Lower bound:**

$$\inf([x]) = \underline{x} \quad (1.2)$$

- **Upper bound:**

$$\sup([x]) = \bar{x} \quad (1.3)$$

- **Center or medium:**

$$m([x]) = \frac{(\bar{x} + \underline{x})}{2} \quad (1.4)$$

- **Width:**

$$w([x]) = \bar{x} - \underline{x} \quad (1.5)$$

- **Radius:**

$$r([x]) = \frac{(\bar{x} - \underline{x})}{2} \quad (1.6)$$

- **Amplitude:**

$$|[x]| = \max\{|\underline{x}|, |\bar{x}|\} \quad (1.7)$$

1.2.2 Interval vector

An interval vector $[\mathbf{x}]$ in \mathbb{R}^n also called box, is the cartesian product of n intervals. It can be written in the following form:

$$[\mathbf{x}] = [\underline{\mathbf{x}}, \bar{\mathbf{x}}] = [\underline{x}_1, \bar{x}_1] \times [\underline{x}_2, \bar{x}_2] \times \dots \times [\underline{x}_n, \bar{x}_n] \quad (1.8)$$

Where $\underline{\mathbf{x}} = (\underline{x}_1, \underline{x}_2, \dots, \underline{x}_n)^T$ and $\bar{\mathbf{x}} = (\bar{x}_1, \bar{x}_2, \dots, \bar{x}_n)^T$. The set of all boxes in \mathbb{R}^n will be noted by \mathbb{IR}^n .

Similarly to the scalar interval case, one can associate to an interval vector the following definitions:

- Lower bound of an interval vector:

$$\inf([\mathbf{x}]) = (\underline{x}_1, \underline{x}_2, \dots, \underline{x}_n)^T \quad (1.9)$$

- Upper bound of an interval vector:

$$\sup([\mathbf{x}]) = (\bar{x}_1, \bar{x}_2, \dots, \bar{x}_n)^T \quad (1.10)$$

- Center or medium of an interval vector:

$$m([\mathbf{x}]) = (m([x_1]), m([x_2]), \dots, m([x_n]))^T \quad (1.11)$$

- Width of an interval vector:

$$w([\mathbf{x}]) = \max_{1 \leq i \leq n} (\bar{x}_i - \underline{x}_i) \quad (1.12)$$

- Element-wise width of an interval vector:

$$\mathbb{W}([\mathbf{x}]) = (w([x_1]), w([x_2]), \dots, w([x_n]))^T \quad (1.13)$$

- Radius of an interval vector:

$$r([\mathbf{x}]) = \max_{1 \leq i \leq n} (r([x_i])) \quad (1.14)$$

Moreover, any interval vector $[\mathbf{x}] \in \mathbb{IR}^n$ can be rewritten as follows

$$[\mathbf{x}] = m([\mathbf{x}]) + [\Delta \mathbf{x}] \quad (1.15)$$

where

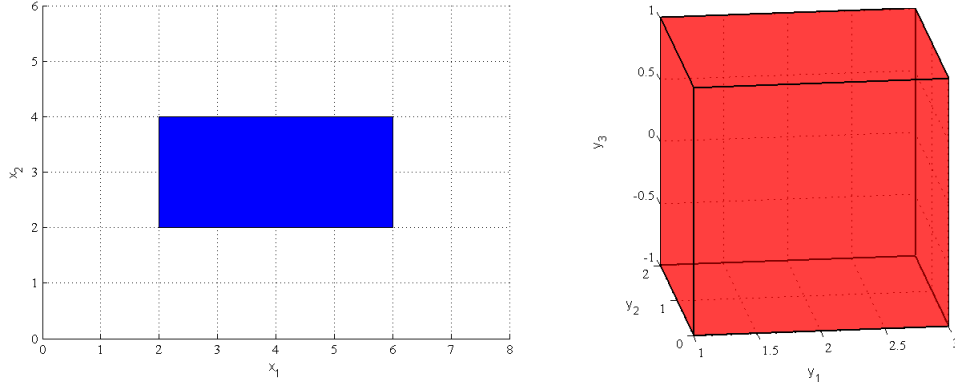
$$[\Delta \mathbf{x}] = \frac{1}{2}[-1 \ 1]\mathbb{W}([\mathbf{x}]) \quad (1.16)$$

- Volume of interval vector:

$$\text{vol}([\mathbf{x}]) = \prod_{i=1}^n w([\mathbf{x}_i]) = (\bar{x}_1 - \underline{x}_1)(\bar{x}_2 - \underline{x}_2) \dots (\bar{x}_n - \underline{x}_n) \quad (1.17)$$

Example 1.2

Let's consider the interval vectors $[\mathbf{x}]$, $[\mathbf{y}]$ of dimension 2 and 3 respectively: $[\mathbf{x}] = [2, 6] \times [2, 4]$ is a box in \mathbb{IR}^2 and $[\mathbf{y}] = [1, 3] \times [0, 2] \times [0, 1/2]$ is a box in \mathbb{IR}^3 . The Figure (1.1) illustrates the graphical representation of the two boxes $[\mathbf{x}]$ and $[\mathbf{y}]$ plotted in 2D and 3D plan respectively.

Figure 1.1: Graphical representation of boxes $[\mathbf{x}]$ (in blue) and $[\mathbf{y}]$ (in red)

1.2.3 Interval matrix

The same reasoning on interval vectors is extended to interval matrices. An interval matrix $[\mathbf{A}] \in \mathbb{IR}^{n \times m}$ is a matrix whose elements are intervals.

$$[\mathbf{A}] = \begin{pmatrix} [a_{1,1}] & \cdots & [a_{1,m}] \\ \vdots & \ddots & \vdots \\ [a_{n,1}] & \cdots & [a_{n,m}] \end{pmatrix} = [\underline{\mathbf{A}}, \overline{\mathbf{A}}] \quad (1.18)$$

Where $\underline{\mathbf{A}} = \begin{pmatrix} \underline{a}_{1,1} & \cdots & \underline{a}_{1,m} \\ \vdots & \ddots & \vdots \\ \underline{a}_{n,1} & \cdots & \underline{a}_{n,m} \end{pmatrix}$ and $\overline{\mathbf{A}} = \begin{pmatrix} \overline{a}_{1,1} & \cdots & \overline{a}_{1,m} \\ \vdots & \ddots & \vdots \\ \overline{a}_{n,1} & \cdots & \overline{a}_{n,m} \end{pmatrix}$ are the lower and upper matrices of the interval matrix $[\mathbf{A}]$

For example, consider the following 2×2 interval matrix

$$[\mathbf{A}] = \begin{pmatrix} [-1, 1] & [0, 3] \\ [2, 6] & [-2, 0] \end{pmatrix} \quad (1.19)$$

where its lower and upper real matrices are:

$$\underline{\mathbf{A}} = \begin{pmatrix} -1 & 0 \\ 2 & -2 \end{pmatrix} \text{ and } \overline{\mathbf{A}} = \begin{pmatrix} 1 & 3 \\ 6 & 0 \end{pmatrix}$$

Remark 1.1

Similarly to the interval vector case, one can associate to a matrix vector the previous definitions (center, width, radius volume...) using the same reasoning.

- **Center or medium of an interval matrix:**

$$m([\mathbf{A}]) = \begin{pmatrix} m_{1,1} & \cdots & m_{1,m} \\ \vdots & \ddots & \vdots \\ m_{n,1} & \cdots & m_{n,m} \end{pmatrix} \quad (1.20)$$

where $m_{i,j} = \frac{a_{i,j} + \bar{a}_{i,j}}{2}$; $1 \leq i \leq n$, $1 \leq j \leq m$

- **Width of an interval matrix:**

$$w([\mathbf{A}]) = \bar{\mathbf{A}} - \underline{\mathbf{A}} \quad (1.21)$$

- **Radius of an interval matrix:**

$$r([\mathbf{A}]) = \frac{(\bar{\mathbf{A}} - \underline{\mathbf{A}})}{2} \quad (1.22)$$

1.2.4 Interval arithmetic

The elementary arithmetic operations on real numbers $\circ \in \{+, -, *, \div\}$ can be extended to intervals over \mathbb{IR} , according to the following principle

$$\forall [x], [y] \in \mathbb{IR} \quad [x] \circ [y] = \{a \circ b \mid a \in [x], b \in [y]\} \quad (1.23)$$

Given two intervals $[x]$ and $[y]$ in \mathbb{IR} the result of the interval operation $[x] \circ [y]$ can be obtained by:

- Addition

$$[x] + [y] = [\underline{x} + \underline{y}, \bar{x} + \bar{y}] \quad (1.24)$$

- Subtraction

$$[x] - [y] = [\underline{x} - \bar{y}, \bar{x} - \underline{y}] \quad (1.25)$$

- Multiplication

$$[x] * [y] = [\min\{\underline{x}\underline{y}, \underline{x}\bar{y}, \bar{x}\underline{y}, \bar{x}\bar{y}\}, \max\{\underline{x}\underline{y}, \underline{x}\bar{y}, \bar{x}\underline{y}, \bar{x}\bar{y}\}] \quad (1.26)$$

$$\alpha[x] = \begin{cases} [\alpha\underline{x}, \alpha\bar{x}] & \text{if } \alpha \geq 0 \\ [\alpha\bar{x}, \alpha\underline{x}] & \text{if } \alpha < 0 \end{cases} \quad (1.27)$$

- Division

$$\frac{1}{[x]} = \begin{cases} \emptyset & \text{if } [x] = [0, 0] \\ [\frac{1}{\bar{x}}, \frac{1}{\underline{x}}] & \text{if } 0 \notin [x] \\ [\frac{1}{\bar{x}}, +\infty] & \text{if } \underline{x} = 0, \bar{x} > 0 \\ [-\infty, \frac{1}{\bar{x}}] & \text{if } \underline{x} < 0, \bar{x} = 0 \\ [-\infty, +\infty] & \text{if } \underline{x} < 0, \bar{x} > 0 \end{cases} \quad (1.28)$$

$$\frac{[x]}{[y]} = [x] \frac{1}{[y]} \quad (1.29)$$

The below interval operations illustrate the application of the interval arithmetic.

- Addition: $[-2, 4] + [1, 3] = [-1, 7]$
- Subtraction: $[0, 7] - [1, 2] = [-2, 6]$
- Multiplication: $[-2, 1] * [3, 4] = [-8, 4]$
- Division: $\frac{[6, 12]}{[2, 3]} = [2, 6]$

We extend the same rules to the case of interval vectors (or boxes). Let's consider two boxes $[\mathbf{x}] = [\mathbf{x}_1] \times [\mathbf{x}_2] \times \dots \times [\mathbf{x}_n]$ and $[\mathbf{y}] = [\mathbf{y}_1] \times [\mathbf{y}_2] \times \dots \times [\mathbf{y}_n]$, the arithmetic operation $\circ \in \{+, -\}$ on two boxes $[\mathbf{x}]$ and $[\mathbf{y}]$ give a box defined as follow:

$$\forall [\mathbf{x}], [\mathbf{y}] \in \mathbb{IR}^n \quad [\mathbf{x}] \circ [\mathbf{y}] = ([x_1] \circ [y_1]) \times ([x_2] \circ [y_2]) \times \dots \times ([x_n] \circ [y_n]) \quad (1.30)$$

For example, let's consider some elementary arithmetic operation on interval vectors

$$[0, 1] \times [1, 3] + [-2, 4] \times [5, 6] = [-2, 5] \times [6, 9]$$

$$[0, 1] \times [2, 3] - [-2, 0] \times [-3, -1] = [0, 3] \times [3, 6]$$

Remark 1.2

If $[\mathbf{A}] \in \mathbf{IR}^{n \times n}$ is an interval matrix and its elements are $[a_{i,j}]$ and $[\mathbf{b}] \in \mathbf{IR}^n$ is an interval vector and its elements are $[b_k]$, then the elements of $[\mathbf{c}] = [\mathbf{A}] * [\mathbf{b}]$ is given by its elements $[c_i]$ given by:

$$[c_i] = \sum_{k=1}^n [a_{i,k}] * [b_k]$$

For example, consider the matrices : $[\mathbf{A}] = \begin{pmatrix} [0, 1] & [2, 3] \\ [1, 2] & [-1, 4] \end{pmatrix}$, $[\mathbf{b}] = \begin{pmatrix} [1, 2] \\ [0, 3] \end{pmatrix}$, the product $[\mathbf{c}] = [\mathbf{A}] * [\mathbf{b}]$ is given as follow

$$[\mathbf{c}] = [\mathbf{A}] * [\mathbf{b}] = \begin{pmatrix} [0, 1] & [2, 3] \\ [1, 2] & [-1, 4] \end{pmatrix} \begin{pmatrix} [1, 2] \\ [0, 3] \end{pmatrix} = \begin{pmatrix} [0, 1][1, 2] + [2, 3][0, 3] \\ [1, 2][1, 2] + [-1, 4][0, 3] \end{pmatrix} = \begin{pmatrix} [0, 11] \\ [-2, 16] \end{pmatrix}$$

1.2.5 Intervals and operations on sets

Since intervals are considered as sets, set operations like equality ($=$), belonging (\in), strict inclusion (\subset), wide inclusion (\subseteq), intersection (\cap) and union (\cup) can be easily defined for intervals. For example, the intersection between two intervals is defined as follow:

$$[x] \cap [y] = \begin{cases} [\max\{\underline{x}, \underline{y}\}, \min\{\bar{x}, \bar{y}\}] & \text{if } \max\{\underline{x}, \underline{y}\} \leq \min\{\bar{x}, \bar{y}\} \\ \emptyset & \text{else} \end{cases} \quad (1.31)$$

Example: The intersection of two intervals is given by:

$$[-1, 2] \cap [0, 4] = [0, 2]$$

In the case of interval vectors $[\mathbf{x}]$ and $[\mathbf{y}]$ in \mathbb{IR}^n , the intersection of two interval vectors is applied element-wise as follows:

$$[\mathbf{x}] \cap [\mathbf{y}] = \begin{cases} \emptyset & \text{if } [x_i] \cap [y_i] = \emptyset \\ [x_i] \cap [y_i] & \text{Otherwise} \end{cases} \quad (1.32)$$

Example: The intersection of two interval vectors $[\mathbf{x}] = [0, 5] \times [1, 3]$ and $[\mathbf{y}] = [3, 4] \times [2, 6]$ is:

$$[\mathbf{x}] \cap [\mathbf{y}] = ([0, 5] \times [1, 3]) \cap ([3, 4] \times [2, 6]) = [3, 4] \times [2, 3]$$

The Figure (1.2) illustrates the intersection of two boxes: $[\mathbf{x}]$ in yellow, $[\mathbf{y}]$ in red, the result of the intersection is the box plotted in red.

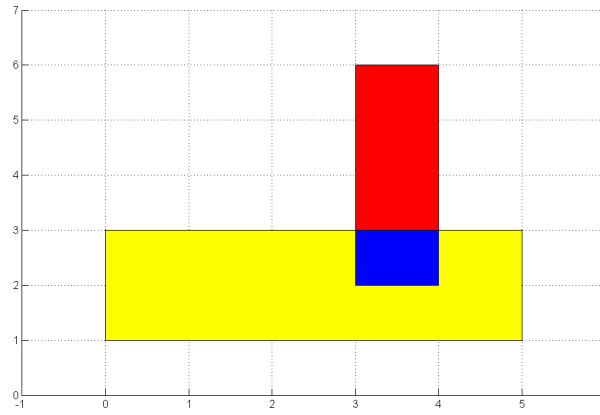


Figure 1.2: Intersection of two interval vectors: $[\mathbf{x}]$ in yellow, $[\mathbf{y}]$ in red, $[\mathbf{x}] \cap [\mathbf{y}]$ in blue

The union (\cup) of two intervals is not generally an interval. The notion of convex-hull union (\sqcup) of two intervals is introduced. It corresponds to the smallest interval containing the union of these two intervals.

$$[x] \sqcup [y] = [\min\{\underline{x}, \underline{y}\}, \max\{\bar{x}, \bar{y}\}] \quad (1.33)$$

For example, consider two intervals $[-2, 1]$ and $[-2, 6]$, the union of these two intervals is given by:

$$[-2, 1] \sqcup [2, 6] = [-2, 6]$$

In the case of interval vectors, the union of two interval vectors $[\mathbf{x}]$ and $[\mathbf{y}]$ in \mathbb{IR}^n is:

$$[\mathbf{x}] \sqcup [\mathbf{y}] = ([x_1] \sqcup [y_1] \times [x_2] \sqcup [y_2] \times \dots \times [x_n] \sqcup [y_n]) \quad (1.34)$$

For example, consider two interval vectors $[\mathbf{x}] = [-2, 1] \times [0, 3]$ and $[\mathbf{y}] = [2, 6] \times [1, 4]$, the union of these two interval vectors is given by:

$$[\mathbf{x}] \sqcup [\mathbf{y}] = [-2, 1] \times [0, 3] \sqcup [2, 6] \times [1, 4] = [-2, 6] \times [0, 4]$$

Figure (1.3) illustrates the union of two disjoint intervals $[x]$ (in yellow) and $[y]$ (in red). The convex-hull union is plotted in green

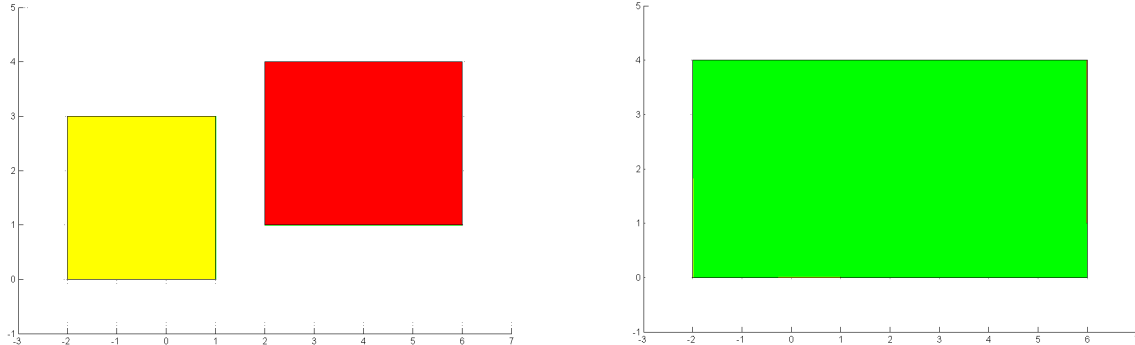


Figure 1.3: Union of two interval vectors: $[x]$ in yellow, $[y]$ in red, $[x] \cup [y]$ in green

1.2.6 Interval norm

1.2.6.1 Interval vector norm

A vector norm of an interval vector is any application $\| \cdot \|: \mathbb{IR}^n \rightarrow \mathbb{R}$ satisfying the following properties:

-

$$\| [x] \| \geq 0, \quad \forall [x] \in \mathbb{IR}^n$$

-

$$\| [x] \| = 0 \iff [x] = 0$$

-

$$\| [\alpha][x] \| = |\alpha| \| [x] \|, \quad \forall [x] \in \mathbb{IR}^n, \quad \forall \alpha \in \mathbb{R}$$

-

$$\| [x] + [y] \| \leq \| [x] \| + \| [y] \|, \quad \forall [x], [y] \in \mathbb{IR}^n$$

So, the maximum norm of given interval vector $[b]$ is defined as

$$\| [b] \| = \max_{1 \leq i \leq n} \{|b_i|\}$$

1.2.6.2 Interval matrix norm

Let's consider the interval matrices $[A], [B] \in \mathbb{M}_{n \times n}$. The application $\| \cdot \|: \mathbb{M} \rightarrow \mathbb{R}$ is a matrix norm if it satisfies the following properties:

•

$$\| [A] \| \geq 0, \quad \forall [A] \in \mathbb{M}$$

•

$$\| [A] \| = 0 \iff [A] = 0$$

•

$$\| [\alpha][A] \| = |\alpha| \| [A] \|, \quad \forall [A] \in \mathbb{M}, \quad \forall \alpha \in \mathbb{R}$$

•

$$\| [A] + [B] \| \leq \| [A] \| + \| [B] \|, \quad \forall [A], [B] \in \mathbb{M}$$

•

$$\| [A][B] \| \leq \| [A] \| \| [B] \|, \quad \forall [A], [B] \in \mathbb{M}$$

We can define maximum norm of a given interval matrix $[A]$ as follow

$$\| [A] \| = \max_{1 \leq i \leq n} \sum_{j=1}^n |a_{ij}|$$

1.2.7 Conservatism

The result of a series of operations between two intervals or more may be pessimist. This pessimism is due to two major reasons: dependency phenomena and wrapping effect.

1.2.7.1 Dependency phenomena

Consider the interval $[x] = [\underline{x}, \bar{x}]$ and elementary operations $\circ \in \{+, -, *, \div\}$. From the definition (1.23), we can compute the result of an operation \circ between $[x]$ and $[x]$ as follows:

$$\forall [x] \in \mathbb{IR} \quad [x] \circ [x] = \{a \circ b \mid a \in [x], b \in [x]\} \quad (1.35)$$

Although we manipulate the same interval $[x]$, the variables a and b are considered as different variables and there is no information that $a = b$. This problem is called dependency phenomena which can be illustrated in the following points:

- **Non existence of zero in subtraction**

In the case of real scalars, the subtraction of two identical terms gives zero. But in the case of intervals, the subtraction of two identical intervals does not give zero, except for degenerated intervals.

For example, consider an interval $[x] = [3, 8]$, then

$$[x] - [x] = [3, 8] - [3, 8] = [3, 8] + [-8, -3] = [-5, 5] \ni 0$$

- **Non existence of unity in division**

In the case of real scalars, the division of two identical terms gives unity. But in the case of intervals, the division of two identical intervals does not give unity, except for degenerated intervals.

For instance, given an interval $[x] = [1, 2]$ then

$$[x]/[x] = [x] * \frac{1}{[x]} = [\frac{1}{2}, 2] \neq 1$$

1.2.7.2 Wrapping effect

The wrapping effect is one major source of conservatism. The wrapping effect is caused by the iterative computation on interval vectors (or interval matrices). One can always use the rotation operator [Moo66] to explain this phenomenon.

Consider successive rotations of a box $[x] = [x_1] \times [x_2]$ using a rotation matrix R .

$$\mathbf{x}(\theta) = \mathbf{R}(\theta)\mathbf{x}_0$$

with

$$\mathbf{R}(\theta) = \begin{pmatrix} \cos\theta & \sin\theta \\ -\sin\theta & \cos\theta \end{pmatrix}$$

where $\mathbf{x}_0 \in [\mathbf{x}_0]$. The evolution of the initial box $[\mathbf{x}_0]$ is governed by the punctual rotation in the plane with respect to the origin gives a rectangle of the same size but with a different orientation. As shown in the Figure (1.4), the representation of this rectangle by a box gives a new bigger rectangle. This phenomena is due to the over-approximation of real solution sets which are parallelepipeds by boxes aligned with the axes of the original mark. Thus, the accumulation of errors related to this over-approximation leads to the explosion of the size of these boxes (see Figure (1.4)).

1.2.8 Inclusion function

Consider a function f from \mathbb{R}^n to \mathbb{R}^m as follows:

$$f : \mathbf{x} \in \mathbb{R}^n \longrightarrow f(\mathbf{x}) \in \mathbb{R}^m \tag{1.36}$$

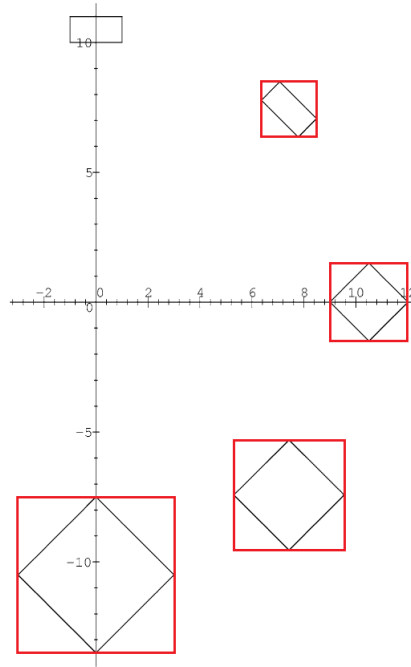


Figure 1.4: Wrapping effect ($\theta = \frac{\pi}{4}$)

The image of a box $[x] \in \mathbb{IR}^n$ by the function f is the set defined as follows:

$$f([x]) = \{f(\mathbf{x}), \forall \mathbf{x} \in [x]\} \tag{1.37}$$

note that $f([x])$ is not necessarily a box of \mathbb{IR}^n , so we introduce the notion of "inclusion function". An inclusion function of f is an interval function denoted by $[f] : \mathbb{IR}^n \longleftrightarrow \mathbb{IR}^m$ that returns a box enclosing $f([x])$:

$$[f]([x]) = [f(\mathbf{x}), \mathbf{x} \in [x]] \tag{1.38}$$

$[f]$ is an inclusion function if and only if:

$$\forall [x] \in \mathbb{IR}^n : f([x]) \subseteq [f]([x])$$

This means that whatever the form of the image $f([x])$, the inclusion function $[f]$ provides a box $[f]([x])$ that contains, in a guaranteed way, the image of $[x]$ by f (see Figure 1.5).

The inclusion function is not unique. There exists an infinity inclusion functions for a given function f depending on how f is written and evaluated in the interval arithmetic framework. The aim is to find a minimal inclusion function $[f^*]$ that provides the smallest box containing $f([x])$ (see Figure 1.5).

For example, consider the function $f(x) = x^2 - x$. In the case of real numbers the two expressions $x^2 - x$ and $x(x - 1)$ provides the same results for any real number x . However, in the case of real intervals, it is possible that the image will be different when we change the expression. For example for $[x] = [2, 4]$ we have:

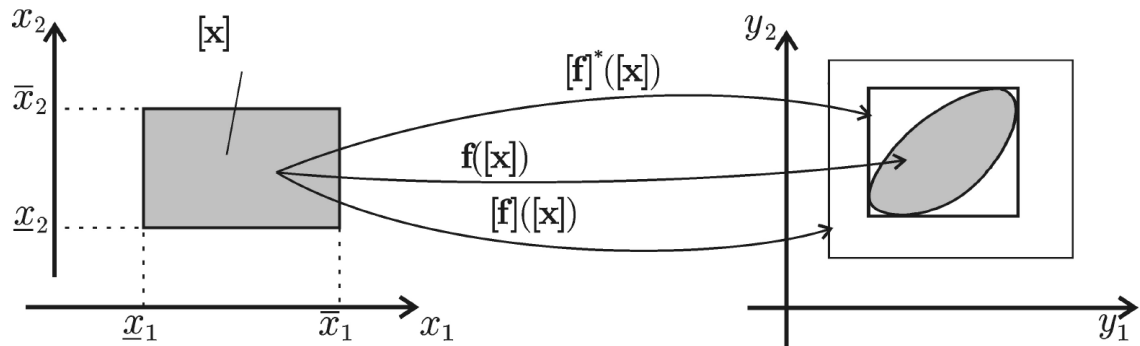


Figure 1.5: Inclusion function

$$\begin{cases} [x]^2 - [x] = [2, 4]^2 - [2, 4] = [0, 14] \\ [x]([x] - 1) = [2, 4]([2, 4] - 1) = [2, 12] \end{cases}$$

This is due to the dependency phenomena presented previously.

1.2.8.1 Properties of inclusion function

1.2.8.2 Monotonicity

An inclusion function $[f]$ is said monotone (in sens of inclusion) if:

$$\forall [x], \forall [y] : [x] \subset [y] \Rightarrow [f]([x]) \subset [f]([y])$$

1.2.8.3 Convergence

An inclusion function $[f]$ is said convergent if for any sequence of boxes $[x_k] \in \mathbb{IR}^n$, we have:

$$\lim_{k \rightarrow +\infty} w([x_k]) = 0 \Rightarrow \lim_{k \rightarrow +\infty} w([f]([x_k])) = 0$$

1.2.8.4 Natural inclusion function

The natural inclusion function consists in replacing all the input variables of the function by the corresponding intervals and all the operators and the elementary functions defining the function by the interval operators and interval functions.

This inclusion function is said convergent if the function f contains only continuous elementary functions as well as continuous operations. The natural inclusion function is minimal if f is continuous and each variable appears only once.

A natural inclusion function is rarely minimal. Pessimism is often introduced when each variable appears multiple times in the expression of f . To explain this lets consider the following function f written in different equivalent expressions f_1, f_2, f_3, f_4 :

$$f_1(x) = x^2 + x$$

$$f_2(x) = x * (x + 2)$$

$$f_3(x) = x * x + 2 * x$$

$$f_4(x) = (x + 1)^2 - 1$$

For $[x] = [-1, 1]$, the natural inclusion function for each expression is obtained as follows:

$$[f_1]([x]) = [x]^2 + [x] = [-2, 3]$$

$$[f_2]([x]) = [x] * ([x] + 1) = [-3, 3]$$

$$[f_3]([x]) = [x] * [x] + [x] = [-3, 3]$$

$$[f_4]([x]) = ([x] + 1)^2 - 1 = [-1, 3]$$

We note that the size of the intervals obtained by these four inclusion functions depends on how f is written, This is due to the dependency phenomenon explained above. In this example, the natural inclusion function $[f_4]([x])$ is minimal inclusion function, it allows to find the smallest interval containing the image of $[x]$ by f .

1.2.8.5 Centered inclusion function

Let's consider the function:

$$f : \mathbb{R}^n \longrightarrow \mathbb{R}$$

To avoid the pessimism due to the dependency phenomenon, the centered inclusion function was introduced [Jau+01]. Using the mean value theorem [Neu90], we obtain:

$$\forall x \in [x], \exists \xi \in [x] : f(x) = f(m([x]) + J(\xi)(x - m([x])))$$

where J is the Jacobean of the function f . Thus we can say that:

$$\forall x \in [x] : f(x) \in f(m([x]) + [J]([x])(x - m([x])))$$

where $[J]$ is the inclusion function of J , so we obtain:

$$f([x]) \subseteq f(m([x]) + [J]([x])([x] - m([x])))$$

Then, the centered inclusion function $[f_c]([x])$ can be defined as:

$$[f_c]([x]) \equiv f(m([x])) + [J]([x])([x] - m([x]))$$

In general, $[f_c]([x])$ gives a less pessimistic result compared to the natural inclusion function when the width of intervals is quite small.

1.2.8.6 Taylor inclusion function

Let's consider the function:

$$f : \mathbb{R}^n \longrightarrow \mathbb{R}$$

The Taylor inclusion function is based on high order Taylor expansion. In our context, we use the order 2 Taylor expansion. The Taylor inclusion function noted $[f_T]([x])$ is defined as follows:

$$[f_T]([x]) = f(m([x])) + J(m([x]))([x] - m([x])) + \frac{1}{2}([x] - m([x]))^T [H]([x])([x] - m([x]))$$

where J is the gradient of f , $[H]([x])$ is the Hessian interval matrix of f and $m([x])$ is the center of the interval $[x]$.

The advantage of such an inclusion function is to use interval arithmetic only at the higher order, usually over a reduced number of operations, and thus greatly reduces the dependency effect.

For example, consider a function $f(x) = x^2 + \sin(x)$, and an interval $[x] = [\frac{2\pi}{3}, \frac{4\pi}{3}]$, let's compare the natural inclusion function $[f_n]([x])$, the centered inclusion function $[f_c]([x])$ and the Taylor inclusion function $[f_T]([x])$.

$$[f_n]([x]) = [x]^2 + \sin([x]) = [3.52046, 18.41199]$$

$$[f_c]([x]) = f(c) + [f']([x])([x] - c) = [1.62022, 18.11899]$$

$$[f_T]([x]) = f(c) + [f'](\pi)([x] - c) + \frac{([x] - c)^2}{2} [f'']([x]) = [4.33706, 16.97362]$$

where $c = m([x])$ is the center of $[x]$.

For this example, since f is increasing in the interval $[x]$, one can determine the minimal inclusion function $[f^*]$:

$$[f^*]([x]) = [\underline{x}^2 + \sin(\underline{x}), \bar{x}^2 + \sin(\bar{x})] = [5.25251, 16.67994]$$

The most precise interval inclusion is the Taylor inclusion function $[f_T]([x])$ which is close to the minimal inclusion function $[f^*]([x])$.

1.3 Invariant sets

Set invariance is a very important concept in control and estimation problems. The notion of invariant sets can be found in [Bla99]. In the literature, techniques for computing invariant sets are mostly related to the computation of levels sets of a Lyapunov function [Bla95] [SG05] or, in others cases, just by the computation of some norm of the system state for describing the boundaries of an invariant set [BC98] [Bla99] [LA03].

Définition 1.1

A set \mathcal{S} is a **Positive Invariant (PI)** set for the dynamic system $\mathbf{x}_{k+1} = \mathbf{A}\mathbf{x}_k$ if

$$\forall \mathbf{x} \in \mathcal{S} : \mathbf{A}\mathbf{x}_{k+1} \in \mathcal{S}$$

Définition 1.2

A set \mathcal{S} is a **Robustly Positive Invariant (RPI)** set for the dynamic perturbed system $\mathbf{x}_{k+1} = \mathbf{A}\mathbf{x}_k + \mathbf{F}\mathbf{w}_k$ if

$$\forall \mathbf{w}_k \in \mathcal{W}, \forall \mathbf{x} \in \mathcal{S} : f(\mathcal{S}, \mathcal{W}) \in \mathcal{S}$$

Définition 1.3

The **minimal Robustly Positive Invariant (mRPI)** is defined as the **RPI** set contained in all possible **RPI** sets.

1.3.1 Ellipsoidal sets

Ellipsoidal sets are widely used in many applications, as identification and estimation and diagnosis, due to their interesting characteristics and the simplicity of their computation. In the context of set-membership estimation, Ellipsoids are frequently used [KV96] [DWP01] [Pol+04].

Définition 1.4 (Ellipsoidal set)

Given a symmetric positive definite matrix $\mathbf{P} := \mathbf{P}^T \succ 0$, a real vector $c \in \mathbb{R}^n$ and a strictly positive real scalar $\rho \in \mathbb{R}_+^*$, the bounded ellipsoid Ψ is defined by the set

$$\Psi = \{x \in \mathbb{R}^n : (x - c)^T \mathbf{P}(x - c) \leq \rho\} \quad (1.39)$$

where \mathbf{P} is the shape matrix of the ellipsoid, c its center and ρ its radius.

Example 1.3

Figure 1.6 illustrates an example of an ellipsoidal set in a two-dimension space with $c = [0 \ 0]^T$, $\mathbf{P} = \begin{bmatrix} 1 & 1 \\ 1 & 4 \end{bmatrix}$ and $\rho = 1$.

Définition 1.5 (Projection of an ellipsoid)

Here, what we mean by projection of an ellipsoid is the computation of upper and lower bounds of an ellipsoid. The projection of an ellipsoid is the hypercube which includes this ellipsoid, it

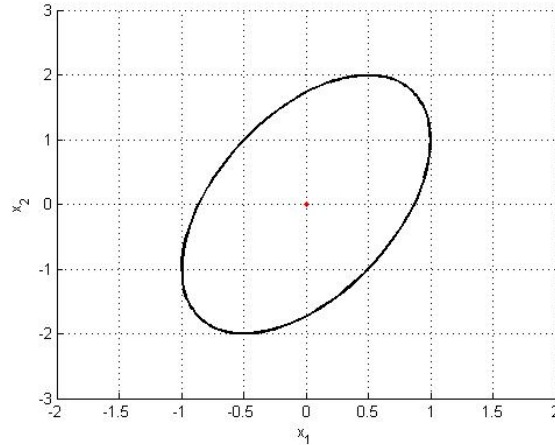


Figure 1.6: Ellipsoidal set

corresponds to the box which its extreme values are the projection on the orthogonal coordinates of the ellipsoidal. As stated in [KV96], the projection of an ellipsoid Ψ can be obtained as follows:

$$\begin{cases} \mathcal{F}(\Psi)_u = c + \text{diag} \left(\left(\frac{\mathbf{P}}{\rho} \right)^{-1/2} \right) \\ \mathcal{F}(\Psi)_l = c - \text{diag} \left(\left(\frac{\mathbf{P}}{\rho} \right)^{-1/2} \right), \end{cases} \quad (1.40)$$

where $\mathcal{F}(\Psi)_u$ and $\mathcal{F}(\Psi)_l$ are the upper and the lower bounds respectively. The notation $\text{diag}(\mathbf{M})$ corresponds to the diagonal elements of the matrix \mathbf{M} .

Remark

In this thesis in particular, we note that for any symmetric positive definite matrix $\mathbf{M} \in \mathbb{R}^{n \times n}$, the matrix $\mathbf{M}^{-1/2}$ is the *elementwise* square-roots of the matrix \mathbf{M}^{-1} .

Example 1.4

Let's go back to the previous example where $c = [0 \ 0]^T$, $\mathbf{P} = \begin{bmatrix} 1 & 1 \\ 1 & 4 \end{bmatrix}$ and $\rho = 1$. The projection of the ellipsoid $\Psi = \{x \in \mathbb{R}^n : (x - c)^T \mathbf{P}(x - c) \leq \rho\}$ is given as follows:

$$\begin{cases} \mathcal{F}(\Psi)_u = c + \text{diag} \left(\left(\frac{\mathbf{P}}{\rho} \right)^{-1/2} \right) = \begin{bmatrix} 1 \\ 2 \end{bmatrix} \\ \mathcal{F}(\Psi)_l = c - \text{diag} \left(\left(\frac{\mathbf{P}}{\rho} \right)^{-1/2} \right) = \begin{bmatrix} -1 \\ -2 \end{bmatrix} \end{cases} \quad (1.41)$$

The Figure (1.7) illustrates the projection of the ellipsoidal set, where the red lines represent the lower bounds and the green lines represent the upper bounds of the ellipsoidal set.

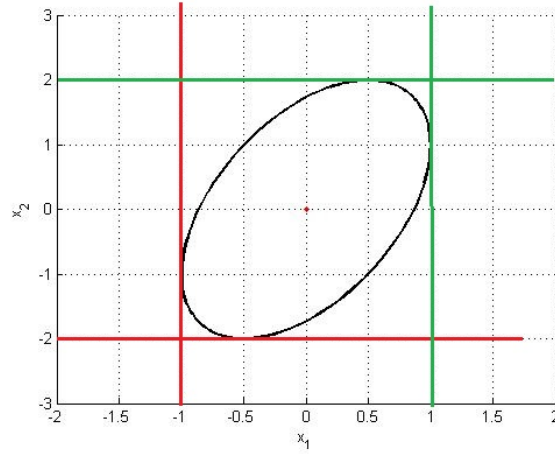


Figure 1.7: Projection of an ellipsoidal set.

1.3.2 Polyhedral sets

The polyhedral set is one of the geometrical forms often used in control and estimation problems. A polyhedral set can be bounded or not, a bounded polyhedral set is called a polytope. There exists two ways to represent geometrically a polyhedral set: (i) half-space representation (definition 1.6), (ii) vertex representation (definition 1.7).

Définition 1.6 (Half-space representation)

A polyhedral set $\mathcal{P} \in \mathbb{R}^n$ can be represented as the intersection of a finite number of closed half-spaces as follows

$$\mathcal{P} = \{x \in \mathbb{R}^n : Ax \leq b\} \quad A \in \mathbb{R}^{m \times n}, \quad b \in \mathbb{R}^m \quad (1.42)$$

In figure (1.8), the half-space representation of a polyhedral set defined by (1.42) where :

$$A = \begin{pmatrix} -1 & 0 \\ 0 & -1 \\ 1 & 1 \\ -1 & 1 \end{pmatrix} \quad \text{and} \quad b = \begin{pmatrix} 1 \\ 1 \\ 1 \\ 1 \end{pmatrix}$$

Définition 1.7 (Vertex representation)

A polyhedral set can be represented using its vertices $\mathcal{V} = \{v_1, v_2, v_3, \dots, v_n\} \in \mathbb{R}^n$. Then, a polytope \mathcal{P} can be defined as the convex hull of the set \mathcal{V}

$$\mathcal{P} = \text{conv}(\mathcal{V}) = \{\alpha_1 v_1, \alpha_2 v_2, \dots, \alpha_n v_n\} \quad (1.43)$$

where α_i are positive scalars and $0 < \alpha_i < 1$, $\sum_{i=1}^n \alpha_i = 1$.

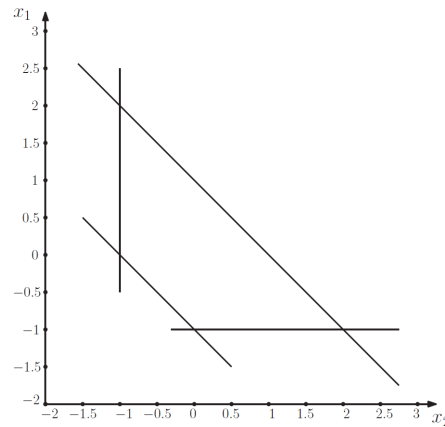


Figure 1.8: Half space representation of a polytope

For example, the Figure (1.9) shows the vertex representation a polytope defined by $\mathcal{V} = \left\{ \begin{pmatrix} 0 \\ -1 \end{pmatrix}, \begin{pmatrix} 0 \\ 2 \end{pmatrix}, \begin{pmatrix} 1.5 \\ 1.5 \end{pmatrix}, \begin{pmatrix} 2 \\ 0.5 \end{pmatrix} \right\}$.

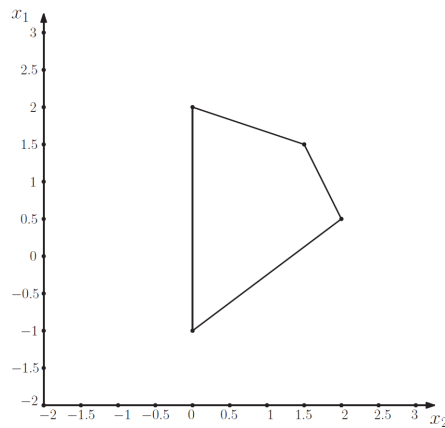


Figure 1.9: Vertex representation of a polytope.

The choice of the polyhedral set representation depends on the context of the problem.

1.3.3 Polyhedral mRPI set computation

Since the theory of Lyapunov has been introduced, the notion of invariant set has been used in many problems concerning the analysis and control of dynamic systems. An important motivation for introducing the invariant sets was the need to analyze the influence of uncertainties on dynamic systems [BM08].

Invariant set is one of the very important tools employed in control system design [Bla99]. In fact, invariant sets are very advantageous because they are defined by the property that

any trajectory starting in such a set will remain in it in the future.

The concept of minimal Robustly Positive Invariant sets (mRPI sets) is a very strong concept used in control, because mRPI sets provide an exact information about the behavior of systems. In practice, it is difficult to compute exactly the mRPI set, except for restrictive classes of systems. In general mRPI sets are approximated, in fact there exists in the literature a number of approaches allowing to characterize the mRPI set for discrete-time linear systems, see for instance [Ola+09] [Ola+10]. Recently [Mar15] proposed an approach to characterize the mRPI set for discrete-time linear systems assumed to be stable with unknown but bounded disturbances. The approach is based on the computation of "ellipsoidal" invariant sets which are obtained by using the Bounded Real Lemma, After that, a **RPI** outer-approximation of the minimal "polyhedral" **RPI** set for the system is obtained by applying a shrinking process.

In the rest of this Section we will summarize the mRPI sets computation method presented in [Mar15].

Let's consider a discrete-time linear system

$$\mathbf{x}_{k+1} = \mathbf{A}\mathbf{x}_k + \mathbf{E}\mathbf{w}_k \quad (1.44)$$

where $\mathbf{x}_k \in \mathbb{R}^n$ is the current state vector and $\mathbf{w}_k \in \mathbb{R}^m$ is an unknown disturbance vector which can be bounded as follow: $|\mathbf{w}_k| \leq \bar{\mathbf{w}}$ where $\bar{\mathbf{w}} = \sup\{|\mathbf{w}|\}$. One assume that the eigenvalues of $\mathbf{A} \in \mathbb{R}^{n \times n}$ are inside the unit circle.

1.3.3.1 Computing an ellipsoidal RPI set

To compute an RPI set for the system 1.44, we use the Lyapunov theory (see for instance [Bla99]). Let's consider a Lyapunov function $V(\mathbf{x})$ of the system (1.44):

$$V(\mathbf{x}_k) = \mathbf{x}_k^T \mathbf{P} \mathbf{x}_k \geq 0 \quad (1.45)$$

Suppose there exists a positive definite matrix $\mathbf{P} = \mathbf{P}^T > 0$ and a scalar $\gamma > 0$ verifying the following dissipation inequality (Bounded Real Lemma):

$$V(\mathbf{x}_k) - V(\mathbf{x}_{k+1}) \leq \gamma^2 \mathbf{w}_k^T \mathbf{w}_k - \mathbf{x}_k^T \mathbf{x}_k \quad (1.46)$$

Replacing (1.45) in (1.46) and by using the dynamics (1.44), we find

$$\mathbf{x}_k^T (\mathbf{A}^T \mathbf{P} \mathbf{A} - \mathbf{P} + \mathbf{I}) \mathbf{x}_k + \mathbf{x}_k^T (\mathbf{A}^T \mathbf{P} \mathbf{E}) \mathbf{w}_k + \mathbf{w}_k^T (\mathbf{E}^T \mathbf{P} \mathbf{A}) \mathbf{x}_k + \mathbf{w}_k^T (\mathbf{E}^T \mathbf{P} \mathbf{E} - \gamma^2 \mathbf{I}) \mathbf{w}_k \leq 0 \quad (1.47)$$

The inequality (1.47) can be re-written as the following Linear Matrix Inequality (LMI):

$$\begin{pmatrix} \mathbf{x}_k \\ \mathbf{w}_k \end{pmatrix}^T \begin{pmatrix} \mathbf{A}^T \mathbf{P} \mathbf{A} - \mathbf{P} + \mathbf{I} & \mathbf{A}^T \mathbf{P} \mathbf{E} \\ \mathbf{E}^T \mathbf{P} \mathbf{A} & \mathbf{E}^T \mathbf{P} \mathbf{E} - \gamma^2 \mathbf{I} \end{pmatrix} \begin{pmatrix} \mathbf{x}_k \\ \mathbf{w}_k \end{pmatrix} \leq 0 \quad (1.48)$$

Before, let's remind the principle of Schur complement

Définition 1.8

Schur complement [Boy+94]. Consider the following LMI:

$$\begin{bmatrix} \mathbf{Q}(x) & \mathbf{S}(x) \\ \mathbf{S}^T(x) & \mathbf{R}(x) \end{bmatrix} \succ 0, \quad (1.49)$$

where $\mathbf{Q}(x)$, $\mathbf{R}(x)$ are symmetric matrices and $\mathbf{Q}(x)$, $\mathbf{R}(x)$ and $\mathbf{S}(x)$ are affine in x . Then this LMI is equivalent to:

$$\begin{cases} \mathbf{Q}(x) \succ 0, \\ \mathbf{Q}(x) - \mathbf{S}(x)\mathbf{R}^{-1}(x)\mathbf{S}^T(x) \succ 0, \end{cases} \quad (1.50)$$

or

$$\begin{cases} \mathbf{R}(x) \succ 0, \\ \mathbf{R}(x) - \mathbf{S}^T(x)\mathbf{Q}^{-1}(x)\mathbf{S}(x) \succ 0. \end{cases} \quad (1.51)$$

Thus, using the Schur complement, the equation (1.48) can be expressed as follows

$$\mathbf{A}^T\mathbf{P}\mathbf{A} - \mathbf{P} + \mathbf{I} - \mathbf{A}^T\mathbf{P}\mathbf{E}(\mathbf{E}^T\mathbf{P}\mathbf{E} - \gamma^2\mathbf{I})^{-1}\mathbf{E}^T\mathbf{P}\mathbf{A} \leq 0 \quad (1.52)$$

Knowing that $\mathbf{w}^T\mathbf{w} \leq \overline{\mathbf{w}}^T\overline{\mathbf{w}}$, from the dissipation inequality (1.46) we get:

$$V(\mathbf{x}_k) - V(\mathbf{x}_{k+1}) \leq \gamma^2\overline{\mathbf{w}}^T\overline{\mathbf{w}} - \mathbf{x}^T\mathbf{x} \quad (1.53)$$

Let's consider a ball

$$B_w = \{\mathbf{x} \in \mathbb{R}^n : \mathbf{x}^T\mathbf{x} \leq \gamma^2\overline{\mathbf{w}}^T\overline{\mathbf{w}}\} \quad (1.54)$$

If $\mathbf{x}^T\mathbf{x} \geq \gamma^2\overline{\mathbf{w}}^T\overline{\mathbf{w}}$, then outside the ball B_w the increment of the Lyapunov function is negative, which implies that a level set of the Lyapunov function $\Omega_c = \{\mathbf{x} : V(\mathbf{x}) = \mathbf{x}^T\mathbf{P}\mathbf{x} \leq \gamma^2\overline{\mathbf{w}}^T\overline{\mathbf{w}}\}$ that contains the set B_w is an attractive invariant set.

We put $r^2 = \gamma^2\overline{\mathbf{w}}^T\overline{\mathbf{w}}$. Since $\mathbf{x}^T\mathbf{x} \leq r^2 \implies \mathbf{x}^T\mathbf{P}\mathbf{x} \leq \lambda_{max}(\mathbf{P})r^2$ which means that the set Ω_c contains the ball B_r where $B_r = \{\mathbf{x} : \mathbf{x}^T\mathbf{x} \leq r^2\}$, this implies that the ellipsoidal set Ψ :

$$\Psi = \{\mathbf{x} \in \mathbb{R}^n : \mathbf{x}^T\mathbf{P}\mathbf{x} \leq \lambda_{max}(\mathbf{P})\gamma^2\overline{\mathbf{w}}^T\overline{\mathbf{w}}\} \quad (1.55)$$

contains the ball B_w and we can deduct that the ellipsoidal set Ψ is an attractive invariant set.

1.3.3.2 Polyhedral RPI sets from Ellipsoidal RPI sets

Once an ellipsoidal RPI set of the system 1.44 is computed, for a computational considerations we are interested to compute polyhedral RPI sets from ellipsoidal ones. to do that we proceed as follows:

A polyhedral RPI set Φ_v with v vertices is computed, using the fact that if Φ_v is between the initial RPI set $\bar{\Psi}$ and its one-step ahead RPI set $\bar{\Psi}^+$ then Φ_v is an RPI set.

$$\bar{\Psi}^+ \subseteq \Phi_v \subseteq \bar{\Psi} \quad (1.56)$$

An interesting method to compute a polyhedral set, which verifies the inclusion condition (1.56), is proposed in [Ale+07]. Here, it is possible to use the invariant set (1.55) to compute an ellipsoidal set $\bar{\Psi}$ as follows:

$$\bar{\Psi} = \{\mathbf{x} \in \mathbb{R}^n : \mathbf{x}^T \mathbf{P} \mathbf{x} \leq \lambda_{max}(\mathbf{P}) \gamma^2 \mu \bar{\mathbf{w}}^T \bar{\mathbf{w}}\} \quad (1.57)$$

For a given $\mu \geq 1$, using (1.53) we can compute the one-step ahead ellipsoidal RPI set:

$$\bar{\Psi}^+ = \{\mathbf{x} \in \mathbb{R}^n : \mathbf{x}^T \mathbf{P} \mathbf{x} \leq (\mu \lambda_{max}(\mathbf{P}) - \mu + 1) \gamma^2 \bar{\mathbf{w}}^T \bar{\mathbf{w}}\} \quad (1.58)$$

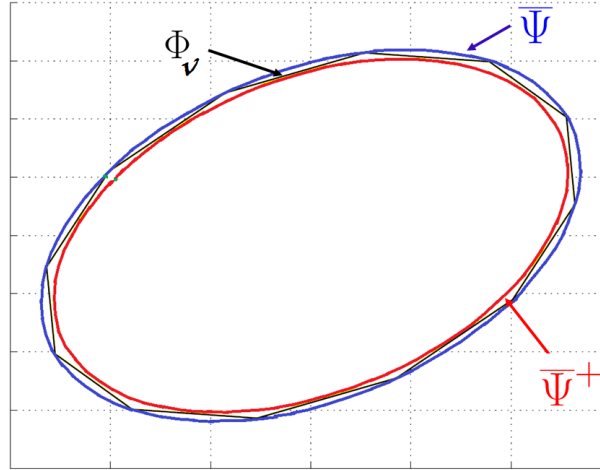


Figure 1.10: Computation of polyhedral RPI set from ellipsoidal ones

1.3.3.3 Shrinking polyhedral RPI sets

We assume that $\forall k \geq 0, \mathbf{w}_k \in \Delta$. A sequence of polyhedral RPI sets can be recursively built starting with an initial invariant set Φ_v as follows:

$$\Phi_{k+1} = \mathbf{A} \Phi_k \oplus \mathbf{E} \Delta, \quad \Phi_0 = \Phi_v \quad (1.59)$$

where \oplus is the Minkowski sum of sets, Φ_{k+1} corresponds to the image of Φ_k . Φ_{k+1} corresponds to a new RPI set included into the initial RPI set. Since the set Φ_0 is a contractive invariant, we can conclude that for any iteration k the following relation is verified:

$$\Omega_\infty \subseteq \Phi_{k+1} \subseteq \Phi_k \subseteq \Phi_0 \quad (1.60)$$

if $k \rightarrow \infty$ then $\Phi_k \rightarrow \Omega_\infty$. Ω_∞ is the exact mRPI set for (1.44).

To simplify the computation, the recursion (1.59) can be written as follows:

$$\Phi_k = \mathbf{A}^k \Phi_0 \oplus \left(\sum_{i=1}^k \mathbf{A}^{i-1} \right) \mathbf{E} \Delta, \quad \Phi_0 = \Phi_v \quad (1.61)$$

Putting $\Omega_k = \left(\sum_{i=1}^k \mathbf{A}^{i-1} \right) \mathbf{E} \Delta$, and taken the fact that

$$\Omega_\infty = \lim_{k \rightarrow +\infty} \Omega_k = \sum_{i=1}^{\infty} \mathbf{A}^{i-1} \mathbf{E} \Delta \oplus \Omega_k \quad (1.62)$$

$$\Omega_\infty = \lim_{k \rightarrow +\infty} \Omega_k = \left(\sum_{i=k+1}^{\infty} \mathbf{A}^{i-1} \right) \mathbf{E} \Delta \oplus \Omega_k \quad (1.63)$$

We conclude that

$$\Omega_k \subset \Omega_\infty \quad (1.64)$$

Using the equations (1.61) and (1.62) we have:

$$\Phi_k = \mathbf{A}^k \Phi_0 \oplus \Omega_k \subset \mathbf{A}^k \Phi_0 \oplus \Omega_\infty \quad (1.65)$$

Since the eigenvalues of \mathbf{A} are strictly inside the unit circle then $\lim_{k \rightarrow +\infty} \mathbf{A}^k \Phi_0 = 0$, we can conclude that the set Ω_∞ is the smallest RPI set for the dynamic system (1.44).

Note that the recursion (1.59) can be stopped when there exists k^* such that

$$\mathbf{A}^{k^*} \Phi_0 \subseteq \mathbb{B}^n(\epsilon) \quad (1.66)$$

For a given ball $\mathbb{B}^n(\epsilon) = \{\mathbf{x} \in \mathbb{R}^n : \mathbf{x}^T \mathbf{x} \leq \epsilon\}$.

The stopping condition (1.66) can not be evaluated easily because of the unknown size of the set $\mathbf{A}^{k^*} \Phi_0$. So, we can use the bound of this set as follows:

$$\mathbf{A}^{k^*} \Phi_0 \subseteq \rho(k^*) \Phi_0 \quad (1.67)$$

Then, the stop criteria if the recursion (1.59) becomes

$$\rho(k^*) \Phi_0 \subseteq \mathbb{B}^n(\epsilon) \quad (1.68)$$

where $\rho(k) = \beta^k$, with $0 < \beta < 1$ is a scalar satisfying the following inequality:

$$\mathbf{A}^T \mathbf{P} \mathbf{A} - \beta^2 \mathbf{P} \leq 0 \quad (1.69)$$

Remind that the matrix \mathbf{P} is the one obtained by solving the LMI (1.48). Using the equation (1.65), we conclude that the set Φ_{k^*} is an outer approximation of the mRPI set with a precision $\mathbb{B}^n(\epsilon)$.

1.3.3.4 Shrinking Index

It is more interesting to measure the relative error of the outer-approximation of the mRPI set Φ_{k^*} with respect to the theoretical mRPI set Ω_∞ . To do this we introduce a relative shrinking index to estimate this relative error.

Consider that there exists a constant $\mu \geq 1$ such that the mRPI set Ω_∞ is included in the ball B_w :

$$B_w = \{\mathbf{x} \in \mathbb{R}^n : \mathbf{x}^T \mathbf{x} \leq \mu \gamma^2 \bar{\mathbf{w}}^T \bar{\mathbf{w}}\} \quad (1.70)$$

We can estimate the upper-bound of the outer-approximation error, at any iteration $k > 0$ and for a given initial RPI set $\Phi_0 = \Phi_v$ verifying the inclusion condition (1.56) :

$$\beta^k \Phi_v \subset \beta^k \sqrt{\frac{\mu \lambda_{max}(\mathbf{P})}{\lambda_{min}(\mathbf{P})}} \Omega_\infty \quad (1.71)$$

The term $\bar{\rho}_k$ defined as follow, represents the shrinking index that characterizes the precision of the mRPI outer-approximation:

$$\bar{\rho}_k = \beta^k \sqrt{\frac{\mu \lambda_{max}(\mathbf{P})}{\lambda_{min}(\mathbf{P})}} \quad (1.72)$$

We can summarize the procedure of computing an outer approximation of mRPI set in the following algorithm:

Algorithm 1 Computation of the outer-approximation of the mRPI set

Require: Matrices $\mathbf{A}, \mathbf{E}, \Delta$. The desired precision ϵ .

- 1: Find matrix \mathbf{P} and the minimum γ satisfying the LMI (1.48)
 - 2: Compute the polyhedral RPI Φ_v satisfying the inclusion condition (1.56).
 - 3: Set $k = 0$.
 - 4: Set $\Phi_0 = \Phi_v$
 - 5: **repeat**.
 - 6: Increment k by 1.
 - 7: Compute Φ_k using the equation (1.59).
 - 8: Until the condition (1.66) is satisfied.
 - 9: **return** The mRPI set approximation Φ_{k^*} .
-

Example 1.5

Let us consider the following stable discrete-time linear system,

$$\mathbf{x}_{k+1} = \begin{pmatrix} 0.2 & 0.2 \\ -0.2 & 0.5 \end{pmatrix} \mathbf{x}_k + \begin{pmatrix} 0 \\ 1 \end{pmatrix} \mathbf{w}_k \quad (1.73)$$

The state disturbance is assumed completely unknown but bounded $\forall k, \|\mathbf{w}_k\| \leq 1$. By solving the LMI (1.48) we obtain the minimum $\gamma = 1.8741$ and the positive matrix

$$\mathbf{P} = \begin{pmatrix} 3.0264 & -0.9271 \\ -0.9271 & 2.1636 \end{pmatrix}$$

In the Figure (1.11), the blue and red ellipsoids show the initial RPI set $\bar{\Psi}$ and its one-step ahead RPI set $\bar{\Psi}^+$ respectively. The polyhedral RPI set Φ_v satisfying the inclusion condition (1.56) is depicted in black, it has 12 vertices.

The figure (1.11) illustrates the shrinking process starting by the initial polyhedral RPI set $\Phi_0 = \Phi_v$ according to the dynamics (1.59), the shrinking process is stopped at $k^* = 8$ to guarantee that the outer estimation of the mRPI set is achieved with a shrinking index $\bar{\rho}_k \leq 4.4e^{-3}$ (with $\beta = 0.473$ and $\epsilon = 4.4e^{-3}$). The outer-approximation of the mRPI set Φ_{k^*} is represented by the green polyhedron.

The Figure (1.12) represents the shrinking index, as a function of the number of iterations.

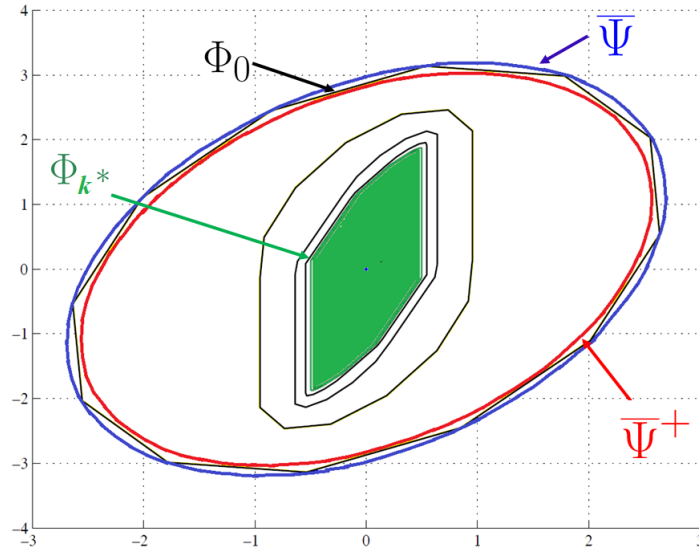


Figure 1.11: Shrinking an initial polyhedral RPI set Φ_0 to get an RPI outer-approximation Φ_{k^*} of the mRPI

1.4 Conclusion

This chapter has been devoted to introduce the basic notions and principles on which the contributions of this thesis are based on. First, several basic definitions and properties about interval analysis are addressed. We highlighted the importance of using intervals and also the main problems encountered while manipulating the intervals such as dependency phenomena and wrapping effect. Secondly, some definitions and properties of ellipsoidal set are addressed.

In addition, we have introduced, the definition of invariant sets and illustrated an algorithm for computing approximations of the minimal Robustly Positive Invariant set for discrete-time linear systems. The algorithm is based on the computation of invariant sets using the Bounded Real Lemma and a suitable shrinking procedure.

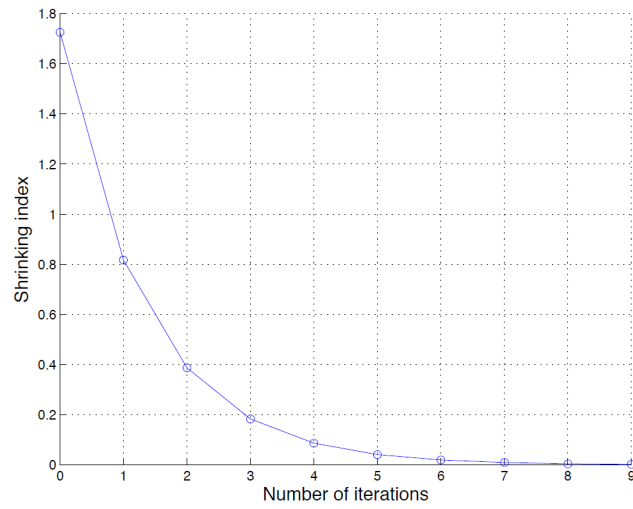


Figure 1.12: Shrinking index with respect to the number of iterations k

The next chapter focuses on the design of a set-membership observer design based on ellipsoidal RPI sets for discrete-time linear systems.

Observers based on ellipsoidal invariant sets for linear systems

Contents

2.1	Introduction	39
2.2	Problem statement	41
2.3	Set-membership observer design	42
2.3.1	H_∞ Observer gain design	43
2.3.2	Computing ellipsoidal RPI sets	44
2.3.3	Shrinking of ellipsoidal RPI sets	46
2.3.4	Characterizing the evolution of the RPI sets	49
2.4	The set-membership observer implementation	51
2.5	A numerical example	52
2.6	Conclusion	54

2.1 Introduction

The concept of set invariance has already applied to design state observers. The work presented in [DP05] proposes a state observer based on polyhedral invariant sets for discrete-time linear systems subject to unknown but bounded persistent disturbances and measurement noise, it has been shown that the estimation error can be forced to remain inside a polyhedral set by means of a suitable output injection. Recently, [TLW17] proposed a robust actuator fault estimation approach for dynamic systems combining the unknown input observer and the invariant sets. These approaches characterize only a unique invariant set, non necessarily the minimal RPI set, and does not characterize its possible evolution for any time-instant.

It is of great interest to design set invariant based observers with low complexity and less computational cost and making possible the characterization of the state bounds over the whole time horizon. This will be the core idea of this chapter and one of the main contributions of this thesis.

In this chapter, we explore the concept of Robustly Positive Invariant (RPI) sets to design a set-membership observer for discrete-time linear systems perturbed by unknown but bounded

disturbances. In particular, we explore the use of RPI sets with ellipsoidal form to frame the estimation error. We use the ellipsoidal invariant sets for two main reasons:

1. Invariant sets allow to provide state bounds in a deterministic and guaranteed way, while keeping the invariance property;
2. Ellipsoidal sets have an interesting geometry which make them easy to manipulate, the characteristics of ellipsoidal sets can be exploited to obtain more simple implementable solutions.

The proposed set-membership observer provides deterministic state bounds that are build as the sum of the punctual estimated system states and its corresponding estimation errors bounds. The design of the proposed observer is based on the solutions of a few number of Linear Matrix Inequalities that are suitable modified to provide both the observer gain and ellipsoidal RPI sets. The obtained RPI sets are used to frame the estimation error in a very simple and accurate way. The observer synthesis process can includes an *a posteriori* steady-state covariance matrix for the estimation errors. This covariance matrix is used to enhance the precision on the computation of the estimation error bounds and to obtain less conservative dissipation inequality used in the Bounded real lemma formulation.

Some of the most important advantages of the proposed observer are:

- ✓ The proposed approach is based on an explicit solution of the estimation-bounding problem, this allow to reduce the on-line computation costs compared to set-membership observers that exist in literature ;
- ✓ For an n -order systems, the order of set-membership observer is reduced to $n+1$ instead of $2n$ order in the case of interval observers. This allows to implement this observer for high order systems in industrial applications;
- ✓ The set-membership observer design can be considered as an extension of the H_∞ observer synthesis, this facilitate its eligibility for solving engineering problems ;
- ✓ The observer design require as data problem the knowledge of only the bounds of the disturbance. Moreover, the observer design could include additional information about the disturbance nature. Here, we propose to use the variance of the disturbance together with their bounds to design the observer ;
- ✓ The proposed approach allows us to combine computation of stochastic sets (based on the information about the disturbance variance) together with the computation of deterministic sets (based on the knowledge of the disturbance bounds);
- ✓ The proposed observer is very simple and easy to implement compared to set-membership observers available in the literature, since it uses a simple explicit solution for computing the estimation error bounds.

This chapter is organized as follows: Section 2.2 presents the class of linear systems used in this chapter and formulates the state estimation problem. The design of the proposed observer is presented in the Section 2.3, this section is divided into four subsections: a first subsection dedicated to H_∞ observer gain design, a second subsection devoted to computing ellipsoidal RPI sets, the third and fourth subsections are dedicated to characterize the evolution of the ellipsoidal RPI sets. Section 2.4 is then dedicated to the observer implementation. A numerical example is studied in order to show the performance of the proposed observer. This chapter ends with a conclusion.

2.2 Problem statement

The class of systems addressed in this chapter is that of discrete-time linear systems assumed to be perturbed by unknown but bounded disturbances:

$$\begin{cases} \mathbf{x}_{k+1} = \mathbf{A}\mathbf{x}_k + \mathbf{B}\mathbf{u}_k + \mathbf{F}\mathbf{d}_k \\ \mathbf{y}_k = \mathbf{C}\mathbf{x}_k + \mathbf{Z}\mathbf{v}_k \end{cases} \quad (2.1)$$

where $\mathbf{x}_k \in \mathbb{R}^n$ is the state vector, $\mathbf{u}_k \in \mathbb{R}^{n_u}$ is the input vector and $\mathbf{y}_k \in \mathbb{R}^{n_y}$ is the measured output vector. The vectors $\mathbf{d}_k \in \mathbb{R}^{n_d}$ and $\mathbf{v}_k \in \mathbb{R}^{n_v}$ are unknown state disturbances and unknown measurement noises, respectively. The vector of total disturbances regrouping state disturbances and measurement noise, i.e. $[\mathbf{d}_k \ \mathbf{v}_k]^T$, is assumed to belong to a bounded set which includes the zero, even if this assumption is not satisfied an appropriate translation can be used. The matrices $\mathbf{A}, \mathbf{B}, \mathbf{F}, \mathbf{C}, \mathbf{Z}$ have appropriated dimensions. We assume that the pair (\mathbf{A}, \mathbf{C}) is observable. The considered problem is to compute at each time-instant the state bounds containing, in a guaranteed way, all possible state vectors of the system (2.1).

Suppose one can design a Luenberger observer:

$$\hat{\mathbf{x}}_{k+1} = (\mathbf{A} - \mathbf{L}\mathbf{C})\hat{\mathbf{x}}_k + \mathbf{B}\mathbf{u}_k + \mathbf{L}\mathbf{y}_k \quad (2.2)$$

where $\hat{\mathbf{x}}_k$ is the state estimation vector and \mathbf{L} is the observer gain matrix that assures the Schur stability of the matrix $(\mathbf{A} - \mathbf{L}\mathbf{C})$.

The estimation error at a given instant k can be defined as follows:

$$\mathbf{e}_k := \mathbf{x}_k - \hat{\mathbf{x}}_k \quad (2.3)$$

From (2.1) and (2.2) one can obtain the dynamics of the estimation error as follows:

$$\mathbf{e}_{k+1} = \mathbf{A}_o\mathbf{e}_k + \mathbf{E}\mathbf{w}_k \quad (2.4)$$

where $\mathbf{A}_o = (\mathbf{A} - \mathbf{L}\mathbf{C})$, $\mathbf{E} = [\mathbf{F} \quad -\mathbf{L}\mathbf{Z}]$ and $\mathbf{w}_k \in \mathbb{R}^m$, defined as $\mathbf{w}_k := \begin{pmatrix} \mathbf{d}_k \\ \mathbf{v}_k \end{pmatrix}$.

From the equation (2.4), we notice that on one hand, the observer gain \mathbf{L} assures the stability of estimation error dynamics and on another hand, the observer gain intervenes on the

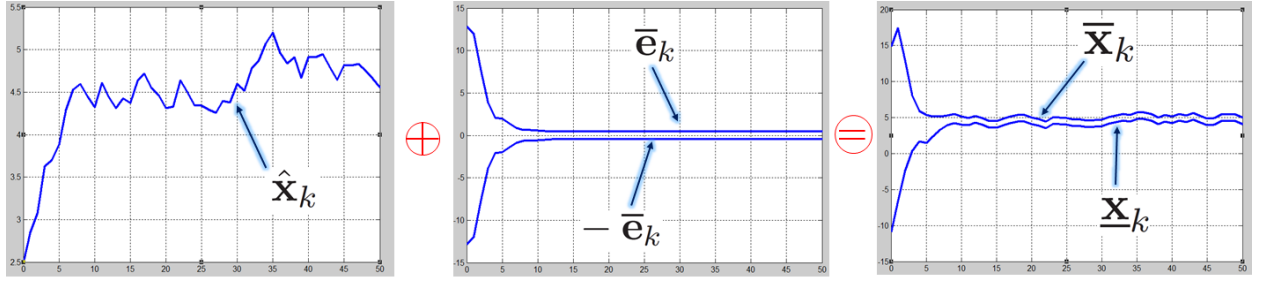


Figure 2.1: Principle of the proposed approach

amplification or on the attenuation of the disturbances \mathbf{w}_k . Hence, the choice of an adequate gain is paramount to solve the trade-off between convergence speed and error amplification.

Let's assume that the estimation error is bounded and the bound of the estimation error, denoted $\bar{\mathbf{e}}_k$ is known. At each time-instant, the real state vector is included between a lower and upper bounds defined as follows:

$$\hat{\mathbf{x}}_k - \bar{\mathbf{e}}_k \leq \mathbf{x}_k \leq \hat{\mathbf{x}}_k + \bar{\mathbf{e}}_k \quad (2.5)$$

In other words, at every time-instant we can guarantee that the system state belongs to a set defined by the vectors $\underline{\mathbf{x}}_k := \hat{\mathbf{x}}_k - \bar{\mathbf{e}}_k$ and $\bar{\mathbf{x}}_k := \hat{\mathbf{x}}_k + \bar{\mathbf{e}}_k$ i.e:

$$\underline{\mathbf{x}}_k \leq \mathbf{x}_k \leq \bar{\mathbf{x}}_k \quad (2.6)$$

In this case, a set-membership observer could be implemented as follows:

$$\hat{\mathbf{x}}_{k+1} = (\mathbf{A} - \mathbf{LC})\hat{\mathbf{x}}_k + \mathbf{B}\mathbf{u}_k + \mathbf{L}y_k \quad (2.7)$$

$$\bar{\mathbf{x}}_k = \hat{\mathbf{x}}_k + \bar{\mathbf{e}}_k \quad (2.8)$$

$$\underline{\mathbf{x}}_k = \hat{\mathbf{x}}_k - \bar{\mathbf{e}}_k \quad (2.9)$$

The set-membership state estimation can be reduced to a computation of the vectors $\bar{\mathbf{x}}_k$ and $\underline{\mathbf{x}}_k$ as the sum the estimation state $\hat{\mathbf{x}}_k$ and a bound of the estimation error $\bar{\mathbf{e}}_k$ and $-\bar{\mathbf{e}}_k$, respectively. The principle of the proposed approach is illustrated in Figure (2.1). The first part of the proposed set-membership observer (2.7) which provides the punctual state estimation $\hat{\mathbf{x}}$ can be designed like any other punctual observer, where the gain \mathbf{L} is computed such that $(\mathbf{A} - \mathbf{LC})$ is Schur stable.

In (2.8) and (2.9), computing the state bounds $\bar{\mathbf{x}}_k$ (respectively $\underline{\mathbf{x}}_k$) returns to compute the error bound $\bar{\mathbf{e}}_k$. To do that we propose a new method based on the computation of ellipsoidal Robustly Positive Invariant (RPI) sets. Such sets are used to compute suitable deterministic bounds of the estimation error \mathbf{e}_k .

2.3 Set-membership observer design

In this Section, we will describe the proposed method for:

- Computing the observer gain \mathbf{L} by using an H_∞ design approach.
- Characterizing the evolution of the estimation error bounds by using RPI sets.

2.3.1 H_∞ Observer gain design

Proposition 2.1

Consider the system (2.1). The observer gain \mathbf{L} , allowing to attenuate the effect of the disturbances on the estimation error (i.e the H_∞ norm of the system (2.4) is lower than $\gamma > 0$), exists if there exists a symmetric positive definite matrix \mathbf{P} and a matrix \mathbf{U} satisfying the following LMI (with dimension $m = n_d + n_v$):

$$\begin{pmatrix} -\mathbf{P} + \mathbf{I}_n & 0_{n \times m} & \mathbf{A}^T \mathbf{P} - \mathbf{C}^T \mathbf{U}^T \\ 0_{m \times n} & -\gamma^2 \mathbf{I}_m & [\mathbf{P}\mathbf{F} \quad -\mathbf{U}\mathbf{Z}]^T \\ \mathbf{P}\mathbf{A} - \mathbf{U}\mathbf{C} & [\mathbf{P}\mathbf{F} \quad -\mathbf{U}\mathbf{Z}] & -\mathbf{P} \end{pmatrix} \preceq 0 \quad (2.10)$$

Moreover, the observer gain \mathbf{L} will be:

$$\mathbf{L} = \mathbf{P}^{-1} \mathbf{U} \quad (2.11)$$

Proof. Consider the estimation error dynamics (2.4). An H_∞ observer is intended to attenuate the effect of the system's disturbances \mathbf{w}_k on the estimation error \mathbf{e}_k .

$$\min_{\mathbf{L} \in \mathbb{R}^{n_x \times n_y}} \gamma^2 \quad \text{subject to} \quad \frac{\|\mathbf{e}_k\|_2^2}{\|\mathbf{w}_k\|_2^2} \leq \gamma^2 \quad (2.12)$$

Let's consider a Lyapunov function $\mathbf{V}(\mathbf{e}_k) = \mathbf{e}_k^T \mathbf{P} \mathbf{e}_k$ of the system (2.4) where \mathbf{P} is a symmetric positive definite matrix and γ a positive scalar verifying the following *dissipation* inequality:

$$\mathbf{V}(\mathbf{e}_{k+1}) - \mathbf{V}(\mathbf{e}_k) \leq -\mathbf{e}_k^T \mathbf{e}_k + \gamma^2 \mathbf{w}_k^T \mathbf{w}_k \quad (2.13)$$

then

$$\mathbf{e}_{k+1}^T \mathbf{P} \mathbf{e}_{k+1} - \mathbf{e}_k^T \mathbf{P} \mathbf{e}_k + \mathbf{e}_k^T \mathbf{e}_k - \gamma^2 \mathbf{w}_k^T \mathbf{w}_k \leq 0 \quad (2.14)$$

we replace (2.4) in (2.14) we obtain

$$(\mathbf{A}_o \mathbf{e}_k + \mathbf{E} \mathbf{w}_k)^T \mathbf{P} (\mathbf{A}_o \mathbf{e}_k + \mathbf{E} \mathbf{w}_k) - \mathbf{e}_k^T \mathbf{P} \mathbf{e}_k + \mathbf{e}_k^T \mathbf{e}_k - \gamma^2 \mathbf{w}_k^T \mathbf{w}_k \leq 0 \quad (2.15)$$

$$\mathbf{e}_k^T (\mathbf{A}_o^T \mathbf{P} \mathbf{A}_o - \mathbf{P} + \mathbf{I}_n) \mathbf{e}_k + \mathbf{e}_k^T (\mathbf{A}_o^T \mathbf{P} \mathbf{E}) \mathbf{w}_k + \mathbf{w}_k^T (\mathbf{E}^T \mathbf{P} \mathbf{A}_o) \mathbf{e}_k + \mathbf{w}_k^T (\mathbf{E}^T \mathbf{P} \mathbf{E} - \gamma^2 \mathbf{I}_m) \mathbf{w}_k \leq 0 \quad (2.16)$$

$$\begin{pmatrix} \mathbf{e}_k \\ \mathbf{w}_k \end{pmatrix}^T \begin{pmatrix} \mathbf{A}_o^T \mathbf{P} \mathbf{A}_o - \mathbf{P} + \mathbf{I}_n & \mathbf{A}_o^T \mathbf{P} \mathbf{E} \\ \mathbf{E}^T \mathbf{P} \mathbf{A}_o & \mathbf{E}^T \mathbf{P} \mathbf{E} - \gamma^2 \mathbf{I}_m \end{pmatrix} \begin{pmatrix} \mathbf{e}_k \\ \mathbf{w}_k \end{pmatrix} \leq 0 \quad (2.17)$$

The gain \mathbf{L} intervenes implicitly in the previous inequality because $\mathbf{A}_o = \mathbf{A} - \mathbf{L}\mathbf{C}$. To find \mathbf{L} , the matrix \mathbf{P} and the minimum scalar γ satisfying the following inequality:

$$\begin{pmatrix} \mathbf{A}_o^T \mathbf{P} \mathbf{A}_o - \mathbf{P} + \mathbf{I}_n & \mathbf{A}_o^T \mathbf{P} \mathbf{E} \\ \mathbf{E}^T \mathbf{P} \mathbf{A}_o & \mathbf{E}^T \mathbf{P} \mathbf{E} - \gamma^2 \mathbf{I}_m \end{pmatrix} \preceq 0 \quad (2.18)$$

The equation (2.18) can not be solved as an LMI because it contains non linear terms, we are going to transform it in order to obtain an LMI that can be resolved using the classical existent tools. First, one can rewrite (2.18) as follows:

$$\begin{pmatrix} -\mathbf{P} + \mathbf{I}_n & 0_{n \times m} \\ 0_{m \times n} & -\gamma^2 \mathbf{I}_m \end{pmatrix} + \begin{pmatrix} \mathbf{A}_o^T \mathbf{P} \mathbf{A}_o & \mathbf{A}_o^T \mathbf{P} \mathbf{E} \\ \mathbf{E}^T \mathbf{P} \mathbf{A}_o & \mathbf{E}^T \mathbf{P} \mathbf{E} \end{pmatrix} \preceq 0 \quad (2.19)$$

Then, we apply the Schur complement (Definition 1.8) for the inequality (2.19), we obtain:

$$\begin{pmatrix} -\mathbf{P} + \mathbf{I}_n & 0_{n \times m} & \mathbf{A}_o^T \mathbf{P} \\ 0_{m \times n} & -\gamma^2 \mathbf{I}_m & \mathbf{E}^T \mathbf{P} \\ \mathbf{P} \mathbf{A}_o & \mathbf{P} \mathbf{E} & -\mathbf{P} \end{pmatrix} \preceq 0 \quad (2.20)$$

Replacing $\mathbf{A}_o = (\mathbf{A} - \mathbf{L}\mathbf{C})$ and $\mathbf{E} = [\mathbf{F} \quad -\mathbf{L}\mathbf{Z}]$ in (2.20), we get:

$$\begin{pmatrix} -\mathbf{P} + \mathbf{I}_n & 0_{n \times m} & \mathbf{A}^T \mathbf{P} - \mathbf{C}^T \mathbf{L}^T \mathbf{P} \\ 0_{m \times n} & -\gamma^2 \mathbf{I}_m & [\mathbf{P}\mathbf{F} \quad -\mathbf{P}\mathbf{L}\mathbf{Z}]^T \\ \mathbf{P}\mathbf{A} - \mathbf{P}\mathbf{L}\mathbf{C} & [\mathbf{P}\mathbf{F} \quad -\mathbf{P}\mathbf{L}\mathbf{Z}] & -\mathbf{P} \end{pmatrix} \preceq 0 \quad (2.21)$$

by performing a suitable change of variable in (2.21), i.e. $\mathbf{U} := \mathbf{P}\mathbf{L}$, we obtain the following LMI:

$$\begin{pmatrix} -\mathbf{P} + \mathbf{I}_n & 0_{n \times m} & \mathbf{A}^T \mathbf{P} - \mathbf{C}^T \mathbf{U}^T \\ 0_{m \times n} & -\gamma^2 \mathbf{I}_m & [\mathbf{P}\mathbf{F} \quad -\mathbf{U}\mathbf{Z}]^T \\ \mathbf{P}\mathbf{A} - \mathbf{U}\mathbf{C} & [\mathbf{P}\mathbf{F} \quad -\mathbf{U}\mathbf{Z}] & -\mathbf{P} \end{pmatrix} \preceq 0 \quad (2.22)$$

Once the matrices \mathbf{P} , \mathbf{U} and the minimum scalar γ are found, the observer gain \mathbf{L} can be computed as:

$$\mathbf{L} = \mathbf{P}^{-1} \mathbf{U} \quad (2.23)$$

□

Thus, the first part of the set-membership state observer, equation (2.7), is completely defined. The problem now is to compute suitable bounds of the estimation error (i.e $\bar{\mathbf{e}}_k$) in order to implement (2.8) and (2.9). This will be the objective of the next subsection.

2.3.2 Computing ellipsoidal RPI sets

Proposition 2.2

Consider the system (2.4) with bounded disturbances $\forall k \geq 0$, $\mathbf{w}^T \mathbf{w} \leq \bar{\mathbf{w}}^T \bar{\mathbf{w}}$, where $\bar{\mathbf{w}}^T \bar{\mathbf{w}} = \sup\{\mathbf{w}^T \mathbf{w}\}$. If there exists a symmetric definite matrix \mathbf{P} and a scalar $\gamma \geq 0$ verifying the condition (2.20), then the ellipsoidal set Φ defined below is a robustly invariant set for the system (2.4):

$$\Phi := \{\mathbf{e} \in \mathbb{R}^n : \mathbf{e}^T \mathbf{P} \mathbf{e} \leq \lambda_{\max}(\mathbf{P}) \gamma^2 \bar{\mathbf{w}}^T \bar{\mathbf{w}}\} \quad (2.24)$$

where $\lambda_{\max}(\mathbf{P})$ is the maximum eigenvalue of the matrix \mathbf{P}

Furthermore, the steady-state bounds of the estimation error, denoted by $\bar{\mathbf{e}}_\infty$ can be obtained as follows:

$$\bar{\mathbf{e}}_\infty = \text{diag} \left(\left(\frac{\mathbf{P}}{\lambda_{\max}(\mathbf{P})\gamma^2\bar{\mathbf{w}}^T\bar{\mathbf{w}}} \right)^{-1/2} \right) \quad (2.25)$$

Proof. Considering that the norm-2 of the disturbances can be bounded as $\mathbf{w}^T\mathbf{w} \leq \bar{\mathbf{w}}^T\bar{\mathbf{w}}$. Then, from (2.13) we have:

$$\mathbf{V}(\mathbf{e}_{k+1}) - \mathbf{V}(\mathbf{e}_k) \leq -\mathbf{e}_k^T\mathbf{e}_k + \gamma^2\bar{\mathbf{w}}^T\bar{\mathbf{w}} \leq 0 \quad (2.26)$$

if $\mathbf{e}_k^T\mathbf{e}_k \geq \gamma^2\bar{\mathbf{w}}^T\bar{\mathbf{w}}$, that means that outside the ball

$$B_w := \{\mathbf{e}_k \in \mathbb{R}^n : \mathbf{e}_k^T\mathbf{e}_k \leq \gamma^2\bar{\mathbf{w}}^T\bar{\mathbf{w}}\} \quad (2.27)$$

the increment of the Lyapunov function, i.e. $\mathbf{V}(\mathbf{e}_{k+1}) - \mathbf{V}(\mathbf{e}_k)$, is negative, this implies that any level set of the Lyapunov function $\Omega := \{\mathbf{e} \in \mathbb{R}^n : \mathbf{e}^T\mathbf{P}\mathbf{e} \leq c\}$ that contains the ball B_w is an attractive invariant set. A value of c which guarantees that the ball B_w is included into the set Ω can be calculated as $c = \gamma^2\bar{\mathbf{w}}^T\bar{\mathbf{w}}$. Thus, the set Φ defined below is an attractive invariant set for the system (2.4):

$$\Phi := \{\mathbf{e} \in \mathbb{R}^n : \mathbf{e}^T\mathbf{P}\mathbf{e} \leq \lambda_{\max}(\mathbf{P})\gamma^2\bar{\mathbf{w}}^T\bar{\mathbf{w}}\} \quad (2.28)$$

Now, using the projection of the ellipsoidal sets (definition 1.5), steady-state bounds on \mathbf{e}_k (i.e. for $k \rightarrow \infty$) can be computed by:

$$\bar{\mathbf{e}}_\infty = \text{diag} \left(\left(\frac{\mathbf{P}}{\lambda_{\max}(\mathbf{P})\gamma^2\bar{\mathbf{w}}^T\bar{\mathbf{w}}} \right)^{-1/2} \right) \quad (2.29)$$

□

Remark 2.1

The set Ω defined as follows:

$$\Omega := \{\mathbf{e} \in \mathbb{R}^n : -\bar{\mathbf{e}}_\infty \leq \mathbf{e} \leq \bar{\mathbf{e}}_\infty\} \quad (2.30)$$

is an hypercube which includes the ellipsoidal RPI set (2.24) The Figure (2.2) shows the ellipsoidal RPI set defined in (2.24) and the hypercube defined in (2.30) which includes the ellipsoidal RPI set (2.24).

Remark 2.2

The above bounds on \mathbf{e}_k presents two drawbacks:

- (i) Those bounds only characterize the steady-state regime of the estimation error;
- (ii) The used ellipsoidal RPI set could present an important volume, providing very conservative bounds of the estimation error.

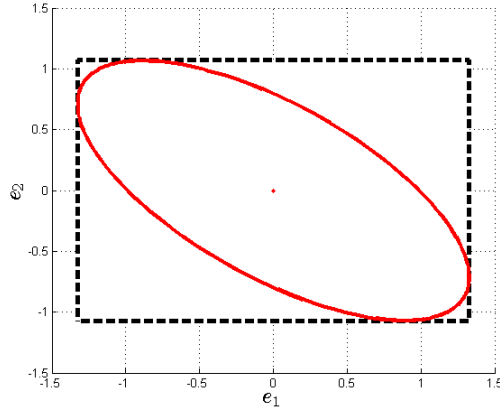


Figure 2.2: The hypercube Ω (in dashed black lines) including the ellipsoidal RPI set Φ (in red) in steady-state regime

In the next section, we will propose a method to reduce the size (the volume) of the obtained RPI sets to enhance the precision of the obtained bounds. In addition to this, we will use the evolution of the Lyapunov level sets, describing the RPI sets, for finding suitable bounds of the estimation error for any instant-time $k > 0$.

2.3.3 Shrinking of ellipsoidal RPI sets

2.3.3.1 Suitable modification of the dissipation matrix

The condition (2.20) can be modified in order to obtain a more general LMI by considering a dissipation matrix \mathbf{Q} .

Proposition 2.3

For a given symmetric definite matrix \mathbf{P} and a scalar $\gamma \geq 0$ verifying the condition (2.20), and considering the existence of a symmetric positive definite matrix \mathbf{Q} such that the following LMI holds:

$$\begin{pmatrix} -\mathbf{P} + \mathbf{Q} & 0_{n \times m} & \mathbf{A}_o^T \mathbf{P} \\ 0_{m \times n} & -\gamma^2 \mathbf{I}_m & \mathbf{E}^T \mathbf{P} \\ \mathbf{P} \mathbf{A}_o & \mathbf{P} \mathbf{E} & -\mathbf{P} \end{pmatrix} \preceq 0 \quad (2.31)$$

Then, a smaller (minimal volume) ellipsoidal RPI set can be obtained as follows:

$$\Psi := \left\{ \mathbf{e} \in \mathbb{R}^n : \mathbf{e}^T \mathbf{P} \mathbf{e} \leq \frac{1}{\lambda} \gamma^2 \bar{\mathbf{w}}^T \bar{\mathbf{w}} \right\} \quad (2.32)$$

where, for all vector \mathbf{e} different to zero, the scalar λ satisfy

$$\lambda \leq \frac{\mathbf{e}^T \mathbf{Q} \mathbf{e}}{\mathbf{e}^T \mathbf{P} \mathbf{e}} \leq 1 \quad (2.33)$$

Proof. It is possible to shrink the ellipsoidal RPI set (2.28) by finding a novel condition of the negative increments of the Lyapunov function. That is, assuming the existence of a symmetric

positive definite matrix \mathbf{Q} , we can modify (2.26) to obtain the following less conservative dissipation inequality:

$$\mathbf{V}(\mathbf{e}_{k+1}) - \mathbf{V}(\mathbf{e}_k) \leq -\mathbf{e}_k^T \mathbf{Q} \mathbf{e}_k + \gamma^2 \bar{\mathbf{w}}^T \bar{\mathbf{w}} \leq 0 \quad (2.34)$$

which holds if $\mathbf{e}_k^T \mathbf{Q} \mathbf{e}_k \geq \gamma^2 \bar{\mathbf{w}}^T \bar{\mathbf{w}}$.

Thus the LMI (2.22), used to compute observer gain, can be transformed into a more general LMI which consider any dissipation matrix \mathbf{Q} , that is:

$$\begin{pmatrix} -\mathbf{P} + \mathbf{Q} & 0_{n \times m} & \mathbf{A}^T \mathbf{P} - \mathbf{C}^T \mathbf{U}^T \\ 0_{m \times n} & -\gamma^2 \mathbf{I}_m & [\mathbf{P} \mathbf{F} \quad -\mathbf{U} \mathbf{Z}]^T \\ \mathbf{P} \mathbf{A} - \mathbf{U} \mathbf{C} & [\mathbf{P} \mathbf{F} \quad -\mathbf{U} \mathbf{Z}] & -\mathbf{P} \end{pmatrix} \preceq 0 \quad (2.35)$$

Once the matrix \mathbf{P} and the minimum scalar γ have been computed from (2.35) for any initial dissipation matrix \mathbf{Q} . A new and refined matrix \mathbf{Q} can be obtained, in a second time, by minimizing the volume of the ellipsoid defined by this matrix. That is, find \mathbf{Q} which minimizes $-\ln \det(\mathbf{Q})$ and verifies the following LMI:

$$\begin{pmatrix} \mathbf{A}_o^T \mathbf{P} \mathbf{A}_o - \mathbf{P} + \mathbf{Q} & \mathbf{A}_o^T \mathbf{P} \mathbf{E} \\ \mathbf{E}^T \mathbf{P} \mathbf{A} & \mathbf{E}^T \mathbf{P} \mathbf{E} - \gamma^2 \mathbf{I}_m \end{pmatrix} \preceq 0 \quad (2.36)$$

In this way, a smaller ellipsoidal RPI set can be obtained as follows:

$$\Psi := \left\{ \mathbf{e} \in \mathbb{R}^n : \mathbf{e}^T \mathbf{P} \mathbf{e} \leq \frac{1}{\lambda} \gamma^2 \bar{\mathbf{w}}^T \bar{\mathbf{w}} \right\} \quad (2.37)$$

where, for all vector \mathbf{e} , the scalar λ satisfy

$$\lambda \leq \frac{\mathbf{e}^T \mathbf{Q} \mathbf{e}}{\mathbf{e}^T \mathbf{P} \mathbf{e}} \leq 1 \quad (2.38)$$

which is known as the **Rayleigh quotient** (see [Par74] for instance). The scalar λ satisfying (2.38) can be obtained as the minimum generalized eigenvalue of the pair (\mathbf{Q}, \mathbf{P}) .

The ellipsoid (2.37) represents the smallest level set of the Lyapunov function which includes the set:

$$B_w^* := \{ \mathbf{e} \in \mathbb{R}^n : \mathbf{e}^T \mathbf{Q} \mathbf{e} \leq \gamma^2 \bar{\mathbf{w}}^T \bar{\mathbf{w}} \} \quad (2.39)$$

The new steady-state bounds is given as follows:

$$\bar{\mathbf{e}}_\infty = \text{diag} \left(\left(\frac{\mathbf{P}}{\frac{1}{\lambda} \gamma^2 \bar{\mathbf{w}}^T \bar{\mathbf{w}}} \right)^{-1/2} \right) \quad (2.40)$$

□

Remark 2.3

The choice of the dissipation matrix \mathbf{Q} is a degree of freedom that can be used to find small volume RPI sets, and in addition, as we will present later, it allows for including information about the a posteriori estimated state covariance.

If the information about the covariance of the disturbances is available, the approach can exploit this information in order to improve the precision of the estimation error bounds. This will be the object of the next subsection.

2.3.3.2 Using the a posteriori steady-state covariance matrix

If the co-variance matrix of the disturbance $\text{var}(\mathbf{E}\mathbf{w}_k)$ is known, it is possible to obtain a steady-state bounds $\bar{\mathbf{e}}_\infty$ smaller than the one computed in (2.29). Considering that the expected value of $\mathbf{e}_k \in \mathbb{R}^n$ in (2.4) is equal to zero, its steady-state covariance matrix is V . For any real number $t > 0$, we can use the multidimensional **Chebyshev's inequality**:

$$\Pr(\mathbf{e}_k^T V^{-1} \mathbf{e}_k > t^2) \leq \frac{n}{t^2} \quad (2.41)$$

for computing a stochastic ellipsoidal set. Even if this set could have very small volume, this set is not an invariant set because there is a probability that some trajectories of the estimation error \mathbf{e} go out this set. However, its shape matrix can be used to update the dissipation matrix \mathbf{Q} during the observer design.

Remember that the Lyapunov function in (2.34) only decreases if the following condition holds:

$$\mathbf{e}_k^T \mathbf{Q} \mathbf{e}_k > \gamma^2 \bar{\mathbf{w}}_k^T \bar{\mathbf{w}}_k \quad (2.42)$$

Remark that this deterministic condition has the same shape than the inequality (2.41), if we get $\mathbf{Q} = V^{-1}$.

Hence, the problem now is to calculate the matrix V . The steady-state covariance matrix of the estimation error can be obtained by solving the following Lyapunov equation [KDS12]:

$$\mathbf{A}_o V \mathbf{A}_o^T - V = -W \quad (2.43)$$

where W represents the covariance matrix for disturbances $\mathbf{E}\mathbf{w}_k$ in (2.4). In practical applications where the co-variance matrix for disturbances is not available, we can assume that every element of the disturbance vector \mathbf{w}_k is uniform distributed but bounded in a given interval $[a, b]$. In this case, its variance can be computed as

$$W = \text{var}(\mathbf{E}\mathbf{w}_k) = (1/12)(b - a)^2 \mathbf{E}\mathbf{E}^T \quad (2.44)$$

with $\mathbf{w}_k \in [a, b]$

Remark 2.4

Remark that the computation of V is possible once the matrix \mathbf{A}_o is available, i.e. an a priori observer matrix gain \mathbf{L} has to be calculated using an initial and arbitrary matrix \mathbf{Q} , for instance $\mathbf{Q} = \mathbf{I}_n$. After that, a significant reduction of the RPI set volume could be obtained by re-starting the observer design process with the new computed matrix $\mathbf{Q} = V^{-1}$.

The complete observer design process is summarizing in Algorithm 1.

Algorithm 2 set-membership observer design based on ellipsoidal invariant sets.

Require: Matrices $\mathbf{A}, \mathbf{B}, \mathbf{C}, \mathbf{F}$ and \mathbf{Z} describing system (2.1). Initialization of $\mathbf{Q} = \mathbf{I}_n$ and $i = 0$.

- 1: Increment i by one
 - 2: Find matrices \mathbf{P}, \mathbf{U} and the minimum γ who satisfy the LMI (2.35).
 - 3: Compute $\mathbf{L} = \mathbf{P}^{-1}\mathbf{U}$.
 - 4: Compute $\mathbf{A}_o = \mathbf{A} - \mathbf{L}\mathbf{C}$.
 - 5: Compute $\mathbf{E} = [\mathbf{F} \quad -\mathbf{L}\mathbf{Z}]$
 - 6: Using \mathbf{P} and γ , find a new matrix \mathbf{Q} which satisfies the LMI (2.36) which minimizes the volume of the ellipsoid $x^T\mathbf{Q}x \leq 1$.
 - 7: Compute the minimum λ which satisfies (2.38)
 - 8: **if** $i < 2$ **then**
 - 9: Compute the disturbance variance W using (2.44).
 - 10: Obtain the covariance matrix V using (2.43).
 - 11: Do $\mathbf{Q} = V^{-1}$.
 - 12: Go to step 1.
 - 13: **end if**
 - 14: **return** The observer parameters $\mathbf{L}, \mathbf{P}, \gamma$ and λ .
-

Once the Algorithm 2 returns \mathbf{P} , γ and λ , a smaller steady-state bounds on \mathbf{e}_k can be obtained as follows:

$$\bar{\mathbf{e}}_\infty = \text{diag} \left(\left(\left(\frac{\mathbf{P}}{\frac{1}{\lambda}\gamma^2\bar{\mathbf{w}}^T\bar{\mathbf{w}}} \right)^{-1/2} \right) \right) \quad (2.45)$$

In the next Section, we will use the evolution of the Lyapunov level sets, describing the RPI sets, for finding suitable bounds during the whole running i.e. $\forall k > 0$.

2.3.4 Characterizing the evolution of the RPI sets

Proposition 2.4

This proposition allows to characterize at every time instant k , The ellipsoidal RPI set $\bar{\Psi}_k$ which is given as follows:

$$\bar{\Psi}_k := \{\mathbf{e} \in \mathbb{R}^n : \mathbf{e}^T\mathbf{P}\mathbf{e} \leq \mu_k \bar{c}\} \quad (2.46)$$

where $\bar{c} := \frac{1}{\lambda}\gamma^2\bar{\mathbf{w}}^T\bar{\mathbf{w}}$ and μ is the shrinking index given by:

$$\mu_{k+1} = (1 - \lambda)\mu_k + \lambda \quad (2.47)$$

Moreover, the estimation error bound, denoted $\bar{\mathbf{e}}_k$ is obtained as follows:

$$\bar{\mathbf{e}}_k = \text{diag} \left(\left(\left(\frac{\mathbf{P}}{\mu_k \bar{c}} \right)^{-1/2} \right) \right) \quad (2.48)$$

Proof. Suppose that the initial estimation error, denoted \mathbf{e}_0 , is unknown but belongs to an initial bounded set $\mathcal{E}_0 \subset \mathbb{R}^n$.

There exists a scalar $\mu \geq 1$ such that the following condition holds:

$$\mathcal{E}_0 \subset \bar{\Psi} \quad (2.49)$$

with

$$\bar{\Psi} := \left\{ \mathbf{e} \in \mathbb{R}^n : \mathbf{e}^T \mathbf{P} \mathbf{e} \leq \frac{1}{\lambda} \mu \gamma^2 \bar{\mathbf{w}}^T \bar{\mathbf{w}} \right\} \quad (2.50)$$

Then,

$$\mathbf{e}_k^T \mathbf{P} \mathbf{e}_k \leq \frac{1}{\lambda} \mu \gamma^2 \bar{\mathbf{w}}^T \bar{\mathbf{w}} \quad (2.51)$$

Remark that the set (2.50) corresponds to an expansion of the invariant set (2.37). For this reason the set (2.50) is also an invariant set.

From the inequality (2.34), using the relation (2.38) and the fact that $0 < \lambda \leq 1$, we have:

$$\mathbf{V}(\mathbf{e}_{k+1}) \leq \mathbf{V}(\mathbf{e}_k) - \mathbf{e}_k^T \mathbf{Q} \mathbf{e}_k + \gamma^2 \bar{\mathbf{w}}^T \bar{\mathbf{w}} \quad (2.52)$$

$$\mathbf{e}_{k+1}^T \mathbf{P} \mathbf{e}_{k+1} \leq \mathbf{e}_k^T \mathbf{P} \mathbf{e}_k - \mathbf{e}_k^T \mathbf{Q} \mathbf{e}_k + \gamma^2 \bar{\mathbf{w}}^T \bar{\mathbf{w}} \quad (2.53)$$

$$\leq \mathbf{e}_k^T \mathbf{P} \mathbf{e}_k - \lambda \mathbf{e}_k^T \mathbf{P} \mathbf{e}_k + \gamma^2 \bar{\mathbf{w}}^T \bar{\mathbf{w}} \quad (2.54)$$

$$\leq (1 - \lambda) \mathbf{e}_k^T \mathbf{P} \mathbf{e}_k + \gamma^2 \bar{\mathbf{w}}^T \bar{\mathbf{w}} \quad (2.55)$$

$$\leq (1 - \lambda) \frac{1}{\lambda} \mu \gamma^2 \bar{\mathbf{w}}^T \bar{\mathbf{w}} + \gamma^2 \bar{\mathbf{w}}^T \bar{\mathbf{w}} \quad (2.56)$$

$$\leq \left(\frac{1}{\lambda} \mu - \mu + 1 \right) \gamma^2 \bar{\mathbf{w}}^T \bar{\mathbf{w}} \quad (2.57)$$

which describes the set containing the one-step ahead estimation error \mathbf{e}_{k+1} . We can now explicitly compute the one-step ahead RPI set, denoted $\bar{\Psi}^+$, as follows:

$$\bar{\Psi}^+ := \left\{ \mathbf{e} \in \mathbb{R}^n : \mathbf{e}^T \mathbf{P} \mathbf{e} \leq \left(\frac{1}{\lambda} \mu - \mu + 1 \right) \gamma^2 \bar{\mathbf{w}}^T \bar{\mathbf{w}} \right\} \quad (2.58)$$

By defining $\bar{c} := \frac{1}{\lambda} \gamma^2 \bar{\mathbf{w}}^T \bar{\mathbf{w}}$ we have a more compact expression of the expanded invariant set (2.50) and its one-step ahead invariant set evolution (2.58), that is

$$\begin{cases} \bar{\Psi} := \{ \mathbf{e}^T \mathbf{P} \mathbf{e} \leq \mu \bar{c} \} \\ \bar{\Psi}^+ := \{ \mathbf{e}^T \mathbf{P} \mathbf{e} \leq \underbrace{((1 - \lambda)\mu + \lambda)}_{\mu^+} \bar{c} \} \end{cases} \quad (2.59)$$

These expressions can be used to infer a recursive relationship between μ and its one-step ahead value, denoted μ^+ in (2.59). Thus, for a given initial condition $\mu_0 \geq 1$ the dynamics of this scalar, at every time-instant k , obeys:

$$\mu_{k+1} = (1 - \lambda)\mu_k + \lambda \quad (2.60)$$

This dynamics is necessarily stable because it characterizes the contraction of the invariant set (2.50). In addition, μ_k asymptotically converges to 1 as long as the time-instant $k \rightarrow \infty$.

Hence, at every time instant, the invariant sets obeys the following dynamics:

$$\bar{\Psi}_k := \{\mathbf{e} \in \mathbb{R}^n : \mathbf{e}^T \mathbf{P} \mathbf{e} \leq \mu_k \bar{c}\} \quad (2.61)$$

and its ellipsoidal shape matrix can be used to compute a more accuracy bounds for the estimation error. That is,

$$\bar{\mathbf{e}}_k = \text{diag} \left(\left(\frac{\mathbf{P}}{\mu_k \bar{c}} \right)^{-1/2} \right) \quad (2.62)$$

equivalently,

$$\bar{\mathbf{e}}_k = \bar{\mathbf{e}}_\infty \mu_k^{1/2} \quad (2.63)$$

with $\bar{\mathbf{e}}_\infty$ a known constant column vector defined as

$$\bar{\mathbf{e}}_\infty := \text{diag} \left(\left(\frac{\mathbf{P}}{\bar{c}} \right)^{-1/2} \right) \quad (2.64)$$

□

It only remains to compute an appropriated initial value for the scalar μ . To do this, suppose that the initial condition for the estimation error verifies $e(0) \in \mathcal{E}_0 \subseteq B_0$, where, for a given scalar $\gamma_\epsilon \geq 0$, the ball B_0 defined as follows

$$B_0 := \{\mathbf{e} \in \mathbb{R}^n : \mathbf{e}^T \mathbf{e} \leq \gamma_\epsilon^2\} \quad (2.65)$$

will be included into the invariant set

$$\bar{\Psi}_0 := \{\mathbf{e} \in \mathbb{R}^n : \mathbf{e}^T \mathbf{P} \mathbf{e} \leq \lambda_{\max}(\mathbf{P}) \gamma_\epsilon^2\} \quad (2.66)$$

Thus, using (2.61) and (2.66) a suitable initial value of μ verifies:

$$\mu_0 \bar{c} = \lambda_{\max}(\mathbf{P}) \gamma_\epsilon^2 \quad (2.67)$$

and then, we can chose $\mu_0 = \lambda_{\max}(\mathbf{P}) \gamma_\epsilon^2 / \bar{c}$.

2.4 The set-membership observer implementation

Once the Algorithm 1 returns the observer parameters \mathbf{L} , \mathbf{P} , γ and λ , and after to initialize the scalar μ in a suitable way. The dynamical equations of the set-membership observer will be implemented as follows:

$$\hat{\mathbf{x}}_{k+1} = (\mathbf{A} - \mathbf{L}\mathbf{C})\hat{\mathbf{x}}_k + \mathbf{B}\mathbf{u}_k + \mathbf{L}\mathbf{y}_k \quad (2.68)$$

$$\mu_{k+1} = (1 - \lambda)\mu_k + \lambda \quad (2.69)$$

$$\bar{\mathbf{x}}_k = \hat{\mathbf{x}}_k + \bar{\mathbf{e}}_\infty \mu_k^{1/2} \quad (2.70)$$

$$\underline{\mathbf{x}}_k = \hat{\mathbf{x}}_k - \bar{\mathbf{e}}_\infty \mu_k^{1/2} \quad (2.71)$$

where $\bar{\mathbf{e}}_\infty$ is a known constant column vector defined in (2.64).

The initial condition for the scalar μ can be obtained as:

$$\mu_0 = \frac{\lambda_{max}(\mathbf{P})}{\bar{c}} \quad (2.72)$$

For any initial estimation error insides a given ball with radius $\gamma_\epsilon > 0$, i.e.

$$\mathbf{e}_0^T \mathbf{e}_0 \leq \gamma_\epsilon$$

with $\mathbf{e}_0 := \mathbf{x}_0 - \hat{\mathbf{x}}_0$.

Recall that we assume that the initial estimation error is bound, and its bound is known, that is γ_ϵ is known. This value allows to properly initialize the scalar μ using (2.72).

The implementation of the proposed set-membership observer is relatively simple, since it only requires to extend the punctual observer dynamics by including a scalar dynamical equation. Thus, the order of the set-membership state observer will be only of $n + 1$, for any n -order system.

2.5 A numerical example

Consider a second order linear discrete-time system (2.1) with matrices:

$$\mathbf{A} = \begin{pmatrix} 0.2 & 0.2 \\ 0 & 0.5 \end{pmatrix}, \mathbf{B} = \begin{pmatrix} 1 \\ 1 \end{pmatrix}, \mathbf{F} = \begin{pmatrix} 0 \\ 0.1 \end{pmatrix}, \mathbf{C} = (1 \ 0)$$

and $\mathbf{Z} = 0.1$.

After applying the Algorithm 2, the obtained matrices which describe the set-membership state observer are:

$$\mathbf{L} = \begin{pmatrix} 0.5453 \\ 0.8919 \end{pmatrix}, \quad \mathbf{P} = 1e3 \begin{pmatrix} 2.5084 & -0.8209 \\ -0.8209 & 0.4749 \end{pmatrix}$$

and the scalars: $\gamma = 2.3223$ and $\lambda = 0.6289$.

We suppose that for all k , the disturbances \mathbf{w}_k are random variables with uniform distribution but bounded by the vector $\bar{\mathbf{w}} = (1 \ 1)^T$. That is, $\forall k > 0, -\bar{\mathbf{w}} \leq \mathbf{w}_k \leq \bar{\mathbf{w}}$.

In this example, we consider a constant system input $\mathbf{u}_k = 1$ for time-instants $k < 9$. After the time-instant $k \geq 9$ the system input vanishes.

The set-membership state observer has been implemented using equations (3.63)-(3.66). The initial conditions for the observer states $\hat{\mathbf{x}}$ and the scalar μ are: $\hat{\mathbf{x}}_0 = (0 \ 0)^T$ and $\mu_0 =$

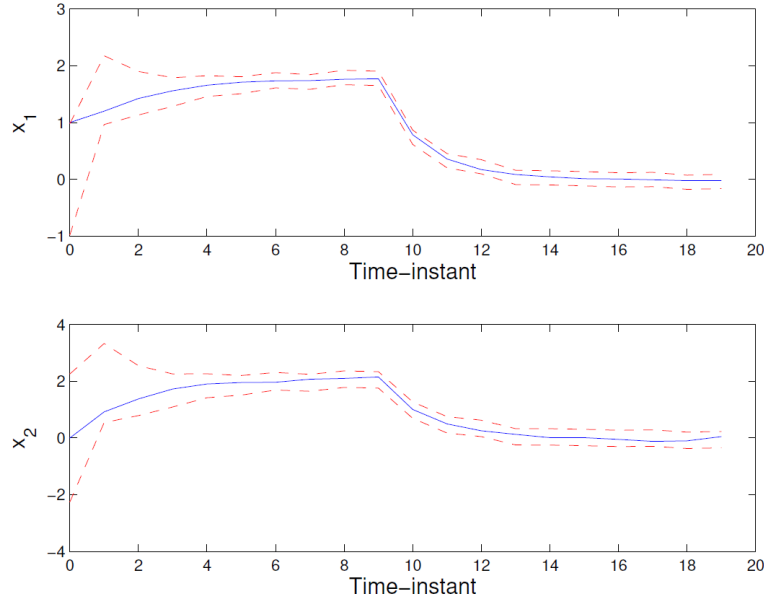


Figure 2.3: Set-membership estimation. The dashed lines correspond to the bounds obtained from the set-membership state observer. For comparison, the solid lines corresponds to the real system state.

163.17, respectively. The latter has been computed using (2.72) by considering $(-1 \ 0)^T \leq \mathbf{x}_0 \leq (1 \ 0)^T$ and then $\gamma_\epsilon = 1$.

Figure 3.3 illustrates the state enclosures. The dashed lines correspond to the bounds obtained from the set-membership state observer. For comparison, we have included the solid lines which corresponds to the real system state. Remark that the obtained bounds are very accuracy for both transient and steady-state periods.

Figure 3.5 depicts the behavior of the scalar μ_k during the whole period of the estimation. Remark that even if its value starts at 163.17, it converges asymptotically to 1 with a behavior compatible with the estimation error dynamics.

In Figure 3.6, the solid-line ellipsoid corresponds to the obtained RPI set used for computing *deterministic* bounds of the estimation error (for $\mu = 1$). The dashed-line corresponds to the stochastic ellipsoidal defined by (2.41) with $t = 3$. Remark that the obtained RPI set has taken a shape that is very close to that characterizing the states covariances. The latter set represents the set of possible values of the estimation error with a probability greater than 77.78%. Thus, according to the Chebyshev's inequality (2.41) there is a probability of obtaining estimation errors outside this set with a probability less or equal to 22.22%. However, for initial conditions starting inside the RPI set (solid-line ellipsoid), it is possible to conclude that, for all $k > 0$, the estimation error always remains inside this set.

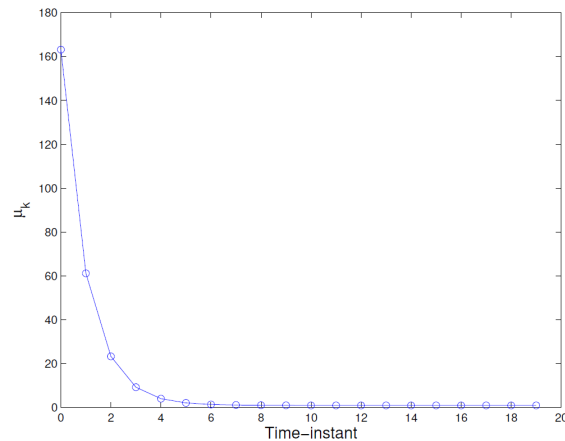


Figure 2.4: Evolution of the scalar μ_k . This scalar characterizes the contraction of the initial RPI set. The value of μ_k converges to 1 as $k \rightarrow \infty$.

2.6 Conclusion

This chapter has presented a new set-membership observer design method based on ellipsoidal robustly invariant sets for discrete-time linear systems perturbed by unknown but bounded disturbances. The set-membership observer provides a deterministic state interval that is build as the sum of the estimated system states and its corresponding estimation error bounds. The proposed approach is based on the solutions of a few number of Linear Matrix Inequalities that are suitable modified to provide both observer parameters and ellipsoidal Robustly Positive Invariant sets. The latter are used to frame the estimation error in a very simple and accurate way.

The enhanced precision on the computation of the estimation error bounds has been possible thanks to the use of the *a posteriori* calculated covariance matrix that allows, in a second time, to better describe the dissipation equation used in the Bounded-real lemma formulation. A numerical example illustrates the behavior of such set-membership observer and shows its easy implementation.

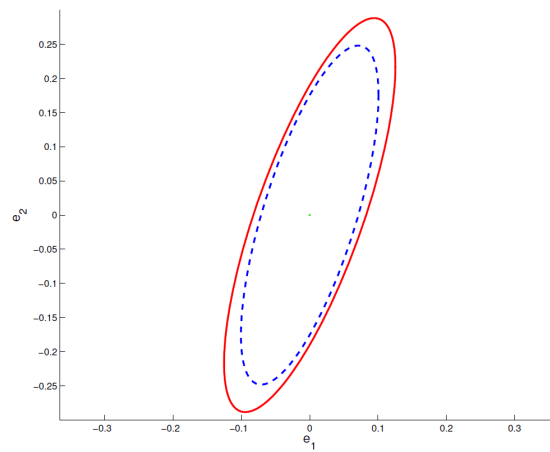


Figure 2.5: Invariant set and states covariances. The solid line corresponds to the obtained RPI set used for computing *deterministic* bounds of the estimation error. The dashed line corresponds to the stochastic ellipsoidal defined by (2.41) with $t = 3$.

Observers based on ellipsoidal invariant sets for LPV systems

Contents

3.1	Introduction	57
3.1.1	Linear Parameter Varying systems	58
3.1.2	Polytopic decomposition of a LPV model	60
3.2	Problem statement	61
3.3	Set-membership design for LPV systems	62
3.3.1	H_∞ Observer gain design	62
3.3.2	Computing ellipsoidal RPI sets	64
3.3.3	Evolution of ellipsoidal RPI sets	66
3.4	Set-membership observer design algorithm for LPV systems	68
3.4.1	Two iterations-based observer synthesis	68
3.4.2	Using the a posteriori steady-state covariance matrix	69
3.5	Set-membership observer implementation for LPV systems	70
3.5.1	Observer dynamical equations	70
3.5.2	Initialization of the scalar μ	71
3.6	A numerical examples	72
3.6.1	Example 1	72
3.6.2	Example 2	73
3.7	Conclusion	76

3.1 Introduction

The set-membership observer presented in the Chapter 2 was addressed for the class of linear systems. It is interesting to be able to apply this observer to a large class of systems such non linear systems and switched systems. It has been shown that a Linear Parameter Varying (LPV) equivalent representation can be an appealing alternative to deal with non linear systems and switched systems.

It exists in the literature some interval observers for LPV systems, for example: the work of [WBR15] developed an interval observer design methodology for linear parameter varying discrete-time systems with parametric uncertainty, the observer gain that ensures the stability and cooperativity of the estimation error is computed as a convex semi-definite programming problem. In the context of continuous systems, [Che+13] proposed an interval observers design for continuous-time LPV and non-negative systems where the cooperativity and stability are expressed in terms of matrix inequalities.

In this chapter we present the extension of the set-membership observer based on ellipsoidal invariant sets presented in the Chapter 2 for the Linear Parameters Varying (LPV) discrete-time systems.

This chapter is organized as follows: Section 3.2 is devoted to the problem statement. The section 3.3 presents the set-membership observer design for LPV systems, this Section is composed of three subsections: a first subsection presents the H_∞ observer gain design, a second subsection shows how to compute ellipsoidal RPI sets and the third subsection dedicated to characterize the evolution of ellipsoidal RPI sets bounding the estimation error at each time-instant. Section 3.4 summarize the set-membership design via an algorithm. The Section 3.5 is devoted to the implementation of the proposed observer. In Section 3.6, an example of LPV system is addressed in order to show the performance of the proposed observer. We finish this chapter with a conclusion.

Before addressing the design and implementation of the observer, let's start with a small reminder about the LPV systems and their importance.

3.1.1 Linear Parameter Varying systems

LPV modeling is one of the major tools used in modeling and control of a large class of systems. LPV systems are more representative for real systems taking into consideration more dynamics and more information on varying parameters. In fact, LPV systems ensure a good approximation of a non linear model by using a state space varying parameters representation that is close to the real dynamical behavior. The Figure (3.1) shows the importance of LPV systems as a bridge between the Non Linear (NL) systems and Linear Time Invariant (LTI) systems. The LPV systems can be seen as a combination of several LTI systems each time the varying parameters takes values in the set of variations. The advantage of the LPV system is that it keeps a linear structure which allows to use several synthesis and analysis mathematical tools for linear systems.

Définition 3.1

In general, a discrete-time LPV system can be represented by the following space-state representation:

$$\begin{cases} \mathbf{x}_{k+1} = \mathbf{A}(\rho(\cdot)) \mathbf{x}_k + \mathbf{B}(\rho(\cdot)) \mathbf{u}_k + \mathbf{F}(\rho(\cdot)) \mathbf{d}_k \\ \mathbf{y}_k = \mathbf{C}(\rho(\cdot)) \mathbf{x}_k + \mathbf{Z}(\rho(\cdot)) \mathbf{v}_k \end{cases} \quad (3.1)$$

where at least one of the matrices $\mathbf{A}(\rho(\cdot))$, $\mathbf{B}(\rho(\cdot))$, $\mathbf{F}(\rho(\cdot))$, $\mathbf{C}(\rho(\cdot))$, $\mathbf{Z}(\rho(\cdot))$ depend on the

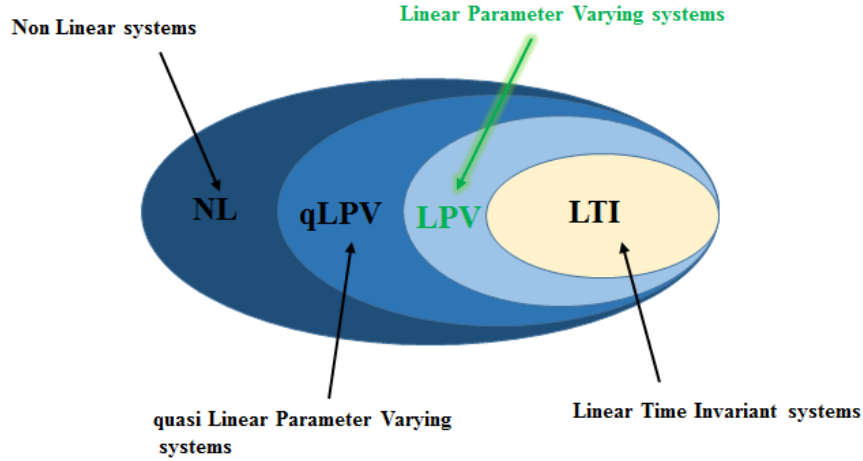


Figure 3.1: Relation between the different classes of systems

parameter vector $\rho = \rho_k$. The scheduling parameter vector $\rho(\cdot) \in \mathbb{R}^L$ is a time-varying measurable parameter vector, where L is the number of varying parameters.

The systems of the type (3.1) can be modeled by different class of systems:

- if $\rho(\cdot) = \rho = \mathbf{constant}$, then the system (3.1) is a Linear Time Invariant (LTI) system.
- if $\rho(\cdot) = \rho(t)$ where the time dependency is explicit, then the system (3.1) is a Linear Time Varying (LTV) system.
- if $\rho(\cdot) = \theta(t)$ with $\theta(t)$ being an external measurable parameter, then the system (3.1) is a Linear Parameter Varying (LPV) system.
- if $\rho(\cdot) = \theta(t)$ with $\theta(t)$ being an uncertain and non measurable parameter, then the system (3.1) is an uncertain (LTI or LTV) system.
- if $\rho(\cdot) = \rho(x(t))$ depends on the state vector, then the system (3.1) is a quasi-Linear Parameter Varying (qLPV) system.

Several representations of the LPV systems are available in the literature:

- Polynomial representation [Rug81]
- Linear Fractional Transformation (LFT) representation [BSL07]
- Polytopic decomposition [MAB05]

In our context, we are going to use the polytopic decomposition.

3.1.2 Polytopic decomposition of a LPV model

Polytopic decomposition of a LPV model is one of the most useful model transformation allowing a LPV model to be written in terms of a convex hull of linear models. In particular, the LPV system matrices can be modeled as convex hulls of linear matrices. Those linear matrices are obtained using all possible extreme values of the scheduling parameter. The polytopic decomposition, see for instance [MAB05], can be formulated as follows:

Proposition 3.1

(See [CDD08]) Consider the LPV system (3.1), for a given scheduling parameter $\rho \in \Omega_\rho$, there exist a column vector $\alpha \in \mathbb{R}^N$, formed by positive scalar elements $\alpha_i \geq 0$, $i = \{1, \dots, N\}$, such that

$$\begin{bmatrix} \theta_1^T & \theta_2^T & \dots & \theta_N^T \\ 1 & 1 & \dots & 1 \end{bmatrix} \alpha = \begin{bmatrix} \rho \\ 1 \end{bmatrix} \quad (3.2)$$

where the row vectors $\theta_i \in \mathbb{R}^{1 \times L}$, $i = \{1, \dots, N\}$, are the *a priori* known vertices of the polytopic set $\Omega_\rho \subset \mathbb{R}^L$. \square

Notice that the vector α is formed by elements satisfying: $\alpha_i \geq 0$ and $\sum_{i=1}^N \alpha_i = 1$. Therefore the state-space matrices can be written in a polytopic form as follows:

$$\mathbf{M}(\rho) = \sum_{i=1}^N \alpha_i \mathbf{M}_i \quad (3.3)$$

where each matrix \mathbf{M}_i can be obtained using its corresponding vertex θ_i , as follows: $\mathbf{M}_i = \mathbf{M}(\theta_i)$, for $i = \{1, \dots, N\}$. Remark that all matrices \mathbf{M}_i can be computed *offline*. These matrices together with α , solution of (3.2), can be used *online* for computing the matrix $\mathbf{M}(\rho)$.

Example 3.1

Let's consider an LPV system with 2 varying parameters $\rho_1 \in [\underline{\rho}_1, \bar{\rho}_1]$ and $\rho_2 \in [\underline{\rho}_2, \bar{\rho}_2]$. The polytope Ω_ρ is formed of 4 vertices $\theta_1, \theta_2, \theta_3$ and θ_4 . The polytope can be obtained as follows:

$$\Omega_\rho = \text{convexhull}\{\theta_1, \theta_2, \theta_3, \theta_4\} \quad (3.4)$$

where

$$\theta_1 = (\underline{\rho}_1, \underline{\rho}_2)$$

$$\theta_2 = (\bar{\rho}_1, \underline{\rho}_2)$$

$$\theta_3 = (\bar{\rho}_1, \bar{\rho}_2)$$

$$\theta_4 = (\underline{\rho}_1, \bar{\rho}_2)$$

with $L = 2$ and $N = 4$. The figure 3.2 illustrates the polytope Ω_ρ used for polytopic representation of an LPV system with 2 parameters.

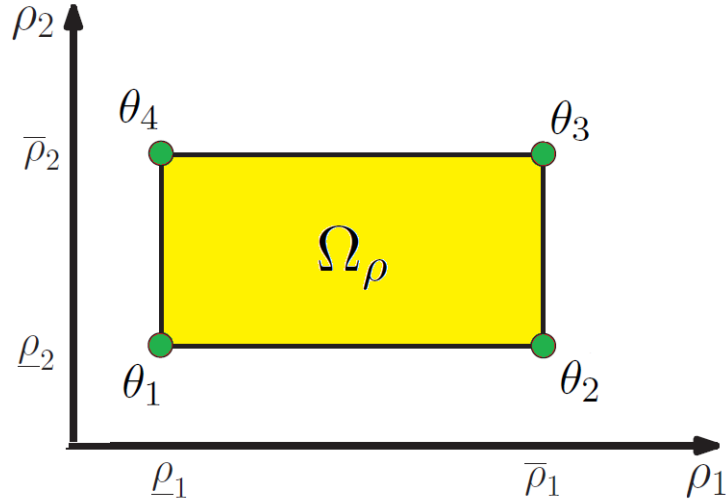


Figure 3.2: Example of a polytope Ω_ρ for polytopic representation of an LPV system with 2 varying parameters.

3.2 Problem statement

Let's consider the LPV discrete-time system represented by the following dynamic equations:

$$\begin{cases} \mathbf{x}_{k+1} = \mathbf{A}(\rho_k)\mathbf{x}_k + \mathbf{B}(\rho_k)\mathbf{u}_k + \mathbf{F}(\rho_k)\mathbf{d}_k \\ \mathbf{y}_k = \mathbf{C}\mathbf{x}_k + \mathbf{Z}\mathbf{v}_k \end{cases} \quad (3.5)$$

where $\mathbf{x}_k \in \mathbb{R}^n$ is the state vector, $\mathbf{u}_k \in \mathbb{R}^{n_u}$ is the input vector and $\mathbf{y}_k \in \mathbb{R}^{n_y}$ is the measured output vector. The vectors \mathbf{w}_k and \mathbf{v}_k are unknown state disturbances and unknown measurement noises assumed to be unknown but bounded with known bounds. The matrices \mathbf{C} , \mathbf{Z} are constant matrices with appropriated dimensions. In the case where \mathbf{C} and \mathbf{Z} depends on ρ , it is possible to rewrite the system (3.5) by including an output filter to assure new matrices \mathbf{C}^* and \mathbf{Z}^* independent on ρ .

The matrices $\mathbf{A}(\rho_k)$, $\mathbf{B}(\rho_k)$, $\mathbf{F}(\rho_k)$ are state-space matrices parameterized by the scheduling parameter vector ρ_k , we assume that these matrices are affinely dependent on ρ_k . The scheduling parameter vector ρ is a time-varying measurable parameter vector. In this work, it is assumed that all possible values of ρ_k belong to a given bounded polytopic set Ω_ρ . The pair $(\mathbf{A}(\rho_k), \mathbf{C})$ is assumed detectable for all values of $\rho_k \in \Omega_\rho$.

Suppose now we can design the following LPV observer:

$$\hat{\mathbf{x}}_{k+1} = \tilde{\mathbf{A}}(\rho_k)\hat{\mathbf{x}}_k + \mathbf{B}(\rho_k)\mathbf{u}_k + \mathbf{L}(\rho_k)\mathbf{y}_k \quad (3.6)$$

Where $\tilde{\mathbf{A}}(\rho_k) = \mathbf{A}(\rho_k) - \mathbf{L}(\rho_k)\mathbf{C}$. The estimation error is given $\mathbf{e}_k := \mathbf{x}_k - \hat{\mathbf{x}}_k$, the dynamics of the estimation error can be obtained from (3.5) and (3.6), as follows:

$$\mathbf{e}_{k+1} = \tilde{\mathbf{A}}(\rho_k)\mathbf{e}_k + \mathbf{E}(\rho_k)\mathbf{w}_k \quad (3.7)$$

where $\mathbf{E}(\rho_k) = [\mathbf{F}(\rho_k) \quad -\mathbf{L}(\rho_k)\mathbf{Z}]$ and $\mathbf{w}_k \in \mathbb{R}^m$, defined as $\mathbf{w}_k := \begin{pmatrix} \mathbf{d}_k \\ \mathbf{v}_k \end{pmatrix}$.

The disturbance vector \mathbf{w}_k is assumed to belong to a bounded i.e $\mathbf{w}_k \in \mathbb{W} \subset \mathbb{R}^m$. We assume that the disturbance \mathbf{w}_k can be bounded as follows $\mathbf{w}_k^T \mathbf{w}_k \leq \bar{\mathbf{w}}^T \bar{\mathbf{w}}$ for all $k \geq 0$, where $\bar{\mathbf{w}} = \sup\{\mathbf{w}_k\}$.

The reasoning is the same as in Chapter 2, we suppose that we know exactly the bounds of the estimation error, denoted $\bar{\mathbf{e}}_k$. At each time-instant, the real state is included between a lower and upper bounds defined as follows:

$$\hat{\mathbf{x}}_k - \bar{\mathbf{e}}_k \leq \mathbf{x}_k \leq \hat{\mathbf{x}}_k + \bar{\mathbf{e}}_k \quad (3.8)$$

Then, at every time-instant we can guarantee that the system state belongs an hypercube defined by the vectors $\underline{\mathbf{x}}_k := \hat{\mathbf{x}}_k - \bar{\mathbf{e}}_k$ and $\bar{\mathbf{x}}_k := \hat{\mathbf{x}}_k + \bar{\mathbf{e}}_k$ i.e :

$$\underline{\mathbf{x}}_k \leq \mathbf{x}_k \leq \bar{\mathbf{x}}_k \quad (3.9)$$

Then, a set-membership observer for the LPV system (3.5) can be implemented as follows:

$$\hat{\mathbf{x}}_{k+1} = (\mathbf{A}(\rho_k) - \mathbf{L}(\rho_k)\mathbf{C})\hat{\mathbf{x}}_k + \mathbf{B}(\rho_k)\mathbf{u}_k + \mathbf{L}(\rho_k)\mathbf{y}_k \quad (3.10)$$

$$\bar{\mathbf{x}}_k = \hat{\mathbf{x}}_k + \bar{\mathbf{e}}_k \quad (3.11)$$

$$\underline{\mathbf{x}}_k = \hat{\mathbf{x}}_k - \bar{\mathbf{e}}_k \quad (3.12)$$

The set-membership observer problem returns to compute the punctual state estimation $\hat{\mathbf{x}}_k$ and the estimation error bounds $\bar{\mathbf{e}}_k$. Once this task is performed, we just have to compute the vectors $\bar{\mathbf{x}}_k$ and $\underline{\mathbf{x}}_k$ as the sum of both state estimation and its corresponding estimation error bounds. These aspect will be illustrated in the next sections.

3.3 Set-membership design for LPV systems

3.3.1 H_∞ Observer gain design

The punctual state estimation $\hat{\mathbf{x}}_k$ is given by (3.10) where the observer gain matrix $\mathbf{L}(\rho_k)$ can be written in a polytopic form, i.e. $\mathbf{L}(\rho_k) = \sum_{i=1}^N \alpha_i \mathbf{L}_i$. The H_∞ gain synthesis is quite similar to the one presented in the previous chapter (see (2.22)) where the H_∞ gain is intended to minimize the impact of the system disturbances \mathbf{w}_k on the estimation error. Theorem 3.1 allows the computation of the H_∞ observer gain.

Theorem 3.1

Consider the system (3.7) and a given matrix $\mathbf{Q} > 0$. The observer gains \mathbf{L}_i which minimize the H_∞ norm of the system (3.7) are found if there exist symmetric positive definite matrices \mathbf{P} , a positive scalar $\gamma > 0$ and matrices \mathbf{U}_i satisfying the following condition:

$$\text{for } i = \{1, \dots, N\} \quad \begin{pmatrix} -\mathbf{P} + \mathbf{Q} & 0_{n \times m} & \mathbf{A}_i^T \mathbf{P} - \mathbf{C}^T \mathbf{U}_i^T \\ \star & -\gamma^2 \mathbf{I}_m & [\mathbf{P}\mathbf{F}_i \quad -\mathbf{U}_i \mathbf{Z}]^T \\ \star & \star & -\mathbf{P} \end{pmatrix} \preceq 0 \quad (3.13)$$

Moreover, the observer gain matrices can be obtained as

$$\mathbf{L}_i = \mathbf{P}^{-1} \mathbf{U}_i$$

observer gain matrix $\mathbf{L}(\rho)$ can be written in a polytopic form:

$$\mathbf{L}(\rho_k) = \sum_{i=1}^N \alpha_i \mathbf{L}_i$$

Proof. The proof is obtained by performing the same reasoning as in the Proposition 2.1. Let's consider the following candidate Lyapunov function for the system (3.7):

$$V(\mathbf{e}_k) = \mathbf{e}_k^T \mathbf{P} \mathbf{e}_k \geq 0 \quad (3.14)$$

Suppose the existence of semi positive definite matrix \mathbf{P} and a positive scalar γ verifying the following dissipation inequality:

$$V(\mathbf{e}_{k+1}) - V(\mathbf{e}_k) \leq -\mathbf{e}_k^T \mathbf{Q} \mathbf{e}_k + \gamma^2 \mathbf{w}_k^T \mathbf{w}_k \quad (3.15)$$

by replacing (3.14) in (3.15) and using the estimation error dynamics (3.7), we obtain:

$$\begin{aligned} & \mathbf{e}_k^T (\tilde{\mathbf{A}}(\rho_k)^T \mathbf{P} \tilde{\mathbf{A}}(\rho_k) - \mathbf{P} + \mathbf{Q}) \mathbf{e}_k + \mathbf{e}_k^T (\tilde{\mathbf{A}}(\rho_k)^T \mathbf{P} \mathbf{E}(\rho_k)) \mathbf{w}_k \\ & + \mathbf{w}_k^T (\mathbf{E}(\rho_k)^T \mathbf{P} \tilde{\mathbf{A}}(\rho_k)) \mathbf{e}_k + \mathbf{w}_k^T (\mathbf{E}(\rho_k)^T \mathbf{P} \mathbf{E}(\rho_k) - \gamma^2 \mathbf{I}_m) \mathbf{w}_k \leq 0 \end{aligned} \quad (3.16)$$

For any $\begin{pmatrix} \mathbf{e}_k \\ \mathbf{w}_k \end{pmatrix} \neq 0$, this inequality can be written in the following matrix form:

$$\begin{pmatrix} \tilde{\mathbf{A}}(\rho_k)^T \mathbf{P} \tilde{\mathbf{A}}(\rho_k) - \mathbf{P} + \mathbf{Q} & \tilde{\mathbf{A}}(\rho_k)^T \mathbf{P} \mathbf{E}(\rho_k) \\ \mathbf{E}(\rho_k)^T \mathbf{P} \tilde{\mathbf{A}}(\rho_k) & \mathbf{E}(\rho_k)^T \mathbf{P} \mathbf{E}(\rho_k) - \gamma^2 \mathbf{I}_m \end{pmatrix} \preceq 0 \quad (3.17)$$

Let's write this condition as follows:

$$\begin{pmatrix} -\mathbf{P} + \mathbf{Q} & 0_{n \times m} \\ 0_{m \times n} & -\gamma^2 \mathbf{I}_m \end{pmatrix} + \begin{pmatrix} \tilde{\mathbf{A}}(\rho_k)^T \mathbf{P} \tilde{\mathbf{A}}(\rho_k) & \tilde{\mathbf{A}}(\rho_k)^T \mathbf{P} \mathbf{E}(\rho_k) \\ \mathbf{E}(\rho_k)^T \mathbf{P} \tilde{\mathbf{A}}(\rho_k) & \mathbf{E}(\rho_k)^T \mathbf{P} \mathbf{E}(\rho_k) \end{pmatrix} \preceq 0 \quad (3.18)$$

then, by using the Schur complement we obtain:

$$\begin{pmatrix} -\mathbf{P} + \mathbf{Q} & 0_{n \times m} & \tilde{\mathbf{A}}(\rho_k)^T \mathbf{P} \\ 0_{m \times n} & -\gamma^2 \mathbf{I}_m & \mathbf{E}(\rho_k)^T \mathbf{P} \\ \mathbf{P} \tilde{\mathbf{A}}(\rho_k) & \mathbf{P} \mathbf{E}(\rho_k) & -\mathbf{P} \end{pmatrix} \preceq 0 \quad (3.19)$$

We can rewrite condition (3.19) at every vertex of the polytopic model (see for instance [AGB95]), as follows:

$$\text{For } i = 1, \dots, N; \quad \begin{pmatrix} -\mathbf{P} + \mathbf{Q} & 0_{n \times m} & \tilde{\mathbf{A}}_i^T \mathbf{P} \\ 0_{m \times n} & -\gamma^2 \mathbf{I}_m & \mathbf{E}_i^T \mathbf{P} \\ \mathbf{P} \tilde{\mathbf{A}}_i & \mathbf{P} \mathbf{E}_i & -\mathbf{P} \end{pmatrix} \preceq 0 \quad (3.20)$$

where $\tilde{\mathbf{A}}_i := (\mathbf{A}_i - \mathbf{L}_i \mathbf{C})$ and $\mathbf{E}_i = [\mathbf{F}_i \quad -\mathbf{L}_i \mathbf{Z}]$.

Notice that the existence of \mathbf{P} means that the family of systems, described by matrices $\tilde{\mathbf{A}}_i$ and \mathbf{E}_i , for $i = \{1, \dots, N\}$, share the **common Lyapunov function** $V(\mathbf{e}_k) = \mathbf{e}_k^T \mathbf{P} \mathbf{e}_k$

$$\begin{pmatrix} -\mathbf{P} + \mathbf{Q} & 0_{n \times m} & \mathbf{A}_i^T \mathbf{P} - \mathbf{C}^T \mathbf{L}_i^T \mathbf{P} \\ \star & -\gamma^2 \mathbf{I}_m & [\mathbf{P} \mathbf{F}_i \quad -\mathbf{P} \mathbf{L}_i \mathbf{Z}]^T \\ \star & \star & -\mathbf{P} \end{pmatrix} \preceq 0 \quad (3.21)$$

. By substitution, we have Now by performing a change of variable in (3.21), i.e. $\mathbf{U}_i := \mathbf{P} \mathbf{L}_i$, to transforming this condition in a LMI, we obtain the following condition:

$$\begin{pmatrix} -\mathbf{P} + \mathbf{Q} & 0_{n \times m} & \mathbf{A}_i^T \mathbf{P} - \mathbf{C}^T \mathbf{U}_i^T \\ \star & -\gamma^2 \mathbf{I}_m & [\mathbf{P} \mathbf{F}_i \quad -\mathbf{U}_i \mathbf{Z}]^T \\ \star & \star & -\mathbf{P} \end{pmatrix} \preceq 0 \quad (3.22)$$

which corresponds to that proposed in (3.13).

Once the matrices \mathbf{P} , \mathbf{U}_i and the minimum scalar γ are found, the state observer gain matrices \mathbf{L}_i can be obtained as $\mathbf{L}_i = \mathbf{P}^{-1} \mathbf{U}_i$ because $\mathbf{U}_i := \mathbf{P} \mathbf{L}_i$. \square

The problem now is to compute suitable bounds of the estimation error $\bar{\mathbf{e}}_k$. Here, the presented synthesis allows to design the observer gain and in the same time allows to compute ellipsoidal RPI sets bounding the estimation error at every instant time. This aspect is one the main novelties of this contribution. The next section is dedicated to the computation of ellipsoidal RPI sets bounding the estimation error.

3.3.2 Computing ellipsoidal RPI sets

The statement of the following theorem allows to compute the ellipsoidal RPI sets used later to bound the estimation errors.

Theorem 3.2

Consider the system (3.7) with bounded disturbances. If there exist a common symmetric positive definite matrix \mathbf{P} and a scalar $\gamma > 0$, for a given matrix \mathbf{Q} verifying the condition (3.20), then the following set Ψ is an RPI set for system (3.7):

$$\Psi := \left\{ \mathbf{e} \in \mathbb{R}^n : \mathbf{e}^T \mathbf{P} \mathbf{e} \leq \frac{1}{\lambda} \gamma^2 \bar{\mathbf{w}}^T \bar{\mathbf{w}} \right\} \quad (3.23)$$

where, for a given non-zero vector \mathbf{e} , the scalar $\lambda > 0$ satisfies

$$\lambda \leq \frac{\mathbf{e}^T \mathbf{Q} \mathbf{e}}{\mathbf{e}^T \mathbf{P} \mathbf{e}} \leq 1 \quad (3.24)$$

Proof. Suppose at a given instant k , \mathbf{e}_k belongs to the set (3.23):

$$\mathbf{e}_k^T \mathbf{P} \mathbf{e}_k \leq \frac{1}{\lambda} \gamma^2 \bar{\mathbf{w}}^T \bar{\mathbf{w}} \quad (3.25)$$

From the dissipation inequality (3.15) and relation (3.24), we can write:

$$V(\mathbf{e}_{k+1}) \leq V(\mathbf{e}_k) - \mathbf{e}_k^T \mathbf{Q} \mathbf{e}_k + \gamma^2 \bar{\mathbf{w}}^T \bar{\mathbf{w}} \quad (3.26)$$

$$\mathbf{e}_{k+1}^T \mathbf{P} \mathbf{e}_{k+1} \leq \mathbf{e}_k^T \mathbf{P} \mathbf{e}_k - \mathbf{e}_k^T \mathbf{Q} \mathbf{e}_k + \gamma^2 \bar{\mathbf{w}}^T \bar{\mathbf{w}} \quad (3.27)$$

$$\leq \mathbf{e}_k^T \mathbf{P} \mathbf{e}_k - \lambda \mathbf{e}_k^T \mathbf{P} \mathbf{e}_k + \gamma^2 \bar{\mathbf{w}}^T \bar{\mathbf{w}} \quad (3.28)$$

$$\leq (1 - \lambda) \mathbf{e}_k^T \mathbf{P} \mathbf{e}_k + \gamma^2 \bar{\mathbf{w}}^T \bar{\mathbf{w}} \quad (3.29)$$

Since $0 < \lambda \leq 1$ i.e. $|(1 - \lambda)| < 1$, then by replacing (3.25) into the previous inequality (3.29) we have:

$$\mathbf{e}_{k+1}^T \mathbf{P} \mathbf{e}_{k+1} \leq (1 - \lambda) \frac{1}{\lambda} \gamma^2 \bar{\mathbf{w}}^T \bar{\mathbf{w}} + \gamma^2 \bar{\mathbf{w}}^T \bar{\mathbf{w}} \quad (3.30)$$

$$\leq \frac{1}{\lambda} \gamma^2 \bar{\mathbf{w}}^T \bar{\mathbf{w}} \quad (3.31)$$

This means that \mathbf{e}_{k+1} belongs to the set (3.23):

$$\mathbf{e}_{k+1} \in \Psi \quad (3.32)$$

From (3.25) and (3.32) we conclude that the set (3.23) is a RPI set for the system dynamics (3.7). \square

Furthermore, the RPI set (3.23) belongs to the hypercube Ω defined as follows:

$$\Omega := \{\mathbf{e} \in \mathbb{R}^n : -\bar{\mathbf{e}}_\infty \leq \mathbf{e} \leq \bar{\mathbf{e}}_\infty\} \quad (3.33)$$

with $\bar{\mathbf{e}}_\infty$ a column vector defined as

$$\bar{\mathbf{e}}_\infty := \text{diag} \left(\left(\left(\frac{\mathbf{P}}{\frac{1}{\lambda} \gamma^2 \bar{\mathbf{w}}^T \bar{\mathbf{w}}} \right)^{-1/2} \right) \right) \quad (3.34)$$

Remark 3.1

Consider the dissipation equation (3.15). Remark that the Lyapunov function decreases outside the set B_Q :

$$B_Q := \{\mathbf{e} \in \mathbb{R}^n : \mathbf{e}^T \mathbf{Q} \mathbf{e} \leq \gamma^2 \bar{\mathbf{w}}^T \bar{\mathbf{w}}\} \quad (3.35)$$

Then, from condition (3.24) we have

$$\lambda \mathbf{e}^T \mathbf{P} \mathbf{e} \leq \mathbf{e}^T \mathbf{Q} \mathbf{e} \leq \gamma^2 \bar{\mathbf{w}}^T \bar{\mathbf{w}} \quad (3.36)$$

which means that the RPI set (3.23) includes the set (3.35).

In the next Section, we will compute the bounds of the estimation error at each time-instant $k \geq 0$ thanks to the evolution of the Lyapunov level sets, describing the evolution of RPI sets at each time-instant.

3.3.3 Evolution of ellipsoidal RPI sets

The following theorem allow to characterize the evolution of the estimation error bounds $\bar{\mathbf{e}}_k$.

Theorem 3.3

Consider the system (3.7) satisfying the condition (3.20), suppose there exist a scalar $\mu_k \geq 1$, such that the estimation error \mathbf{e}_k , at the time-instant k , belongs to the RPI set $\bar{\Psi}_k$:

$$\bar{\Psi}_k := \{ \mathbf{e} \in \mathbb{R}^n : \mathbf{e}^T \mathbf{P} \mathbf{e} \leq \mu_k \bar{c} \} \quad (3.37)$$

Then, the one-step ahead estimation error \mathbf{e}_{k+1} belongs to the RPI set $\bar{\Psi}_{k+1}$:

$$\bar{\Psi}_{k+1} := \{ \mathbf{e} \in \mathbb{R}^n : \mathbf{e}^T \mathbf{P} \mathbf{e} \leq \mu_{k+1} \bar{c} \} \quad (3.38)$$

where the μ_k -dynamics obeys:

$$\mu_{k+1} = (1 - \lambda)\mu_k + \lambda \quad (3.39)$$

with λ a scalar satisfying (3.24) and $\bar{c} := \frac{1}{\lambda} \mu \gamma^2 \bar{\mathbf{w}}^T \bar{\mathbf{w}}$.

Proof. Suppose that, the initial estimation error, denoted \mathbf{e}_0 , is unknown but belongs to an initial bounded set $\mathcal{E}_0 \subset \mathbb{R}^n$. There exist a scalar $\mu \geq 1$ such that the following condition holds:

$$\mathcal{E}_0 \subset \bar{\Psi} \quad (3.40)$$

with

$$\bar{\Psi} := \{ \mathbf{e} \in \mathbb{R}^n : \mathbf{e}^T \mathbf{P} \mathbf{e} \leq \frac{1}{\lambda} \mu \gamma^2 \bar{\mathbf{w}}^T \bar{\mathbf{w}} \} \quad (3.41)$$

Then,

$$\mathbf{e}_k^T \mathbf{P} \mathbf{e}_k \leq \frac{1}{\lambda} \mu \gamma^2 \bar{\mathbf{w}}^T \bar{\mathbf{w}} \quad (3.42)$$

Remark that the set (3.41) corresponds to an expansion of the invariant set (3.23). For this reason the set (3.41) is also an invariant set. From the inequality (3.15) and using the relation (3.24), we have:

$$V(\mathbf{e}_{k+1}) \leq V(\mathbf{e}_k) - \mathbf{e}_k^T \mathbf{Q} \mathbf{e}_k + \gamma^2 \bar{\mathbf{w}}^T \bar{\mathbf{w}} \quad (3.43)$$

$$\mathbf{e}_{k+1}^T \mathbf{P} \mathbf{e}_{k+1} \leq \mathbf{e}_k^T \mathbf{P} \mathbf{e}_k - \mathbf{e}_k^T \mathbf{Q} \mathbf{e}_k + \gamma^2 \bar{\mathbf{w}}^T \bar{\mathbf{w}} \quad (3.44)$$

$$\leq \mathbf{e}_k^T \mathbf{P} \mathbf{e}_k - \lambda \mathbf{e}_k^T \mathbf{P} \mathbf{e}_k + \gamma^2 \bar{\mathbf{w}}^T \bar{\mathbf{w}} \quad (3.45)$$

$$\leq (1 - \lambda) \mathbf{e}_k^T \mathbf{P} \mathbf{e}_k + \gamma^2 \bar{\mathbf{w}}^T \bar{\mathbf{w}} \quad (3.46)$$

$$\leq (1 - \lambda) \frac{1}{\lambda} \mu \gamma^2 \bar{\mathbf{w}}^T \bar{\mathbf{w}} + \gamma^2 \bar{\mathbf{w}}^T \bar{\mathbf{w}} \quad (3.47)$$

$$\leq \left(\frac{1}{\lambda} \mu - \mu + 1 \right) \gamma^2 \bar{\mathbf{w}}^T \bar{\mathbf{w}} \quad (3.48)$$

which describes the set containing the one-step ahead estimation error \mathbf{e}_{k+1} . Thus, it is possible now explicitly compute the one-step ahead RPI set, denoted $\bar{\Psi}^+$, as follows:

$$\bar{\Psi}^+ := \left\{ \mathbf{e} \in \mathbb{R}^n : \mathbf{e}^T \mathbf{P} \mathbf{e} \leq \left(\frac{1}{\lambda} \mu - \mu + 1 \right) \gamma^2 \bar{\mathbf{w}}^T \bar{\mathbf{w}} \right\} \quad (3.49)$$

By defining $\bar{c} := \frac{1}{\lambda} \gamma^2 \bar{\mathbf{w}}^T \bar{\mathbf{w}}$ we have a more compact expression of the expanded invariant set (3.41) and its one-step ahead invariant set evolution (3.49). That is,

$$\begin{cases} \bar{\Psi} & : \mathbf{e}^T \mathbf{P} \mathbf{e} \leq \mu \bar{c} \\ \bar{\Psi}^+ & : \mathbf{e}^T \mathbf{P} \mathbf{e} \leq \underbrace{((1-\lambda)\mu + \lambda)}_{\mu^+} \bar{c} \end{cases} \quad (3.50)$$

These expressions can be used to infer a recursive relationship between μ and its one-step ahead value, denoted μ^+ in (3.50). Thus, for a given initial condition $\mu_0 \geq 1$ the dynamics of this scalar, at every time-instant k , obeys:

$$\mu_{k+1} = (1 - \lambda)\mu_k + \lambda \quad (3.51)$$

and hence the invariant sets obeys the following dynamics:

$$\bar{\Psi}_k := \{\mathbf{e} \in \mathbb{R}^n : \mathbf{e}^T \mathbf{P} \mathbf{e} \leq \mu_k \bar{c}\} \quad (3.52)$$

which completes the proof. \square

The dynamical equation (3.51) is stable because $0 < \lambda \leq 1$. This dynamical equation characterizes the contraction of the invariant set (3.41). Remark that μ_k asymptotically converges to 1 as long as the time-instant $k \rightarrow \infty$.

Corollary 3.1

Consider the system (3.7) and suppose that the initial estimation error \mathbf{e}_0 (i.e. for $k = 0$) is unknown but belongs to an initial bounded set \mathcal{E}_0 . In addition, suppose that there exist $\mu_0 > 1$ such that $\mathcal{E}_0 \subset \bar{\Psi}_0$, $\bar{\Psi}_0$ defined in (3.37). Then, at every time-instant $k > 0$, the estimation error \mathbf{e}_k belongs to the hypercube:

$$\Omega_k := \{\mathbf{e} \in \mathbb{R}^n : -\bar{\mathbf{e}}_k \leq \mathbf{e}_k \leq \bar{\mathbf{e}}_k\} \quad (3.53)$$

with $\bar{\mathbf{e}}_k$ a column vector defined as

$$\bar{\mathbf{e}}_k := \bar{\mathbf{e}}_\infty \mu_k^{1/2} \quad (3.54)$$

where $\bar{\mathbf{e}}_\infty$ is a known constant column vector defined in (3.34), and $\mu_k \geq 1$ obeys:

$$\mu_{k+1} = (1 - \lambda)\mu_k + \lambda \quad (3.55)$$

Proof. Consider the RPI set (3.37). Because we assume that the initial estimation error belongs to this set, then, at every time instant, the estimation error belongs to the hypercube defined by the column vector

$$\bar{\mathbf{e}}_k = \text{diag} \left(\left(\frac{\mathbf{P}}{\mu_k \bar{c}} \right)^{-1/2} \right) \quad (3.56)$$

equivalently,

$$\bar{\mathbf{e}}_k = \bar{\mathbf{e}}_\infty \mu_k^{1/2} \quad (3.57)$$

that can be obtained by replacing (3.34) into (3.56) \square

Algorithm 3 H_∞ set-membership observer design for LPV systems.

Require: Matrices $\mathbf{A}_i, \mathbf{B}_i, \mathbf{F}_i$, for $i = \{1, \dots, N\}$, \mathbf{C} and \mathbf{Z} describing system (3.5). Disturbance covariance matrix \mathbf{W} . Initialization of $\mathbf{Q} = \mathbf{I}_n$.

- 1: **for** i **from** 1 **to** 2 **do**
 - 2: Find matrices \mathbf{P} , \mathbf{U}_i and the minimum γ who satisfy the LMI (2.22).
 - 3: Compute $\mathbf{L}_i = \mathbf{P}^{-1}\mathbf{U}_i$.
 - 4: Compute $\tilde{\mathbf{A}}_i = \mathbf{A}_i - \mathbf{L}_i\mathbf{C}$.
 - 5: Compute $\mathbf{E}_i = [\mathbf{F}_i \quad -\mathbf{L}_i\mathbf{Z}]$
 - 6: Using \mathbf{P} and γ , find a new matrix \mathbf{Q} which satisfies the LMI (3.20) and minimizes $(-\log(\det(\mathbf{Q})))$
 - 7: Compute λ as the minimum generalized eigenvalue of the pair (\mathbf{Q}, \mathbf{P}) .
 - 8: **if** $i = 1$ **then**
 - 9: Estimate the expected covariance matrix \mathbf{V} using (3.61)-(2.43).
 - 10: Do $\mathbf{Q} = \mathbf{V}^{-1}$.
 - 11: **end if**
 - 12: **end for**
 - 13: **return** observer parameters $\mathbf{L}_i, \mathbf{P}, \gamma$ and λ .
-

3.4 Set-membership observer design algorithm for LPV systems

The previous results can be used to perform a set-membership observer synthesis. Remark that the implementation of the observer (7)-(9) can be possible by using the system matrices $\mathbf{A}(\rho_k)$, $\mathbf{B}(\rho_k)$ and \mathbf{C} together with matrices $\mathbf{L}(\rho_k)$, \mathbf{P} , and the scalars γ and λ . In particular, the observer outputs (8)-(9) can use the estimation-error bounds (3.54) which are function of the matrix \mathbf{P} , the scalars γ and λ and the disturbance bounds $\bar{\mathbf{w}}$. Hence, the observer design process has to provide such necessary information. The complete proposed observer design process is summarized in Algorithm 1. The main steps will be explained in the following subsections.

3.4.1 Two iterations-based observer synthesis

The first part of the proposed algorithm uses Theorem 3.1 to compute \mathbf{P} , \mathbf{U}_i and the minimum γ which satisfy the LMI (3.13). Condition (3.13) requires the initialization of the matrix \mathbf{Q} . This matrix can be initialized as $\mathbf{Q} = \mathbf{I}_n$, where \mathbf{I}_n is an n -dimensional identity matrix.

Once \mathbf{P} and γ are found we can use condition (3.20), to find a more suitable matrix \mathbf{Q} . Thus, the matrix \mathbf{Q} becomes the only decision variable in condition (3.20), and can be chosen in order to minimize the volume of the ellipsoid (3.35). This is possible by minimizing $(-\log(\det(\mathbf{Q})))$ as proposed in [Hin06]. This minimization assures that this set is smaller or equal than that defined by the initial matrix \mathbf{Q} .

Now, it is possible to obtain a first version of the scalar λ satisfying (24) by computing λ as the minimum generalized eigenvalue of the pair (\mathbf{Q}, \mathbf{P}) . Remark that this scalar intervenes

into the computation of the estimation error bounds in steady state (3.34) but also intervenes into the computation of the evolution of such bounds, equation (3.54).

At this point, a first version of the matrices \mathbf{L}_i , for $i = \{1, \dots, N\}$, \mathbf{P} , and the scalars γ and λ are available.

The design process can be restarted by using a new initial matrix \mathbf{Q} . Here, the second part of the Algorithm 1 proposes a *suitable* choice of \mathbf{Q} . This choice is based on an *a posteriori* estimated steady-state covariance matrix for system (3.7). The next subsection explains the main motivation of this choice.

3.4.2 Using the a posteriori steady-state covariance matrix

Considering that the expected value of $\mathbf{e}_k \in \mathbb{R}^n$ in (3.7) is equal to zero, its steady-state covariance equal to \mathbf{V} and for any real number $t > 0$, we can use the multidimensional **Chebyshev's inequality**:

$$\Pr(\mathbf{e}_k^T \mathbf{V}^{-1} \mathbf{e}_k > t^2) \leq \frac{n}{t^2} \quad (3.58)$$

for computing a stochastic ellipsoidal set, where the symbol $\Pr(\cdot)$ stands for a probability measure on the probability space \mathbb{R}^n . This set is not an invariant set because there is a probability that some trajectories of the estimation error \mathbf{e} go out this set. However, its shape matrix can be used to update the dissipation matrix \mathbf{Q} during the observer design. Remember that matrix \mathbf{Q} is a symmetric positive definite matrix that can be arbitrarily chosen.

Remember also that the Lyapunov function only decreases if the following condition holds:

$$\mathbf{e}_k^T \mathbf{Q} \mathbf{e}_k > \gamma^2 \bar{\mathbf{w}}_k^T \bar{\mathbf{w}}_k \quad (3.59)$$

Remark that this deterministic condition has the same shape than the inequality (3.58), if we get $\mathbf{Q} = \mathbf{V}^{-1}$. In addition, the number of standard deviations, the real number t in (3.58), can be computed as $t = \sqrt{\gamma^2 \bar{\mathbf{w}}_k^T \bar{\mathbf{w}}_k}$ providing a probability less or equal than n/t^2 that the estimation trajectories can leaves this set (if we assume that the probability distribution of \mathbf{e} is unknown).

Therefore, the ellipsoidal set (3.35) can now be interpreted in an stochastic way.

Here, we propose to calculate the steady-state covariance matrix for system trajectories (3.7) as

$$\mathbf{V} := \frac{1}{N} \sum_{i=1}^N \mathbf{V}_i \quad (3.60)$$

which supposes identical probability of every vertex of the polytopic model. Of course, other possible ways to compute \mathbf{V} for system (3.7) can be used. The steady-state covariance of the estimation error of individual subsystems, denoted here \mathbf{V}_i , $i = \{1, \dots, N\}$, can be obtained by solving the following Lyapunov equation:

$$\tilde{\mathbf{A}}_i \mathbf{V}_i \tilde{\mathbf{A}}_i^T - \mathbf{V}_i = -\mathbf{E}_i \mathbf{W} \mathbf{E}_i^T \quad (3.61)$$

where the symbol \mathbf{W} represents the covariance matrix for disturbances \mathbf{w}_k in (3.7), which is assumed to be known.

In practical applications where the covariance matrix for disturbances is not available, we can assume that every element of the disturbance vector \mathbf{w}_k is uniform distributed but bounded in a given interval $[a \ b]$. In this case, its variance can be computed as

$$\mathbf{W} = \text{var}(\mathbf{w}_k) = \frac{1}{12}(b-a)^2 \mathbf{I}_m \quad (3.62)$$

Remark that the computation of \mathbf{V} is possible once the matrices $\tilde{\mathbf{A}}_i$ and \mathbf{E}_i are available. For this reason, Algorithm 1 iterates one more time using a new initial matrix $\mathbf{Q} = \mathbf{V}^{-1}$.

The synthesis of the set-membership observer is thus carry out in offline way using a two-iterations-based synthesis as it is explained in Section 3.4.1. The next Section presents the main issues concerning the observer implementation.

3.5 Set-membership observer implementation for LPV systems

3.5.1 Observer dynamical equations

Once the Algorithm 1 returns the observer parameters \mathbf{L}_i , \mathbf{P} , γ and λ , and after to initialize the scalar μ in a suitable way. The dynamical equations of the set-membership observer will be implemented as follows:

$$\hat{\mathbf{x}}_{k+1} = (\mathbf{A}(\rho_k) - \mathbf{L}(\rho_k)\mathbf{C})\hat{\mathbf{x}}_k + \mathbf{B}(\rho_k)\mathbf{u}_k + \mathbf{L}(\rho_k)\mathbf{y}_k \quad (3.63)$$

$$\mu_{k+1} = (1 - \lambda)\mu_k + \lambda \quad (3.64)$$

$$\bar{\mathbf{x}}_k = \hat{\mathbf{x}}_k + \bar{\mathbf{e}}_\infty \mu_k^{1/2} \quad (3.65)$$

$$\underline{\mathbf{x}}_k = \hat{\mathbf{x}}_k - \bar{\mathbf{e}}_\infty \mu_k^{1/2} \quad (3.66)$$

with a constant column vector:

$$\bar{\mathbf{e}}_\infty = \text{diag} \left(\left(\frac{\mathbf{P}}{\bar{c}} \right)^{-1/2} \right) \quad (3.67)$$

where $\bar{c} = \frac{1}{\lambda} \gamma^2 \bar{\mathbf{w}}^T \bar{\mathbf{w}}$.

The matrix $\mathbf{L}(\rho)$ can be computed online as follows

$$\mathbf{L}(\rho_k) = \sum_{i=1}^N \alpha_i \mathbf{L}_i \quad (3.68)$$

where $\alpha_i \geq 0$, for $i = \{1, \dots, N\}$, are the elements of the vector $\alpha \in \mathbb{R}^N$ which satisfies (3.2). That is, the vector $\alpha = \alpha_k$ can be obtained online, at every time-instant, as a solution of a linear programming problem.

The initial condition for the scalar μ can be obtained using the procedure proposed in Section 3.5.2.

The implementation of the proposed set-membership observer is relatively simple, since it only requires to extend its dynamics by including a scalar dynamical equation. Thus, the order of the set-membership state observer will be only of $n + 1$, for any n -order system, i.e. for $\mathbf{x} \in \mathbb{R}^n$.

3.5.2 Initialization of the scalar μ

3.5.2.1 Initial estimation error into a known ball

Now we are interesting in computing an appropriated initial value for the scalar μ . To do this, suppose that the initial condition for the estimation error verifies $\mathbf{e}(0) \in \mathcal{E}_0 \subseteq B_0$, where, for a given scalar $\delta \geq 0$, the ball B_0 defined as follows:

$$B_0 := \{\mathbf{e} \in \mathbb{R}^n : \mathbf{e}^T \mathbf{e} \leq \delta^2\} \quad (3.69)$$

will be included into the set

$$\bar{\Psi}_0 := \{\mathbf{e} \in \mathbb{R}^n : \mathbf{e}^T \mathbf{P} \mathbf{e} \leq \lambda_{max}(\mathbf{P}) \delta^2\} \quad (3.70)$$

Thus, using (3.37) and (3.70) a suitable initial value of μ verifies:

$$\mu_0 \bar{c} \geq \lambda_{max}(\mathbf{P}) \delta^2 \quad (3.71)$$

and then, we can chose any $\mu_0 \geq 1$ such that

$$\mu_0 \geq \lambda_{max}(\mathbf{P}) \delta^2 / \bar{c} \quad (3.72)$$

3.5.2.2 Initial estimation error inside a known polytope

Suppose that the initial estimation error set \mathcal{E}_0 is a polytope whose vertices are described by the vectors v_j , $j = \{1, \dots, p\}$, where p is the number of vertices.

In this case the vertices of the set \mathcal{E}_0 have to verify $v_j^T \mathbf{P} v_j \leq \mu_0 \bar{c}$, for all $j = \{1, \dots, p\}$, to guarantee that the set \mathcal{E}_0 is inside a RPI set of the form (3.37). Thus, we can chose μ_0 which solves the following problem:

$$\begin{aligned} & \text{minimize } \mu_0 \\ & \text{subject to} \end{aligned} \quad (3.73)$$

$$\mu_0 \geq 1 \quad (3.73)$$

$$v_j^T \mathbf{P} v_j \leq \mu_0 \bar{c} \quad (3.74)$$

for all $j = \{1, \dots, p\}$.

3.6 A numerical examples

3.6.1 Example 1

Consider a second order discrete-time LPV system (3.5) with matrices:

$$\mathbf{A}(\rho_k) = \begin{pmatrix} 1 & \rho_k \\ 0 & 1 \end{pmatrix}, \mathbf{B}(\rho_k) = \begin{pmatrix} 0 \\ \rho_k \end{pmatrix}, \mathbf{F}(\rho_k) = \begin{pmatrix} 0 \\ \rho_k \end{pmatrix}, \mathbf{C} = \begin{pmatrix} 1 & 0 \end{pmatrix}$$

and $\mathbf{Z} = 0.01$, where the scheduling parameter ρ_k can vary into the interval $(0.050, 0.100)$, as it is depicted in Figure 3.4, i.e. the vertices of the polytopic set Ω_ρ will be $\underline{\rho} = 0.050$ and $\bar{\rho} = 0.100$.

After applying the Algorithm 3, the obtained matrices which describe the set-membership state observer are:

$$\mathbf{L}_1 = \begin{pmatrix} 1.4649 \\ 9.2965 \end{pmatrix}, \mathbf{L}_2 = \begin{pmatrix} 1.9299 \\ 9.2990 \end{pmatrix}$$

$$\mathbf{P} = 1e4 \begin{pmatrix} 3.2498 & -0.3381 \\ -0.3381 & 0.0428 \end{pmatrix}$$

and the scalars: $\gamma = 2.5720$ and $\lambda = 0.4586$.

We suppose that for all k , the disturbances \mathbf{w}_k are random variables with uniform distribution but bounded by the vector $\bar{\mathbf{w}} = [1 \ 1]^T$. That is, $-\bar{\mathbf{w}} \leq \mathbf{w}_k \leq \bar{\mathbf{w}}$.

In this example, we consider a constant system input $\mathbf{u}_k = 10$ for time-instants $k < 10$. After the time-instant $k \geq 10$ the system input is $\mathbf{u}_k = 0$. The set-membership state observer has been implemented using equations (3.63)-(3.66). The initial conditions for the observer states $\hat{\mathbf{x}}$ and the scalar μ are: $\hat{\mathbf{x}}_0 = (0 \ 0)^T$ and $\mu_0 = 117.4504$, respectively. The latter has been computed by solving (3.73)-(3.74) by considering $(-0.1 \ -2)^T \leq \mathbf{x}_0 \leq (0.1 \ 2)^T$.

Figure 3.3 illustrates the behavior of the observer. The dashed lines correspond to the bounds obtained from the set-membership state observer. For comparison, we have included the solid lines which corresponds to the real system state. Remark that the obtained bounds are very accurate for both during the transient and during the steady-state periods.

Figure 3.5 depicts the behavior of the scalar μ_k during the whole period of the estimation. Remark that even if its value starts at 117.4504, it converges asymptotically to 1 with a behavior compatible with the estimation error dynamics.

In Figure 3.6, the solid-line ellipsoid corresponds to the obtained RPI set used for computing *deterministic* bounds of the estimation error (for $\mu = 1$). The dashed-line corresponds to the stochastic ellipsoidal defined by (3.58) with $t = 3.6374$. Remark that the obtained RPI set has taken a shape that is very close to that characterizing the states covariances.

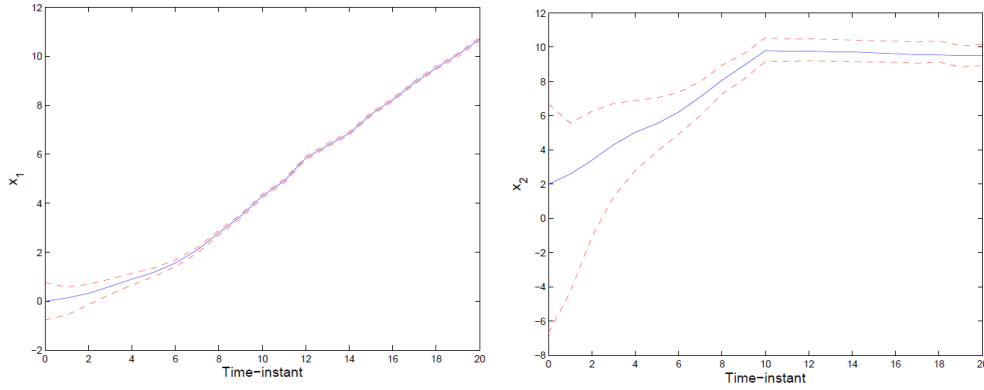


Figure 3.3: Set-membership estimation. The dashed lines correspond to the bounds obtained from the set-membership state observer. For comparison, the solid lines corresponds to the real system state.

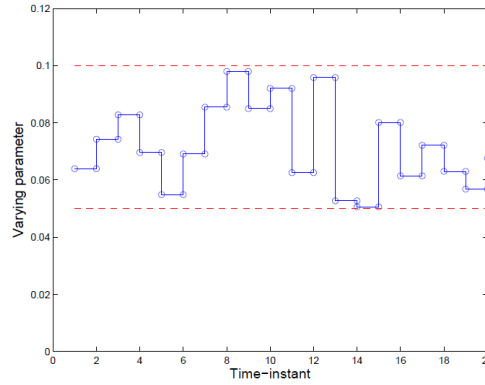


Figure 3.4: The scheduling parameter ρ_k .

3.6.2 Example 2

Consider the following discrete-time Lorenz model, as proposed in [Che+13], written in a LPV form (3.5), with matrices:

$$\mathbf{A}(\rho_k) = \begin{pmatrix} 1 - T_s\sigma & T_s\sigma & 0 \\ 0 & 1 - T_s\eta & -T_s\rho_k(1) \\ 0 & T_s\rho_k(1) & 1 - T_s\rho_k(2) \end{pmatrix}, \quad \mathbf{B}(\rho_k) = \begin{pmatrix} 0 \\ T_s\rho_k(1) \\ 0 \end{pmatrix}, \quad \mathbf{F}(\rho_k) = \begin{pmatrix} 0 \\ T_s\rho_k(1) \\ 0 \end{pmatrix}, \quad \mathbf{C} = (1 \ 0 \ 0)$$

and $\mathbf{Z} = 0$. The constant parameters are $\sigma = 1$, $\eta = 10$ and $T_s = 0.08$. The scheduling parameter $\rho_k = [\rho_k(1) \ \rho_k(2)]^T$ can vary into the following interval

$$\begin{pmatrix} -1 \\ 9 \end{pmatrix} \leq \begin{pmatrix} \rho_k(1) \\ \rho_k(2) \end{pmatrix} \leq \begin{pmatrix} 1 \\ 11 \end{pmatrix} \quad (3.75)$$

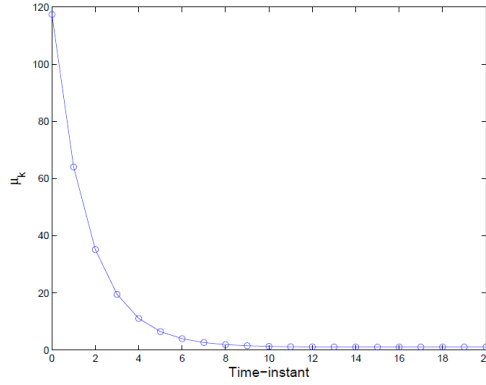


Figure 3.5: Evolution of the scalar μ_k . This scalar characterizes the contraction of the initial RPI set. The value of μ_k converges to 1 as $k \rightarrow \infty$.

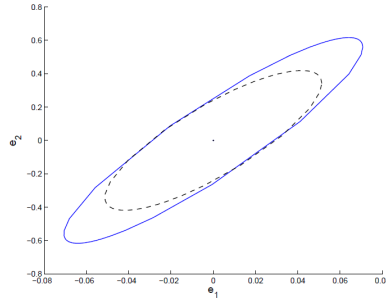


Figure 3.6: Minimal ellipsoidal RPI set and steady-state covariance for the estimation error dynamics. The solid line corresponds to the obtained RPI set used for computing *deterministic* bounds of the estimation error. The dashed line corresponds to the stochastic ellipsoidal defined by (3.58) with a number of standard deviation t equal to 3.6374.

That is, the 4 vertices of the polytopic set Ω_{ρ_k} will be $\theta_1 = [-1 \ 9]$, $\theta_2 = [-1 \ 11]$, $\theta_3 = [1 \ 9]$ and $\theta_4 = [1 \ 11]$.

After applying the Algorithm 2, the obtained matrices which describe the set-membership state observer are, for $i = \{1, 2, 3, 4\}$:

$$\mathbf{L}_1 = \begin{pmatrix} 1.0984 \\ 0.4460 \\ -0.1783 \end{pmatrix}, \quad \mathbf{L}_2 = \begin{pmatrix} 1.0983 \\ 0.4458 \\ -0.1783 \end{pmatrix}, \quad \mathbf{L}_3 = \begin{pmatrix} 1.0984 \\ 0.4460 \\ 0.1783 \end{pmatrix}, \quad \mathbf{L}_4 = \begin{pmatrix} 1.0983 \\ 0.4458 \\ 0.1783 \end{pmatrix}$$

$$\mathbf{P} = 1e3 \begin{pmatrix} 6.7285 & -0.5728 & 0 \\ -0.5728 & 0.2397 & 0 \\ 0 & 0 & 9.9395 \end{pmatrix}$$

and the scalars: $\gamma = 1.2391$ and $\lambda = 0.4884$. These observer parameters have been obtained

by using the following matrix \mathbf{Q} :

$$\mathbf{Q} = 1e3 \begin{pmatrix} 6.1199 & -0.2997 & 0 \\ -0.2997 & 0.1172 & 0 \\ 0 & 0 & 7.1422 \end{pmatrix} \quad (3.76)$$

which corresponds to the inverse of the estimation-error covariance matrix \mathbf{V} , as proposed in Section 3.4.2.

In order to compare the results with respect to those presented in **Efimov2013** in this simulation we consider $\rho_k(1) = x_k(1)$ and $\rho_k(2) = \beta$ with $\beta = 10$. In addition, we suppose that for all time-instants k , the system input $\mathbf{u}_k = 10$ and, the disturbances \mathbf{w}_k are:

$$\mathbf{w}_k = \begin{pmatrix} 2 \sin(0.5T_s k) \\ 0 \end{pmatrix} \quad (3.77)$$

That is, $-\bar{\mathbf{w}} \leq \mathbf{w}_k \leq \bar{\mathbf{w}}$, with $\bar{\mathbf{w}} = [2 \ 0]^T$. The set-membership state observer has been implemented using equations (3.63)-(3.66). The initial conditions for the observer states $\hat{\mathbf{x}}$ and the scalar μ are: $\hat{\mathbf{x}}_0 = (0.5 \ 0 \ 0)^T$ and $\mu_0 = 197.59$, respectively. The latter has been computed by solving (3.73)-(3.74) by considering $(0.5 \ 0 \ 0.5)^T \leq \mathbf{x}_0 \leq (0.5 \ 0 \ -0.5)^T$.

Figure 3.7, 3.8 and 3.9 illustrate the behavior of the observer. The dashed lines correspond to the bounds obtained from the set-membership state observer. For comparison, we have included the solid lines which corresponds to the real system state. Remark that the obtained bounds are very accurate for both during the transient and during the steady-state periods.

Figure 3.10 depicts the behavior of the scalar μ_k during the whole period of the estimation. Remark that even if its value starts at 197.59, it converges asymptotically to 1 with a behavior compatible with the estimation error dynamics.

In Figure 3.11, the yellow ellipsoid corresponds to the obtained RPI set used for computing *deterministic* bounds of the estimation error (for $\mu = 1$). The green one corresponds to the stochastic ellipsoidal defined by (2.41) with $t = \sqrt{\gamma^2 \bar{\mathbf{w}}^T \bar{\mathbf{w}}} = 2.478$. Remark that the obtained RPI set has taken a shape that is very close to that characterizing the states covariances.

In this example the obtained steady state estimation-error bounds are:

$$\bar{\mathbf{e}}_\infty = \begin{pmatrix} 0.0484 \\ 0.2567 \\ 0.0356 \end{pmatrix} \quad (3.78)$$

which are clearly less conservative than that presented in [Che+13]. The complexity of the proposed observer here mainly depends on the number of vertices describing the polytopic set Ω_ρ , see Section 3.1.2. The complexity is then similar to any polytopic LPV observers, see for instance [HMD13].

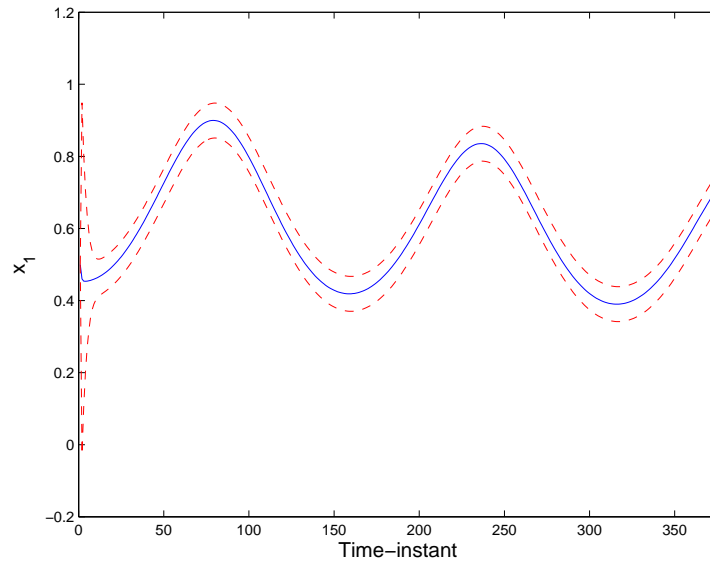
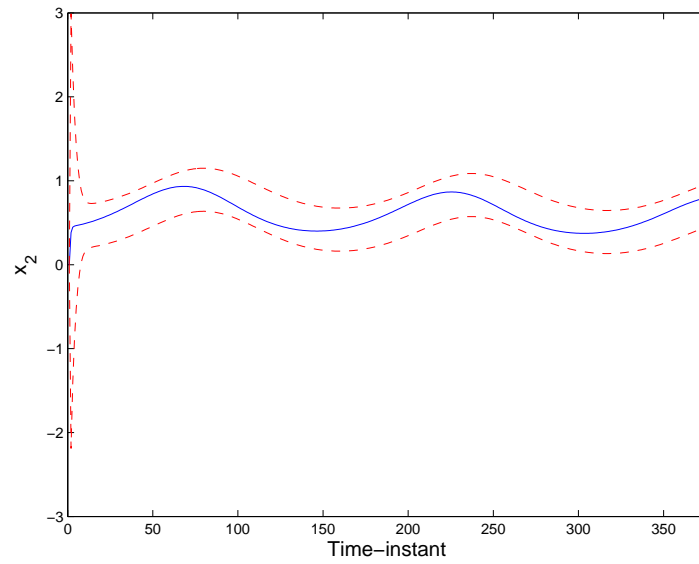
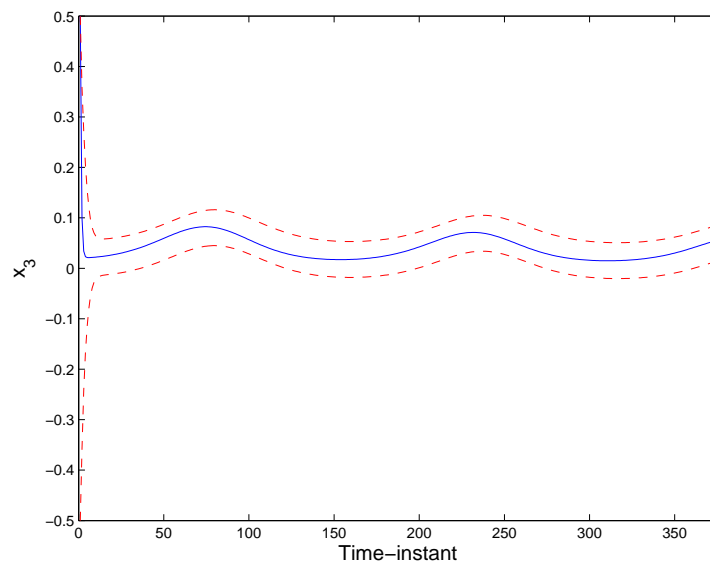


Figure 3.7: Estimated bounds for system state $x_k(1)$.

3.7 Conclusion

In this chapter we have presented an extension of the set-membership observer based on ellipsoidal invariant sets for the more general case of LPV systems. Thanks to the polytopic decomposition of LPV systems, we can transform it into a family of N linear systems (describing a polytopic system). It is shown that the implementation of the observer is very simple, and it is comparable to the implementation of standard state observers.

Figure 3.8: Estimated bounds for system state $x_k(2)$.Figure 3.9: Estimated bounds for system state $x_k(3)$.

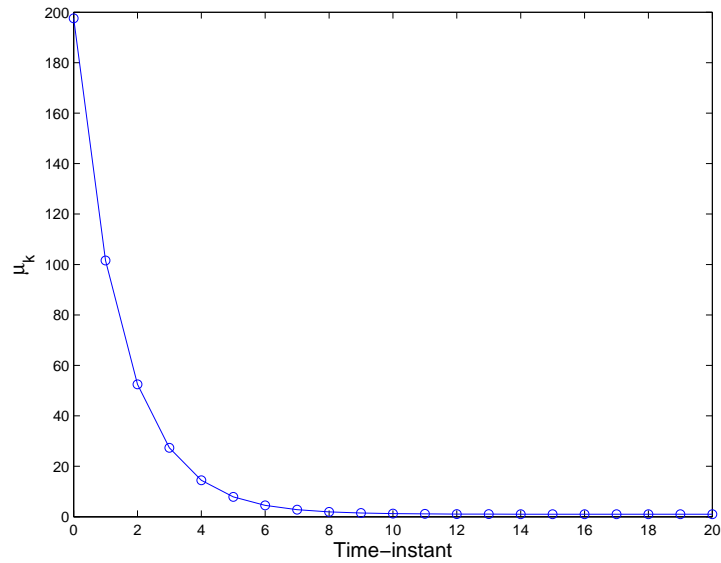


Figure 3.10: Evolution of the scalar μ_k for the second example. This scalar characterizes the contraction of the initial RPI set. The initial value of μ_k guarantee the inclusion of the initial estimation-error set. The value of μ_k converges to 1 as $k \rightarrow \infty$. Remark the fast convergence.

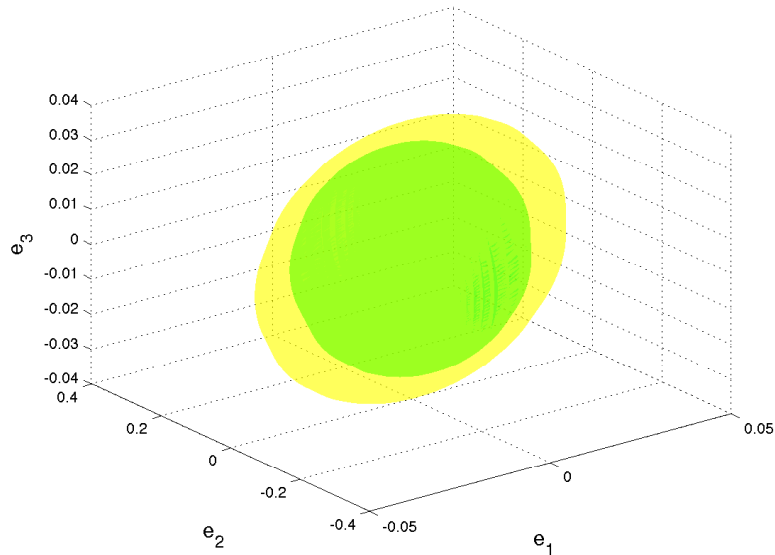


Figure 3.11: Steady state ellipsoidal RPI set, for the estimation error dynamics, which includes an stochastic set with a scalar $t = 2.478$.

Contents

4.1	Introduction	79
4.2	Problem statement	80
4.3	Observers design based on interval analysis	81
4.3.1	H_∞ observer gain design	82
4.3.2	Characterization of all possible estimation errors	82
4.3.3	Convergence towards an outer-approximation of the ultimate-bound	85
4.3.4	Guaranteed framing of the real state vector	85
4.4	Observers design based on intervals and invariant sets	86
4.5	Illustrative examples	89
4.5.1	Example 1	89
4.5.2	Example 2	92
4.6	Extension to a class of nonlinear systems	97
4.6.1	H_∞ observer gain design	98
4.6.2	Interval characterization of the estimation errors	98
4.6.3	Illustrative example	99
4.7	Conclusion	100

4.1 Introduction

During the last decades, various approaches based on interval analysis have been developed to design interval observers. These approaches provide a guaranteed enclosure of all possible state trajectories of the system which are consistent with the mathematical model, the state disturbances and the measurement noises.

We propose in this chapter a new approach to design an interval observer for uncertain linear discrete-time systems, simple to implement, with less computation time and reduced complexity. The set-membership state estimation problem is considered as a punctual state estimation issue coupled with an interval characterization of the estimation error. A non pessimistic numerical scheme to compute a rigorous enclosure of the estimation error is proposed.

This chapter is organized as follows: the problem statement is introduced in Section 4.2, after that Section 4.3 shows the first main contribution of this chapter which is the design of the fully interval observer for uncertain linear discrete-time systems. Section 4.4 is devoted to

the second contribution of this chapter which is combining set invariance theory and interval analysis to design an observer allowing to enhance the precision at the steady-state regime and reducing the on-line computation time. Illustrative examples are presented in the Section 4.5 to show the performance of the proposed observer. An extension of this approach to a class of nonlinear uncertain systems is presented in the Section 4.6. This chapter ends with a conclusion.

4.2 Problem statement

Let's consider again a discrete-time linear system described by (4.1)

$$\begin{cases} \mathbf{x}_{k+1} &= \mathbf{A}\mathbf{x}_k + \mathbf{B}\mathbf{u}_k + \mathbf{F}\mathbf{d}_k \\ \mathbf{y}_k &= \mathbf{C}\mathbf{x}_k + \mathbf{Z}\mathbf{v}_k \end{cases} \quad (4.1)$$

where $\mathbf{x}_k \in \mathbb{R}^{n_x}$ is the state vector, $\mathbf{u}_k \in \mathbb{R}^{n_u}$ is the input vector and $\mathbf{y}_k \in \mathbb{R}^{n_y}$ is the measured output vector and the pair (\mathbf{A}, \mathbf{C}) is assumed observable. The vectors \mathbf{d}_k and \mathbf{v}_k are respectively the state perturbation and the measurement noise which are assumed unknown but bounded with known bounds, i.e:

$$\begin{aligned} \forall k \geq 0, \quad \mathbf{d}_k &\in [\underline{\mathbf{d}}, \bar{\mathbf{d}}] \subset \mathbb{R}^{n_d} \\ \forall k \geq 0, \quad \mathbf{v}_k &\in [\underline{\mathbf{v}}, \bar{\mathbf{v}}] \subset \mathbb{R}^{n_v} \end{aligned} \quad (4.2)$$

where the real vectors $\underline{\mathbf{d}}$ and $\bar{\mathbf{d}}$ (resp. $\underline{\mathbf{v}}, \bar{\mathbf{v}}$) are the lower and upper bounds of the box $[\mathbf{d}]$ (resp. $[\mathbf{v}]$).

Suppose that we can design a Luenberger observer (4.3) for the system (4.1)

$$\hat{\mathbf{x}}_{k+1} = (\mathbf{A} - \mathbf{L}\mathbf{C})\hat{\mathbf{x}}_k + \mathbf{B}\mathbf{u}_k + \mathbf{L}\mathbf{y}_k \quad (4.3)$$

where $\mathbf{L} \in \mathbb{R}^{n_x \times n_y}$ is the observation gain that guarantees the stability of the dynamics of the estimation error.

The estimation error at a given instant k can be calculated as follows:

$$\mathbf{e}_k = \mathbf{x}_k - \hat{\mathbf{x}}_k \quad (4.4)$$

From (4.1) and (4.3) and using (4.4), the dynamics of the estimation error can be obtained as follows:

$$\mathbf{e}_{k+1} = \mathbf{A}_o\mathbf{e}_k + \mathbf{E}\mathbf{w}_k \quad (4.5)$$

where $\mathbf{A}_o = (\mathbf{A} - \mathbf{L}\mathbf{C})$, $\mathbf{E} = [\mathbf{F} \quad -\mathbf{L}\mathbf{Z}]$ and $\mathbf{w}_k = \begin{pmatrix} \mathbf{d}_k \\ \mathbf{v}_k \end{pmatrix}$ with $\mathbf{w}_k \in \mathbb{R}^m$ and $m = n_d + n_v$.

Now suppose that we know at every time-instant a box, denoted by $[\mathbf{e}_k]$, which includes in a guaranteed way all possible estimation error \mathbf{e}_k , i.e:

$$\forall k \geq 0, \quad \mathbf{e}_k \in [\mathbf{e}_k] \quad (4.6)$$

with $[\mathbf{e}_k] = [\underline{\mathbf{e}}_k, \bar{\mathbf{e}}_k]$, where $\underline{\mathbf{e}}_k$ and $\bar{\mathbf{e}}_k$ are the lower and upper bounds of the box $[\mathbf{e}_k]$.

So, at every time-instant, we can guarantee that the real system state \mathbf{x}_k belongs to a box denoted $[\mathbf{x}_k]$ defined as follows: $[\mathbf{x}_k] = \hat{\mathbf{x}}_k + [\mathbf{e}_k]$.

In this case, an interval observer can be designed as follows:

$$\hat{\mathbf{x}}_{k+1} = \mathbf{A}_o \hat{\mathbf{x}}_k + \mathbf{B} \mathbf{u}_k + \mathbf{L} \mathbf{y}_k \quad (4.7)$$

$$[\mathbf{x}_k] = \hat{\mathbf{x}}_k + [\mathbf{e}_k] \quad (4.8)$$

Therefore the set-membership estimation problem is considered as a punctual state estimation issue coupled with an interval characterization of the estimation error. On other words, the proposed interval observer provides at every time-instant an estimated state vector $\hat{\mathbf{x}}_k$ and a bounded box $[\mathbf{e}_k]$ of the estimation error such that the real state vector is included in the box $[\mathbf{x}_k]$ defined by (4.8).

We will present two versions of the proposed observer:

- (i) A fully interval version which requires an on-line characterization of the estimation error boxes.
- (ii) A second version which combines interval analysis with invariant set computation to improve the accuracy of the estimated state enclosure and to allow an off-line characterization of the set of the estimation error.

4.3 Observers design based on interval analysis

In this section we will present the first version of the proposed observer which is a fully interval observer, where the characterization of the boxes including all possible estimation errors is done on-line. The following proposition states the first result.

Proposition 4.1

If the pair (\mathbf{A}, \mathbf{C}) is detectable, then the punctual-interval dynamical system (4.9) - (4.12) is an interval observer for the uncertain system (4.1).

$$\hat{\mathbf{x}}_{k+1} = \mathbf{A}_o \hat{\mathbf{x}}_k + \mathbf{B} \mathbf{u}_k + \mathbf{L} \mathbf{y}_k \quad (4.9)$$

$$[\mathbf{e}_{k+1}] = \mathbf{A}_o^{k+1} [\mathbf{e}_0] + [\mathbf{g}_k] \quad (4.10)$$

$$[\mathbf{g}_{k+1}] = \mathbf{A}_o^{k+1} [\mathbf{g}_0] + [\mathbf{g}_k] \quad (4.11)$$

$$[\mathbf{x}_{k+1}] = \hat{\mathbf{x}}_{k+1} + [\mathbf{e}_{k+1}] \quad (4.12)$$

where

$$\mathbf{A}_o = (\mathbf{A} - \mathbf{L}\mathbf{C})$$

$$\mathbf{E} = (\mathbf{F} - \mathbf{LZ}), \quad [\mathbf{w}] = ([\mathbf{d}], [\mathbf{v}])^T, \quad [\mathbf{g}_0] = \mathbf{E}[\mathbf{w}]$$

The initial condition $\hat{\mathbf{x}}_0$ of the punctual dynamics (4.9) belongs into the initial box $[\mathbf{x}_0]$ of the uncertain system (4.1). Thus, the interval dynamics (4.10),(4.11) is initialized with $[\mathbf{e}_0] = [\mathbf{x}_0] - \hat{\mathbf{x}}_0$.

The punctual Luenberger observer (4.9) generates a nominal state trajectory where the system's uncertainties are neglected. Then, the effect of these uncertainties on the quality of the estimated nominal state trajectory is characterized by the interval dynamics (4.10). Finally, a tight outer-enclosure of all the possible state trajectories of the uncertain system (4.1) is given by the output equation (4.12).

The proof of this Proposition will be presented step by step in the next Subsections 4.3.1, 4.3.2, 4.3.3 and 4.3.4.

4.3.1 H_∞ observer gain design

Let's consider the discrete-time linear system described by (4.1). The observer (4.9) provides the punctual state estimation $\hat{\mathbf{x}}$ where the observer gain \mathbf{L} has to attenuate the effect of the disturbances on the estimation error. To ensure that, an H_∞ observer synthesis similar to the one introduced in the Subsection 2.1 of Chapter 2 is applied. Let's recall the statement of the H_∞ observer gain synthesis:

Proposition 4.2

Considering the estimation error dynamics (4.5). The observer gain \mathbf{L} which allows to attenuate the impact of the disturbances on the estimation error exists if there exists a symmetric positive definite matrices \mathbf{P} and \mathbf{U} satisfying the following LMI:

$$\begin{pmatrix} -\mathbf{P} + \mathbf{I}_n & 0_{n_x \times m} & \mathbf{A}^T \mathbf{P} - \mathbf{C}^T \mathbf{U}^T \\ 0_{m \times n_x} & -\gamma^2 \mathbf{I}_m & [\mathbf{P}\mathbf{F} - \mathbf{U}\mathbf{Z}]^T \\ \mathbf{P}\mathbf{A} - \mathbf{U}\mathbf{C} & [\mathbf{P}\mathbf{F} - \mathbf{U}\mathbf{Z}] & -\mathbf{P} \end{pmatrix} \preceq 0 \quad (4.13)$$

Moreover, the observer gain is obtained as follow:

$$\mathbf{L} = \mathbf{P}^{-1} \mathbf{U} \quad (4.14)$$

Proof. See the Proposition 2.1 and it's proof 2.3.1. □

4.3.2 Characterization of all possible estimation errors

This subsection is dedicated to the interval characterization of the estimation error given by the equation (4.10,4.11). The novelty here is that we propose a non pessimistic scheme to compute a tight enclosure of the estimation error. This result is presented in the following proposition:

Proposition 4.3

For all $\mathbf{e}_0 \in [\mathbf{e}_0]$ and for all $\mathbf{w}_k \in [\mathbf{w}]$, $k = 1, \dots, n$, the interval dynamic defined by the equation ((4.10),4.11) provides a non pessimistic outer enclosure of the estimation error $[\mathbf{e}_k]$ which includes all possible estimation errors generated from the initial set.

Proof. Considering the estimation error given by (4.5). All the possible evolution of this estimation error can be framed by applying interval analysis [Moo66]; [Jau+01],

$$[\mathbf{e}_{k+1}] = \mathbf{A}_o[\mathbf{e}_k] + [\mathbf{g}_0] \quad (4.15)$$

As shown in Figure (4.1), due to the wrapping effect the direct interval iteration (4.15) is too pessimistic [Moo66]; [Jau+01]. In fact, at each iteration a pessimism is introduced and propagated to the next iteration. Consequently, the accumulation of this pessimism on a long period leads to too large enclosures and maybe numerical unstable behavior.

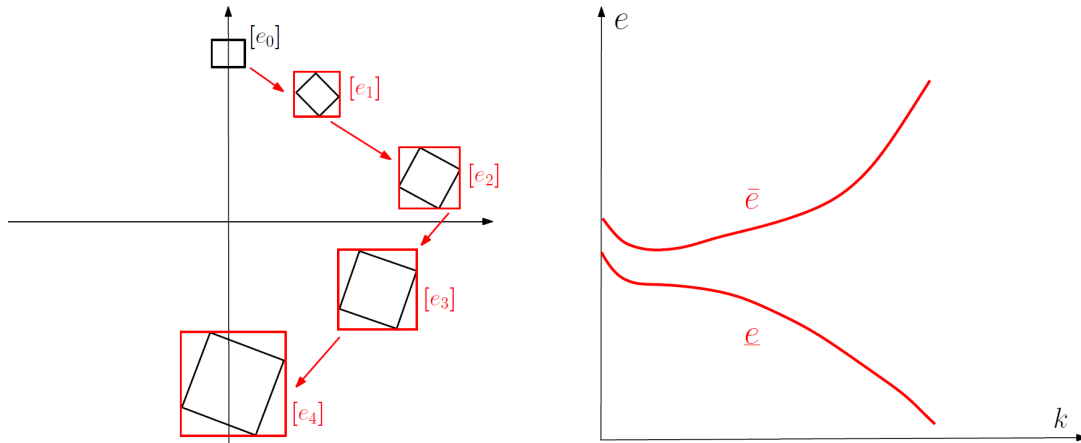


Figure 4.1: Over-estimation linked to the wrapping effect. Usually, framing at each iteration the set of the solutions by an axis-aligned box led to too pessimistic enclosures of the solutions for the large values of k .

To cope with this undesirable wrapping effect, we propose a new expression for (4.15). By definition, any sequence of size $k + 1$ generated by (4.15) from $[\mathbf{e}_0]$ can be presented as follows:

$$\begin{aligned} \mathbf{e}_1 &= \mathbf{A}_o \mathbf{e}_0 + \mathbf{E} \mathbf{w}_0 \in \mathbf{A}_o[\mathbf{e}_0] + [\mathbf{g}_0] \\ \mathbf{e}_2 &= \mathbf{A}_o \mathbf{e}_1 + \mathbf{E} \mathbf{w}_1 = \mathbf{A}_o^2 \mathbf{e}_0 + \mathbf{A}_o \mathbf{E} \mathbf{w}_0 + \mathbf{E} \mathbf{w}_1 \\ &\in \mathbf{A}_o^2[\mathbf{e}_0] + \mathbf{A}_o[\mathbf{g}_0] + [\mathbf{g}_0] \\ &\in \mathbf{A}_o^2[\mathbf{e}_0] + [\mathbf{g}_1] \end{aligned} \quad (4.16)$$

where $[\mathbf{g}_1] = \mathbf{A}_o[\mathbf{g}_0] + [\mathbf{g}_0]$. Now, for the next iteration one gets,

$$\begin{aligned}
 \mathbf{e}_3 &= \mathbf{A}_o \mathbf{e}_2 + \mathbf{E} \mathbf{w}_2 = \mathbf{A}_o^3 \mathbf{e}_0 + \mathbf{A}_o^2 \mathbf{E} \mathbf{w}_0 + \mathbf{A}_o \mathbf{E} \mathbf{w}_1 + \mathbf{E} \mathbf{w}_2 \\
 &\in \mathbf{A}_o^3 [\mathbf{e}_0] + \mathbf{A}_o^2 [\mathbf{g}_0] + \mathbf{A}_o [\mathbf{g}_0] + [\mathbf{g}_0] \\
 &\in \mathbf{A}_o^3 [\mathbf{e}_0] + \mathbf{A}_o^2 [\mathbf{g}_0] + [\mathbf{g}_1] \\
 &\in \mathbf{A}_o^3 [\mathbf{e}_0] + [\mathbf{g}_2]
 \end{aligned} \tag{4.17}$$

where $[\mathbf{g}_2] = \mathbf{A}_o^2 [\mathbf{g}_0] + [\mathbf{g}_1]$. Thus, in the same way, for each iteration $k+1$ one can characterize the estimation error by:

$$\mathbf{e}_{k+1} = \mathbf{A}_o \mathbf{e}_k + \mathbf{E} \mathbf{w}_k \in \mathbf{A}_o^{k+1} [\mathbf{e}_0] + [\mathbf{g}_k] \tag{4.18}$$

where $[\mathbf{g}_k] = \mathbf{A}_o^k [\mathbf{g}_0] + [\mathbf{g}_{k-1}]$.

Hence, it is clear that the equation (4.18) is exactly the interval dynamics (4.10)-(4.11) of the proposed interval observer. In this way one can compute a tight enclosure of all the possible estimation errors without wrapping effect. As illustrated in Figure 4.2, thanks to this new formula one can compute at each time instant t_k , $k \in \{0, \dots, N\}$ the minimal inclusion function of the set of the estimation error. In other terms, there is no dependency phenomenon or wrapping effect in (4.10)-(4.11), which describes the error propagation on the observation horizon. Notice that, the recursive equation (4.11) does not generate conservatism because the vectors \mathbf{w}_k are not the same at each time instant k .

Remark 4.1

In order to reduce the on-line computation, the matrices \mathbf{A}_o^{k+1} , $k = 0, \dots, N$ are computed in an iterative way $\mathbf{A}_o^{k+1} = \mathbf{A}_o^k \mathbf{A}_o$.

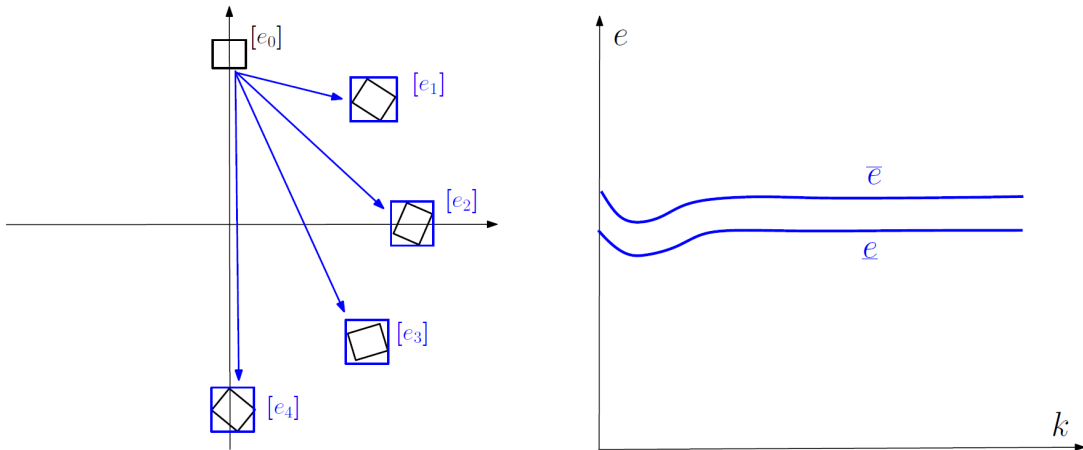


Figure 4.2: Minimal inclusion function, at each time instant k , of the estimation error. No wrapping effect nor the dependency phenomenon in the proposed numerical scheme (4.10).

□

4.3.3 Convergence towards an outer-approximation of the ultimate-bound

The steady state of the interval dynamics (4.10)-(4.11) is bounded by the following limit

$$\lim_{k \rightarrow +\infty} [\mathbf{e}_{k+1}] = \lim_{k \rightarrow +\infty} \mathbf{A}_o^{k+1}[\mathbf{e}_0] + \lim_{k \rightarrow +\infty} [\mathbf{g}_k] \quad (4.19)$$

Since the pair (\mathbf{A}, \mathbf{C}) is observable, the observer gain \mathbf{L} is chosen such that the eigenvalues λ_i of the matrix \mathbf{A}_o satisfy

$$|\lambda_i| < 1, \quad \forall i = 1, \dots, n_x \quad (4.20)$$

Then, based on (4.20) and the properties of Schur stable matrices, one can state that

$$\lim_{k \rightarrow +\infty} \mathbf{A}_o^{k+1} = 0 \quad (4.21)$$

Now, using (4.21) one can show that at the steady state the box generated by (4.11) is bounded

$$[\mathbf{g}_{k+1}] = \lim_{k \rightarrow +\infty} \mathbf{A}_o^{k+1}[\mathbf{g}_0] + [\mathbf{g}_k] = [\mathbf{g}_k] = [\mathbf{g}] \quad (4.22)$$

and the ultimate-bound of the estimation error (4.10) converges towards the same box

$$\lim_{k \rightarrow +\infty} [\mathbf{e}_{k+1}] = \lim_{k \rightarrow +\infty} \mathbf{A}_o^{k+1}[\mathbf{e}_0] + \lim_{k \rightarrow +\infty} [\mathbf{g}_k] = [\mathbf{g}] \quad (4.23)$$

which shows the practical stability of the interval observer introduced in Proposition 4.1. This completes the proof of this proposition.

4.3.4 Guaranteed framing of the real state vector

The output of the observer $[\mathbf{x}_{k+1}]$ described by the equation (4.12) is guaranteed to contain all the possible state trajectories consistent with the mathematical model, the bounds of the state disturbances and the bounds of the measurement noises. For an unknown but bounded initial condition $\forall \mathbf{x}_0 \in [\mathbf{x}_0]$, at each iteration all the possible states are included in $[\mathbf{x}_k]$:

$$\forall k : \quad \mathbf{x}_k \in [\mathbf{x}_k] \quad (4.24)$$

where $[\mathbf{x}_k] = \hat{\mathbf{x}}_k + [\mathbf{e}_k]$

We have

$$\mathbf{x}_k = \hat{\mathbf{x}}_k + \mathbf{e}_k \quad (4.25)$$

The punctual observer (4.9) is initialized at $\hat{\mathbf{x}}_0 \in [\mathbf{x}_0]$, then the initial box of the dynamics of the estimation error (4.10) is $[\mathbf{e}_0] = [\mathbf{x}_0] - \hat{\mathbf{x}}_0$. At each iteration, the interval $[\mathbf{e}_k]$ contains all possible estimation errors. Since, by definition $\mathbf{x}_k - \hat{\mathbf{x}}_k \in [\mathbf{e}_k]$, we can easily deduce that:

$$\forall k, \mathbf{x}_k \in [\mathbf{x}_k] = \hat{\mathbf{x}}_k + [\mathbf{e}_k] \quad (4.26)$$

4.4 Observers design based on intervals and invariant sets

In practice, reducing the on-line computation is required to face with both constraints on the computational resources and the swiftness of the monitored systems. In this subsection, an interval observer with less on-line computation, with respect to the first proposed observer, is introduced. To do that, we propose an off-line method to characterize the set of all the possible estimation errors.

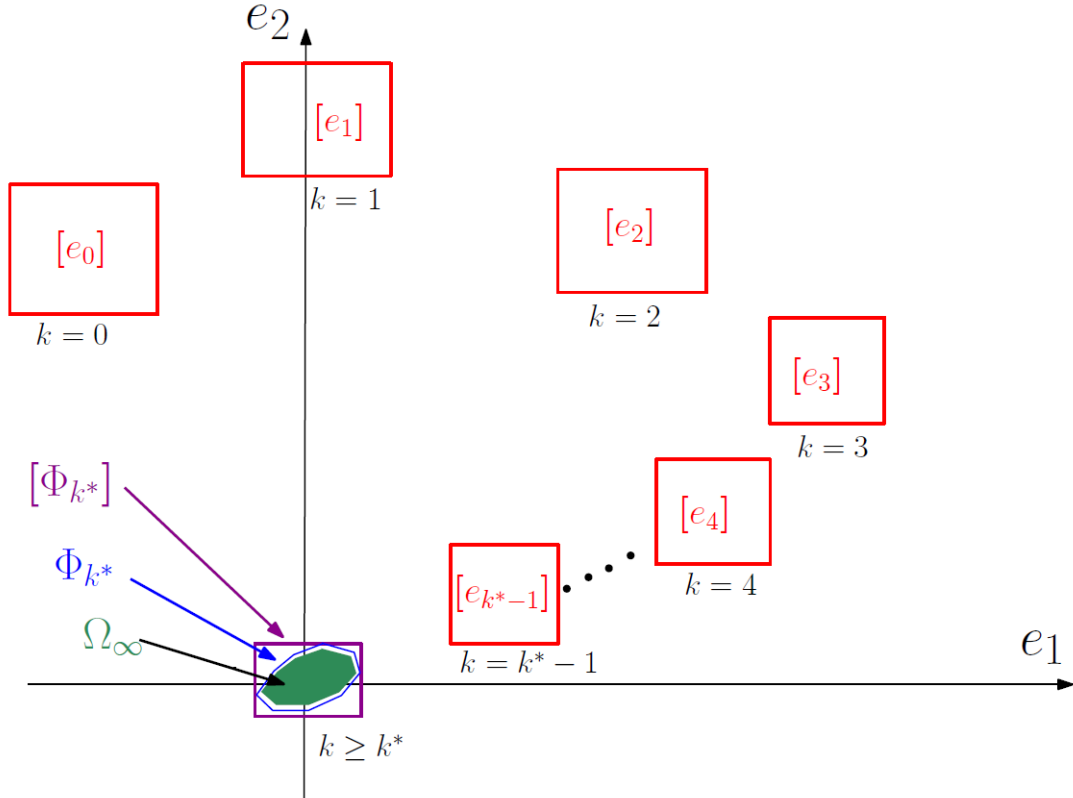


Figure 4.3: Thanks to interval and invariant set computations all the possible estimation errors, for all $k \geq 0$, are characterized by a small finite number k^* of boxes.

As shown in Figure (4.3), this method combines interval and invariant set computations to generate an interval sequence $\{[s_k]\}_{k=0, \dots, k^*}$ with finite number of values k^* such that:

$$\forall k \geq 0, \forall \mathbf{w}_k \in [\mathbf{w}] \quad \mathbf{e}_k \in [s_k] = \begin{cases} [\mathbf{e}_k] & \text{if } k \leq k^* \\ [s_{k^*+1}] = [s_{k^*}] & \text{if } k > k^* \end{cases} \quad (4.27)$$

where k^* is a positive integer. More formally, for $k = 1, 2, \dots, k^* - 1$ the outer-approximation of the estimation error is computed by:

$$\begin{aligned} [s_{k+1}] &= \mathbf{A}_o^{k+1}[\mathbf{e}_0] + [\mathbf{g}_k] \\ [\mathbf{g}_{k+1}] &= \mathbf{A}_o^{k+1}[\mathbf{g}_0] + [\mathbf{g}_k] \end{aligned} \quad (4.28)$$

where $[\mathbf{g}_0] = \mathbf{E}[\Delta \mathbf{w}]$ and $\mathbf{E} = (\mathbf{F} - \mathbf{LZ})$ and the box $[\Delta \mathbf{w}]$ is computed from $[\mathbf{w}]$ as in (1.15) and (1.16).

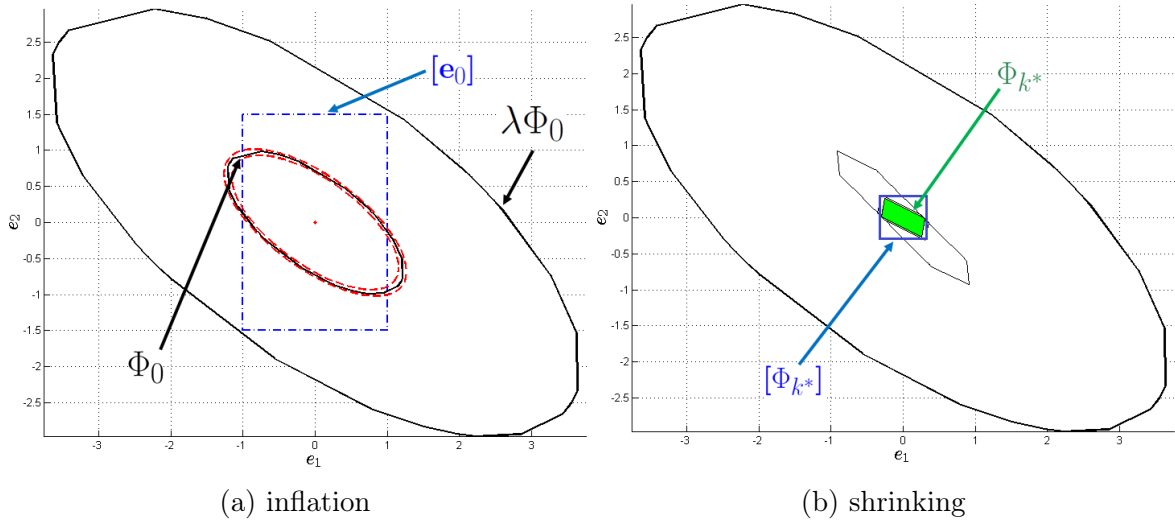


Figure 4.4: The inflation and shrinking procedures used to get the time instant k^* and an outer-approximation $[\Phi_{k^*}]$ of the theoretical mRPI set Ω_∞ of the estimation error at the steady state.

For $k \geq k^*$ we have:

$$[\mathbf{s}_k] = [\Phi_{k^*}] = [\mathbb{B}^{n_x}(\epsilon) \oplus \Omega_\infty] \quad (4.29)$$

where $[\Phi_{k^*}]$ is the smallest box which contains a RPI outer-approximation of the theoretical mRPI set denoted by Ω_∞ of the discrete-time linear system (4.5) with a desired precision defined by the positive real number ϵ . The relative error of the outer-approximation with respect to the set Ω_∞ can be measured by the following shrinking index $\rho(k)$ which characterizes the precision of the outer-approximation of the mRPI set:

$$\rho(k) = \beta^k \sqrt{\frac{\mu \lambda_{\max}(\mathbf{P})}{\lambda_{\min}(\mathbf{P})}} \quad (4.30)$$

where $\mu > 1$ and $\beta \in [0, 1]$ and \mathbf{P} is a symmetric positive definite matrix solution to the LMI (4.13).

Now, to determine the positive integer k^* , let λ be a positive real number such that:

$$[\mathbf{e}_0] \subseteq \lambda \Phi_0 \quad (4.31)$$

where Φ_0 is the initial polyhedral RPI set defined in (1.56) and λ represents the inflation factor. The set Φ_0 is inflated in order to include the initial estimation error set. The inflation procedure is illustrated in Figure 4.4a. Then, based on the stop criterion (4.33), for a given precision ϵ the integer k^* has to satisfy following inclusion:

$$\lambda \beta^{k^*} \Phi_0 \subseteq \mathbb{B}^{n_x}(\epsilon) \quad (4.32)$$

Remark 4.2

Since the polyhedron Φ_0 and the ball $\mathbb{B}^{n_x}(\epsilon)$ contain the origin, k^* can be lower bounded by

$$k^* \geq \frac{\log\left(\frac{\epsilon}{\lambda\|\Phi_0\|}\right)}{\log(\beta)} \quad (4.33)$$

where $\|\cdot\|$ denotes the maximal distance of the extreme values of a set from its origin.

Figure 4.3 shows the interval sequence $\{[\mathbf{s}_k]\}_{k=0,\dots,k^*}$, where the first elements of this sequence are obtained by interval computation (4.11) and the last one is an outer-approximation of the mRPI set Φ_{k^*} of the dynamics of the estimation error.

The second version of the proposed interval observer is stated in the following proposition 4.4.

Proposition 4.4

If the pair (\mathbf{A}, \mathbf{C}) is observable then there exists an observer gain matrix \mathbf{L} , and a positive integer k^* such that the Luenberger-like observer

$$\begin{aligned} \hat{\mathbf{x}}_{k+1} &= \mathbf{A}_o \hat{\mathbf{x}}_k + \mathbf{B} \mathbf{u}_k + \mathbf{L} \mathbf{y}_k + \mathbf{E} \mathbf{w}_c \\ \bar{\mathbf{x}}_{k+1} &= \hat{\mathbf{x}}_{k+1} + \bar{\mathbf{s}}_{k+1} \\ \underline{\mathbf{x}}_{k+1} &= \hat{\mathbf{x}}_{k+1} + \underline{\mathbf{s}}_{k+1} \end{aligned} \quad (4.34)$$

is an interval observer for (4.1). In addition, the vector width of the outer-approximation of the ultimate-bound of the estimation error is lower than

$$\mathbb{W}([\mathbf{s}_{k^*}]) \leq \mathbb{W}([\Phi_{k^*}]) \quad (4.35)$$

where \mathbf{w}_c is the midpoint of the box $[\mathbf{w}]$ where $[\Delta \mathbf{w}] = \frac{1}{2}[-1 \ 1] \mathbb{W}([\mathbf{w}])$ and $[\mathbf{w}] = \mathbf{w}_c + [\Delta \mathbf{w}]$.

Note that, all the values of the finite sequences $k = 1, \dots, k^*$, $\underline{\mathbf{s}}_{k+1}$ and $\bar{\mathbf{s}}_{k+1}$ are available off-line.

Proof. By direct computation one can define the dynamics of the estimation error $\mathbf{e}_{k+1} = \mathbf{x}_{k+1} - \hat{\mathbf{x}}_{k+1}$ as follows

$$\mathbf{e}_{k+1} = \mathbf{A}_o \mathbf{e}_k + \mathbf{E}(\mathbf{w}_k - \mathbf{w}_c) = \mathbf{A}_o \mathbf{e}_k + \mathbf{E} \Delta \mathbf{w}_k \quad (4.36)$$

Since, the pair (\mathbf{A}, \mathbf{C}) is observable there exists an observer gain \mathbf{L} such that the matrix \mathbf{A}_o is Schur stable. In addition, by definition the box $[\Delta \mathbf{w}] = [\mathbf{w}] - \mathbf{w}_c$ contains the origin. Thus, all the required assumptions to find the positive integer k^* and to compute an RPI outer-approximation Φ_{k^*} of the mRPI set Ω_∞ of (4.36) are satisfied. Hence, one can claim that for all $k \geq k^*$ one can set $[\mathbf{s}_k] = [\Phi_{k^*}]$.

Now, to get tight enclosures $[\mathbf{s}_k]$ of the estimation error for $k = 1, \dots, k^* - 1$ one compute the reachable set of (4.36) as follows:

$$\begin{aligned} [\mathbf{s}_{k+1}] &= \mathbf{A}_o^{k+1} [\mathbf{s}_0] + [\mathbf{g}_k] \\ [\mathbf{g}_{k+1}] &= \mathbf{A}_o^{k+1} [\mathbf{g}_0] + [\mathbf{g}_k] \end{aligned} \quad (4.37)$$

where $[\mathbf{s}_0] = [\mathbf{e}_0]$ and $[\mathbf{g}_0] = \mathbf{E}[\Delta\mathbf{w}]$. This completes the proof. \square

4.5 Illustrative examples

4.5.1 Example 1

To show the performance of the proposed robust interval observer, let us consider the following observable discrete-time linear system,

$$\begin{cases} \mathbf{x}_{k+1} = \begin{pmatrix} -1.1267 & -1.3503 \\ 1.1095 & 1.2673 \end{pmatrix} \mathbf{x}_k + \begin{pmatrix} 0.0951 & -0.1977 \\ -0.2894 & 0.1099 \end{pmatrix} \mathbf{u}_k + \begin{pmatrix} -0.1606 \\ 0.1254 \end{pmatrix} \mathbf{d}_k \\ \mathbf{y}_k = (-0.2512 \quad 0.1723) \mathbf{x}_k - 0.1542 \mathbf{v}_k \end{cases} \quad (4.38)$$

where the input vector is defined by $\mathbf{u}_k = (12 + \sin(0.5k), 10 + \cos(0.6k))^T$ and the initial state vector \mathbf{x}_0 is unknown but belongs into a bounded set with perfectly known bounds $[\mathbf{x}_0] = [-3, +3] \times [-3, +3]$. The punctual observer is initialized at $\hat{\mathbf{x}}_0 = (0, 0)^T$ and the real system is initialized at $\mathbf{x}_0 = (1, 1)^T$. The state disturbance and measurement noise are assumed completely unknown but bounded:

$$\forall k, \quad |\mathbf{v}_k| \leq 1 \quad \text{and} \quad |\mathbf{d}_k| \leq 1$$

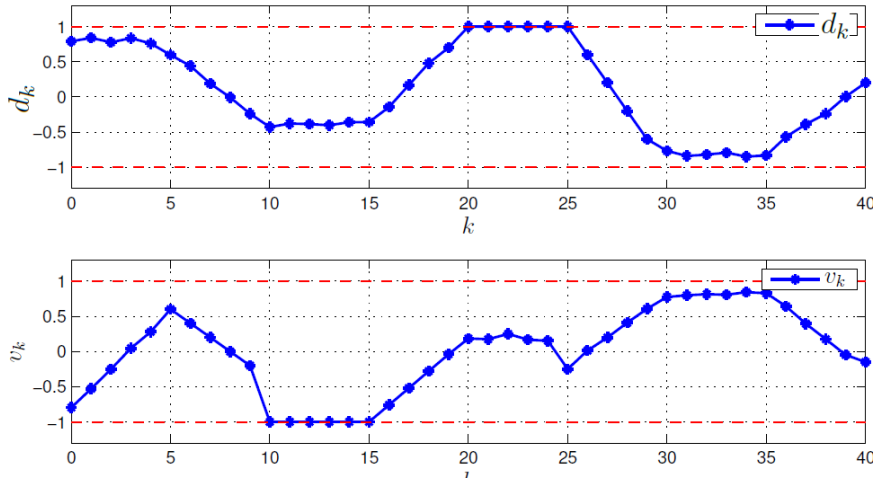


Figure 4.5: The supposed behaviors of the state disturbance and the output noise.

As introduced in Subsection 4.3.1, to attenuate the effect of both state disturbance and measurement noise on the estimation error at the steady state, the optimal observer gain \mathbf{L} has to be computed through the solution of the LMI (4.13). For this example one gets,

$$\gamma = 0.2108, \quad \mathbf{L} = (0.0889, -0.2167)^T$$

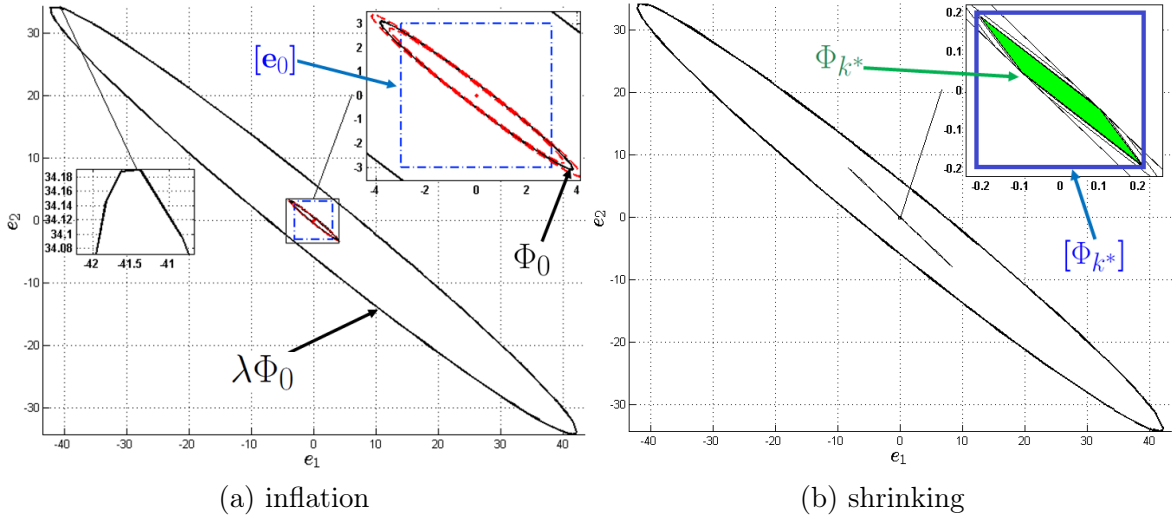


Figure 4.6: Shrinking procedure to get an outer-approximation of the mRPI set of the estimation error at the steady state.

for the positive definite matrix,

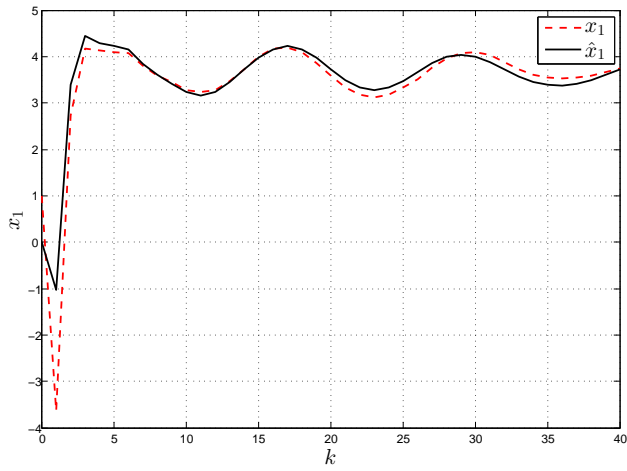
$$\mathbf{P} = \begin{bmatrix} 54.3612 & 65.9833 \\ 65.9833 & 82.5909 \end{bmatrix}$$

With this value of γ one can affirm that at the steady state the effect of the uncertainties $(\mathbf{d}_k, \mathbf{v}_k)$ on the estimation error are well attenuated.

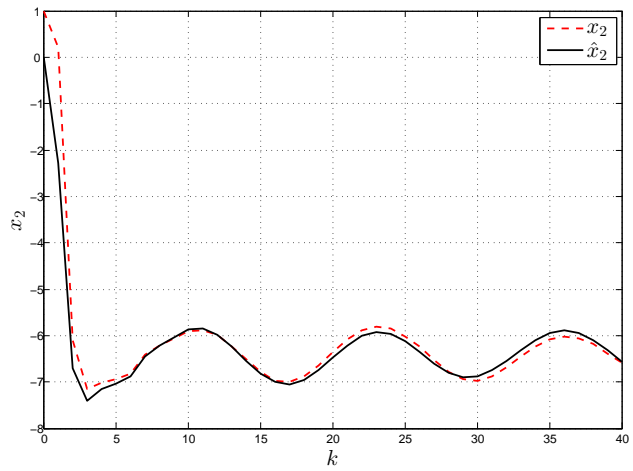
Now, to implement the interval observer (4.34), we need to construct the off-line interval sequence (4.27) of the estimation error. First, we have to determine the positive integer k^* and then to compute the box $[\Phi_{k^*}]$. For this example, the origin is considered as the initial condition of the punctual part of the proposed interval observer $\hat{\mathbf{x}}_0 = (0, 0)^T$. Thus, the initial box of the estimation error is $[\mathbf{e}_0] = [\mathbf{x}_0]$ and then to get the inclusion $[\mathbf{e}_0] \subset \lambda\Phi_0$ the considered inflation factor is $\lambda = 11$.

The inflation procedure is illustrated in Figure 4.6(a), where the polyhedral Φ_0 , confined between the two ellipsoids $\bar{\Psi}, \bar{\Psi}^+$ established for $\mu = 2$, is depicted by the black lines and the box of initial estimation error is plotted by the dashed blue lines. Now, according to (4.33), for $\epsilon = 0.01$ and $\beta = 0.2884$, one gets $k^* = 7$. Then, as shown in Figure 4.6(b), the polyhedral invariant set Φ_{k^*} is computing by the shrinking procedure defined in Subsection 1.3.3 of the Chapter 1. On Figure 4.6, the outer-approximation Φ_{k^*} of the mRPI set of the estimation error at the steady state Ω_∞ , is presented by the green surface and the blue rectangle stands for the minimal box $[\Phi_{k^*}]$ which frames the set $\Phi_{k^*} = \mathbb{B}^{n_x} \oplus \Omega_\infty$.

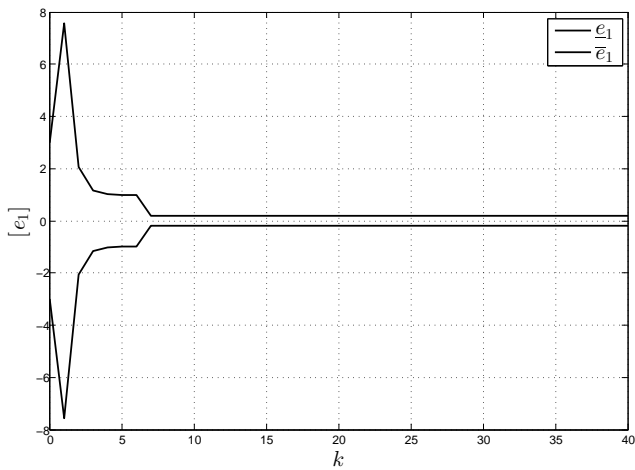
Table 4.1 shows the entries of the finite interval sequence (4.27). Here, it is worth pointing out that all of these entries are off-line computed. Moreover, only these seven interval elements are required to characterize the bounds of the estimation error on the whole simulation period. On the Figures 4.7a and 4.7b, the punctual estimated state variables $\hat{\mathbf{x}}_1, \hat{\mathbf{x}}_2$ provided by the



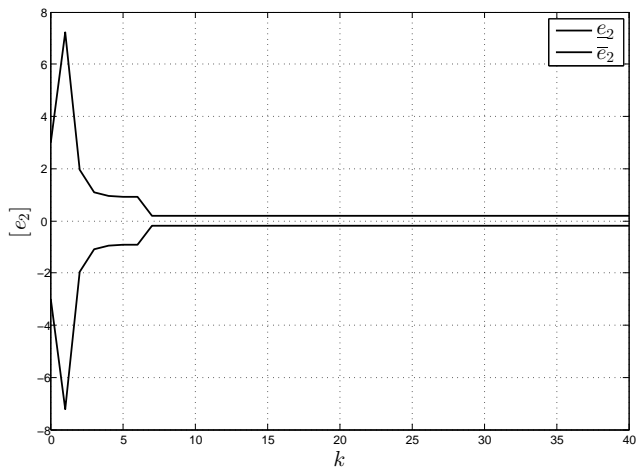
(a) $\hat{\mathbf{x}}_1$ and \mathbf{x}_1



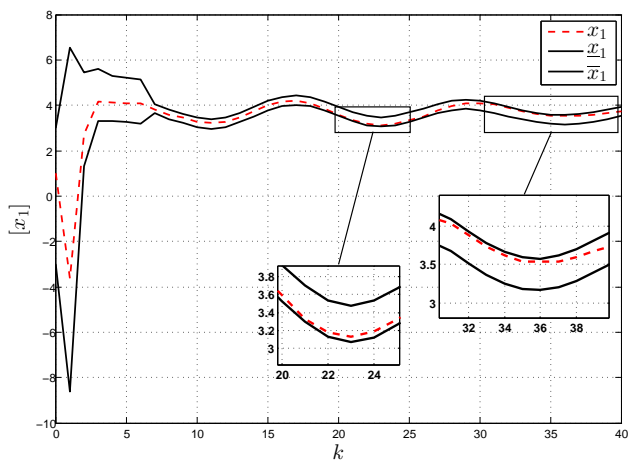
(b) $\hat{\mathbf{x}}_2$ and \mathbf{x}_2



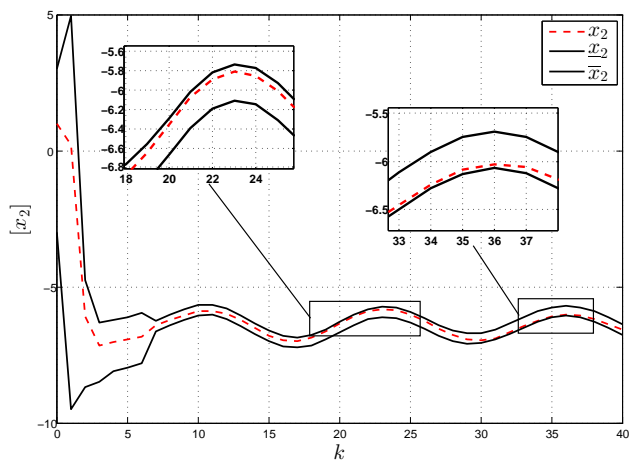
(c) The enclosure of \mathbf{e}_1



(d) The enclosure of \mathbf{e}_2



(e) The enclosure of \mathbf{x}_1



(f) The enclosure of \mathbf{x}_2

Figure 4.7: (a) and (b) show the time evolution of the estimated and the real state trajectories. (c) and (d) plot the guaranteed enclosure of the estimation error. (e) and (f) represent the outer-approximation of all the possible state trajectories

Table 4.1: A finite interval sequence of the time evolution of the estimation error.

$[\mathbf{s}_k], k = 0, \dots, 7$	Box of the off-line estimation error
$[\mathbf{s}_0] = [\mathbf{e}_0]$	$[-3, +3] \times [-3, +3]$
$[\mathbf{s}_1]$	$[-7.5843, +7.5843] \times [-7.2379, +7.2379]$
$[\mathbf{s}_2]$	$[-2.0676, +2.0676] \times [-1.9675, +1.9675]$
$[\mathbf{s}_3]$	$[-1.6003, +1.6003] \times [-1.1008, +1.1008]$
$[\mathbf{s}_4]$	$[-1.0056, +1.0056] \times [-0.9530, +0.9530]$
$[\mathbf{s}_5]$	$[-0.9762, +0.9762] \times [-0.9249, +0.9249]$
$[\mathbf{s}_6]$	$[-0.9704, +0.9704] \times [-0.9194, +0.9194]$
$[\mathbf{s}_7] = [\Phi_7]$	$[-0.2053, +0.2053] \times [-0.1884, +0.1884]$

punctual part of the interval Luenberger-like observer (4.34) are shown by the continuous curves and the real state variables of the system (4.38) are depicted by the dashed lines. Note that, for these simulation results the time evolution of the state disturbance and the output noise are presented in Figure 4.5. In addition, Figures 4.7c and 4.7d show the enclosure of all the possible estimation error over the whole simulation period. Finally, Figures 4.7e and 4.7f plot the guaranteed outer-approximation of all the possible state trajectories of the uncertain system (4.38), generated by the interval observer (4.34). Note that, in this simulation test the elapsed CPU time is 0.428 *ms* (for a processor: Intel Core i3 CPU @ 2.30 GHz). This low computation time is the fruit of the off-line characterization of the feasible set of the estimation error.

4.5.2 Example 2

Now, consider a system of order four described by

$$\begin{cases} \mathbf{x}_{k+1} = \mathbf{A}\mathbf{x}_k + \mathbf{B}\mathbf{u}_k + \mathbf{F}\mathbf{d}_k \\ \mathbf{y}_k = \mathbf{C}\mathbf{x}_k + \mathbf{Z}\mathbf{v}_k \end{cases} \quad (4.39)$$

where the system's matrices are defined as follows:

$$\mathbf{A} = \begin{pmatrix} -0.1321 & 1.1732 & -0.1794 & 0.1522 \\ -0.8148 & 0.1689 & 0.3771 & 0.9308 \\ -0.0871 & 0.4465 & -0.0722 & -0.3125 \\ 0.0804 & 0.2929 & -0.1056 & -0.0631 \end{pmatrix},$$

$$\mathbf{B} = \begin{pmatrix} 0.2598 \\ -0.6342 \\ 0.3125 \\ -0.7458 \end{pmatrix}, \quad \mathbf{F} = \begin{pmatrix} 0.1264 & 0 & 0 & -0.1267 \\ 0 & 0.09321 & 0 & 0 \\ 0.0958 & 0 & 0.1325 & 0 \\ 0.1052 & 0 & 0 & 0.2189 \end{pmatrix}$$

$$\mathbf{C} = (0.3502 \quad 0 \quad 0.9298 \quad 0.2398), \quad \mathbf{Z} = 0.2905$$

and the considered input is

$$\mathbf{u}_k = \frac{\pi}{8}(\sin(0.5k) + \cos(2k)) + \frac{\pi}{4}$$

The feasible bounded domain of the initial state is defined by a box:

$$[\mathbf{x}_0] = [-3, +3] \times [-3, +3] \times [-3, +3] \times [-3, +3]$$

The vector of the state perturbations \mathbf{d}_k is unknown but belongs to the box:

$$\forall k \geq 0, \mathbf{d}_k \in [\mathbf{d}] = [-2, +2] \times [-2, +2] \times [-2, +2] \times [-2, +2]$$

Also the measurement noise \mathbf{v}_k is unknown but evolves in a bounded set:

$$\mathbf{v}_k \in [\mathbf{v}_k] = [-1, +1]$$

For this example the considered time evolution of the state disturbances and the output noise are plotted in Figure 4.8. The observer gain \mathbf{L} is computed through the solution to the LMI

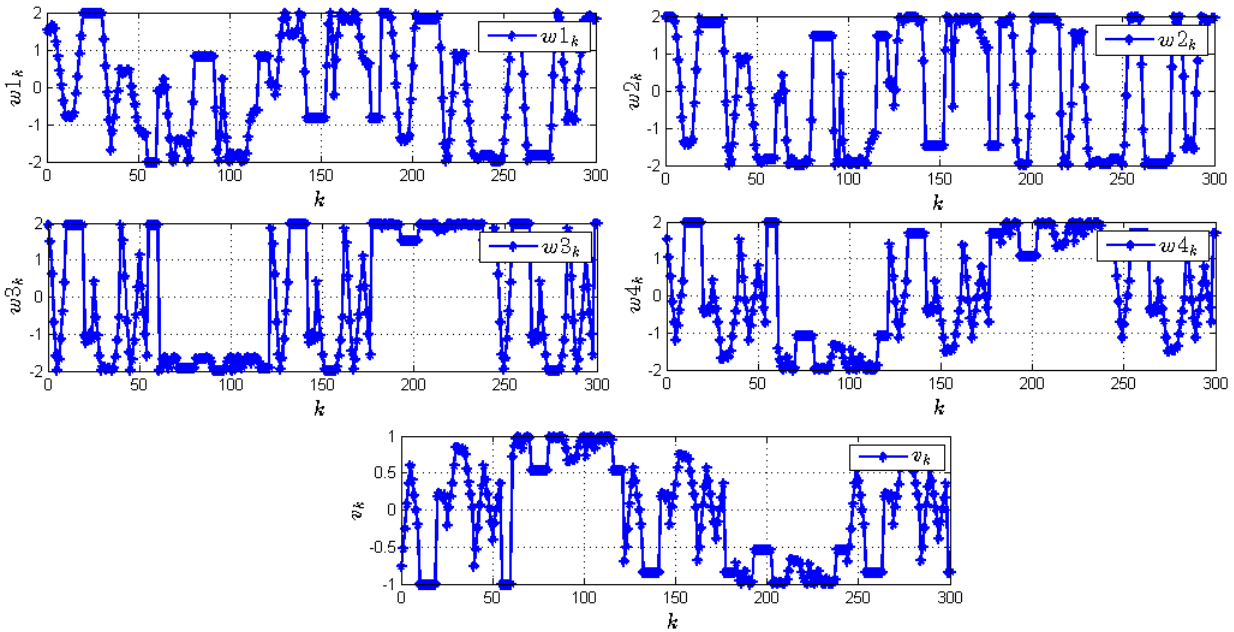


Figure 4.8: Profiles of state disturbances and the measurement noise.

(4.13). So, the obtained optimal gain is,

$$\mathbf{L} = (-0.2946, -0.4998, -0.2811, -0.0008)^T \text{ for } \gamma = 0.6831$$

and for the following positive definite matrix

$$\mathbf{P} = \begin{bmatrix} 3.8087 & -0.8918 & -6.6369 & 0.0963 \\ -0.8918 & 3.1209 & 2.1267 & 0.3579 \\ -6.6369 & 2.1267 & 19.3054 & -4.4521 \\ 0.0963 & 0.3579 & -4.4521 & 7.9044 \end{bmatrix}$$

The other parameters used to characterize off-line the set of all the possible estimation error are:

$$\epsilon = 5 \cdot 10^{-2}, \lambda = 2, \mu = 2, \beta = 0.8781, k^* = 51$$

The initial state of the system is assumed $\mathbf{x}_0 = (2.5, -2.5, 2.5, -2.5)^T$ and that of the punctual part of the interval observer is set at $\hat{\mathbf{x}}_0 = (-2.5, 2.5, -2.5, 2.5)^T \in [\mathbf{x}_0]$.

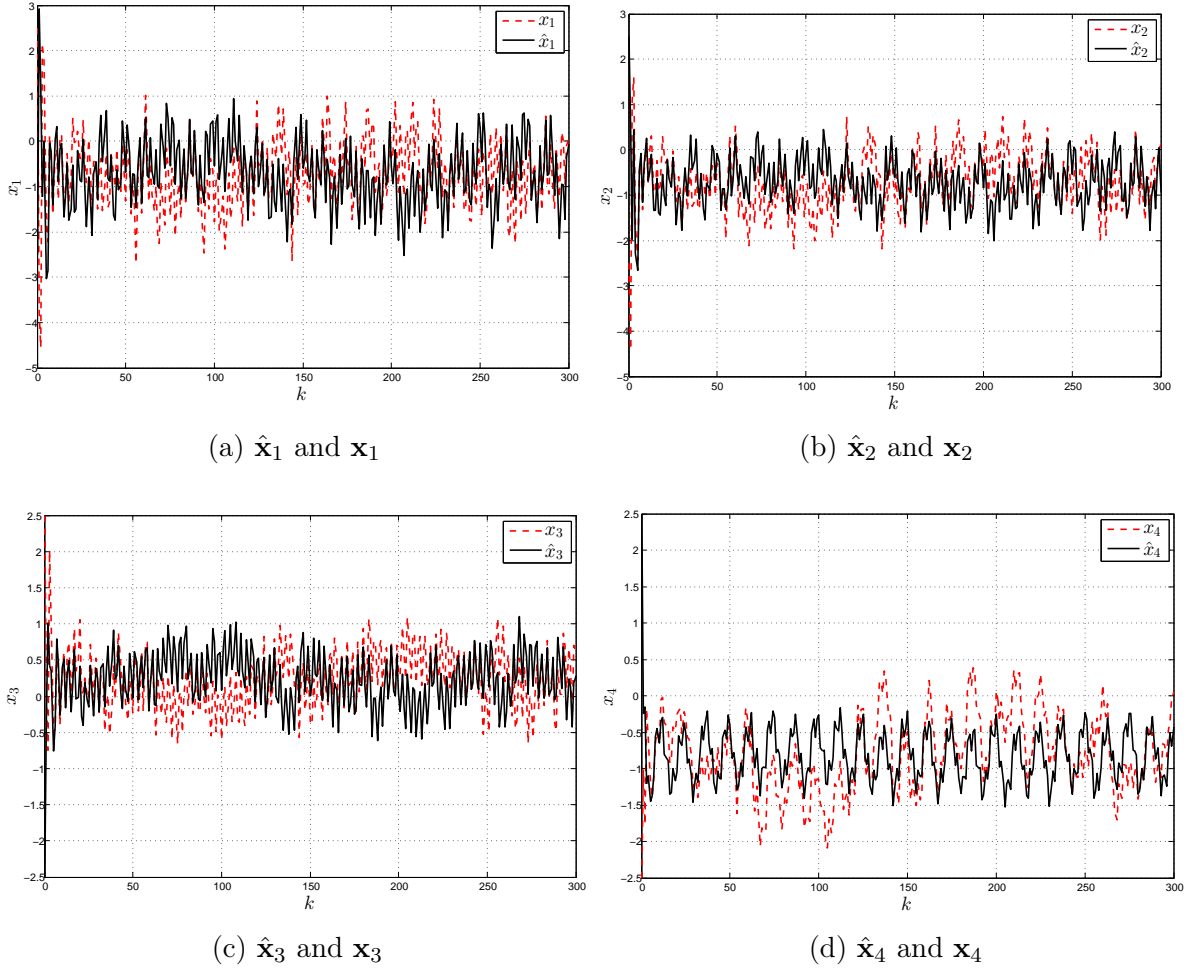


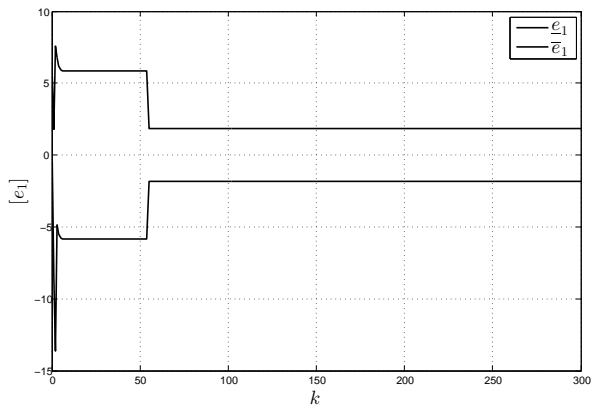
Figure 4.9: Punctual state estimations

The simulation results are shown in the Figures (4.9), (4.10) and (4.11).

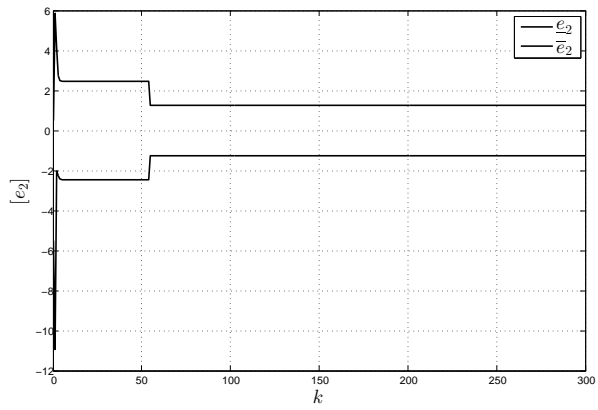
In Figure (4.9), each picture shows the punctual estimation (in black) of the four states, this estimation is obtained using the punctual observer (4.9), the red dashed lines represents the real states.

The Figure (4.10) represents the enclosure of all possible estimation errors where the upper and lower bounds (in black) are obtained using the interval sequence (4.27).

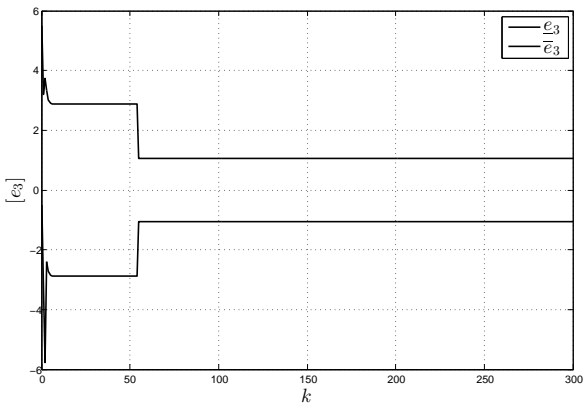
The Figure (4.11) shows the enclosures of the state variables (in black), and the real state



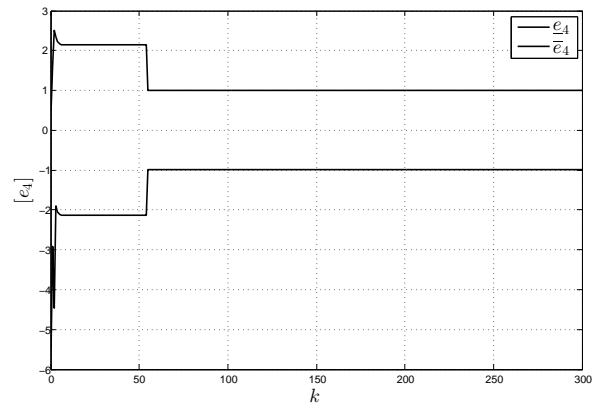
(a) The enclosure of \mathbf{e}_1



(b) The enclosure of \mathbf{e}_2

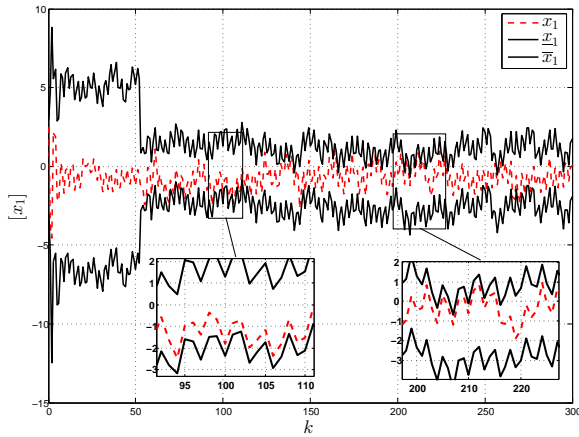


(c) The enclosure of \mathbf{e}_3

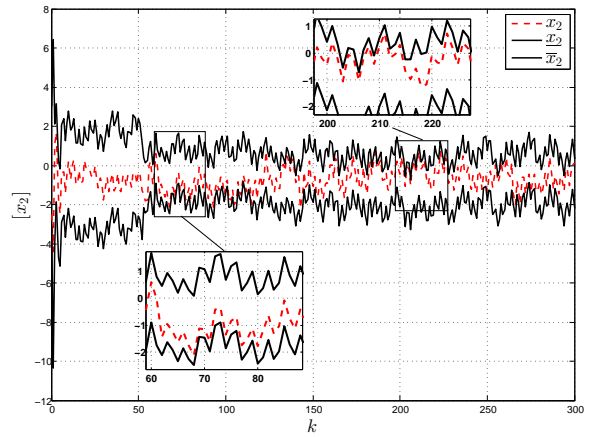


(d) The enclosure of \mathbf{e}_4

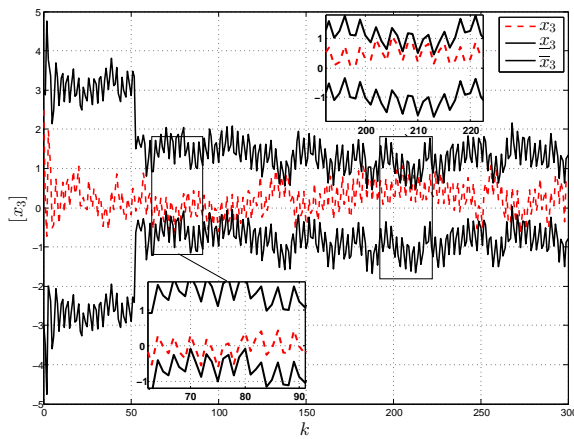
Figure 4.10: Enclosure of the estimation errors



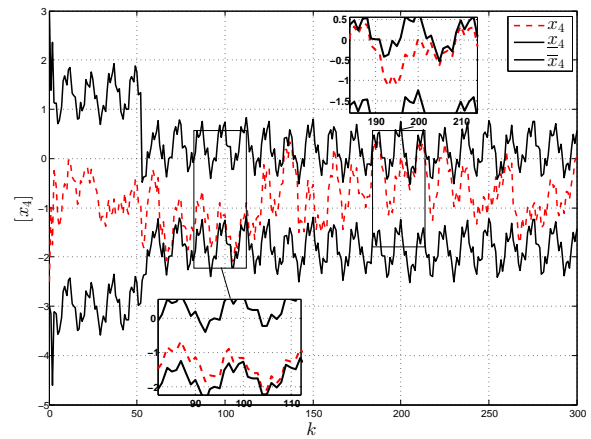
(a) enclosure of $\mathbf{x}_1(k)$



(b) enclosure of $\mathbf{x}_2(k)$



(c) enclosure of $\mathbf{x}_3(k)$



(d) enclosure of $\mathbf{x}_4(k)$

Figure 4.11: The enclosure of all the possible state trajectories of the system

variables are depicted by the red dashed line. Note that, the used computation time in this simulation is 1.606 *ms* (for a processor: Intel Core i3 CPU @ 2.30 GHz). As aforementioned, this weak demand of the computation time is linked to the fact that the characterization of the estimation error is carried off-line. This presents an other important advantage of the proposed interval observer with respect to the existing approaches in the literature.

4.6 Extension to a class of nonlinear systems

The interval observer presented till now is devoted to uncertain linear discrete-time systems. In this section, we will extend the interval observer for a class of uncertain nonlinear systems.

The class of nonlinear system considered in this section can be seen as the sum of a linear term and a nonlinear uncertain term assumed to be bounded. The systems are described by:

$$\begin{cases} \mathbf{x}_{k+1} &= \mathbf{A}\mathbf{x}_k + \mathbf{h}(\mathbf{p}, \mathbf{x}_k) + \mathbf{B}\mathbf{u}_k \\ \mathbf{y}_k &= \mathbf{C}\mathbf{x}_k + \mathbf{Z}\mathbf{v}_k \end{cases} \quad (4.40)$$

$\mathbf{x}_k \in \mathbb{R}^{n_x}$ is the state vector, $\mathbf{u}_k \in \mathbb{R}^{n_u}$ is the input vector and $\mathbf{y}_k \in \mathbb{R}^{n_y}$ is the measured output vector. The initial state is unknown but belongs to initial box $\mathbf{x}_0 \in [\mathbf{x}_0] = [\underline{\mathbf{x}}_0, \bar{\mathbf{x}}_0]$.

The parameter vector $\mathbf{p} \in \mathbb{R}^{n_p}$ is uncertain but belongs to a box $[\mathbf{p}] = [\underline{\mathbf{p}}, \bar{\mathbf{p}}]$. The function $\mathbf{h}(\mathbf{p}, \mathbf{x}_k)$ stands for the uncertain nonlinear part of the system and it is assumed to be bounded, i.e:

$$\forall \mathbf{x}_k \in [\mathbf{x}_k], \quad \forall \mathbf{p}_k \in [\mathbf{p}_k], \quad \forall k \geq 0 : \quad \mathbf{h}(\mathbf{p}, \mathbf{x}_k) \in [\mathbf{h}] = [\underline{\mathbf{h}}, \bar{\mathbf{h}}]$$

The proposed interval observer for the system (4.40) is introduced in the following proposition.

Proposition 4.5

Consider the nonlinear uncertain system (4.40) and assuming that the pair (\mathbf{A}, \mathbf{C}) is detectable, The interval observer for (4.40) is defined by the punctual-interval dynamical system (4.41), (4.42) and (4.44):

$$\hat{\mathbf{x}}_{k+1} = \tilde{\mathbf{A}}\hat{\mathbf{x}}_k + \hat{\mathbf{h}} + \mathbf{B}\mathbf{u}_k + \mathbf{L}\mathbf{y}_k \quad (4.41)$$

$$[\mathbf{e}_{k+1}] = \mathbf{A}_o^{k+1}[\mathbf{e}_0] + [\mathbf{g}_k] \quad (4.42)$$

$$[\mathbf{g}_{k+1}] = \mathbf{A}_o^{k+1}[\mathbf{g}_0] + [\mathbf{g}_k] \quad (4.43)$$

$$[\mathbf{x}_{k+1}] = \hat{\mathbf{x}}_{k+1} + [\mathbf{e}_{k+1}] \quad (4.44)$$

where

$$\begin{aligned} \hat{\mathbf{h}} &= m([\mathbf{h}]) \\ \mathbf{A}_o &= (\mathbf{A} - \mathbf{L}\mathbf{C}) \\ \mathbf{E} &= [\mathbf{I}_{n_x} - \mathbf{L}\mathbf{Z}] \\ [\mathbf{g}_0] &= \mathbf{E} \left(\left[\underline{\mathbf{h}} - \hat{\mathbf{h}}, \bar{\mathbf{h}} - \hat{\mathbf{h}} \right], [\mathbf{v}] \right)^T \end{aligned} \quad (4.45)$$

The initial state $\hat{\mathbf{x}}_0$ of the punctual dynamics (4.41) belongs to the box $[\mathbf{x}_0]$, the interval dynamics (4.42),(4.43) is initialized by the box $[\mathbf{e}_0] = [\mathbf{x}_0] - \hat{\mathbf{x}}_0$.

4.6.1 H_∞ observer gain design

The H_∞ observer gain synthesis is similar to that one presented in Subsection 2.1 of Chapter 2, The only difference is that we replace the matrix F by an identity matrix.

Proposition 4.6

Consider the system (4.40). The observer gain \mathbf{L} exists if there exists a symmetric positive definite matrices \mathbf{P} and \mathbf{U} satisfying the following LMI:

$$\begin{pmatrix} -\mathbf{P} + \mathbf{I}_n & 0_{n_x \times m} & \mathbf{A}^T \mathbf{P} - \mathbf{C}^T \mathbf{U}^T \\ 0_{m \times n_x} & -\gamma^2 \mathbf{I}_m & [\mathbf{P} - \mathbf{U} \mathbf{Z}]^T \\ \mathbf{P} \mathbf{A} - \mathbf{U} \mathbf{C} & [\mathbf{P} - \mathbf{U} \mathbf{Z}] & -\mathbf{P} \end{pmatrix} \preceq 0 \quad (4.46)$$

Moreover, the observer gain is obtained as follow:

$$\mathbf{L} = \mathbf{P}^{-1} \mathbf{U} \quad (4.47)$$

4.6.2 Interval characterization of the estimation errors

The estimation error is defined as follows:

$$\mathbf{e}_k = \mathbf{x}_k - \hat{\mathbf{x}}_k \quad (4.48)$$

From (4.40) and (4.41) and using (4.48), we obtain the dynamics of the estimation error as follows:

$$\mathbf{e}_{k+1} = \mathbf{A}_o \mathbf{e}_k + \mathbf{h}(\mathbf{p}, \mathbf{x}_k, k) - \hat{\mathbf{h}} - \mathbf{L} \mathbf{Z} \mathbf{v}_k \quad (4.49)$$

By taking into account all the system's uncertainties we obtain, in a guaranteed way, the following interval equation:

$$\begin{aligned} [\mathbf{e}_{k+1}] &= \mathbf{A}_o [\mathbf{e}_k] + [\mathbf{h}([\mathbf{p}], [\mathbf{x}], k) - \hat{\mathbf{h}} - \mathbf{L} \mathbf{Z} [\mathbf{v}]] \\ &\subseteq \mathbf{A}_o [\mathbf{e}_k] + [\mathbf{g}_o] \end{aligned} \quad (4.50)$$

Then, one can outer-approximate (4.49) by the following set equality:

$$[\mathbf{e}_{k+1}] = \mathbf{A}_o [\mathbf{e}_k] + [\mathbf{g}_0] \quad (4.51)$$

Subsequently, starting from an initial box $[\mathbf{e}_0]$, we can compute $[\mathbf{e}_{k+1}]$ as follows:

$$\begin{aligned} [\mathbf{e}_{k+1}] &= \mathbf{A}_o^{k+1} [\mathbf{e}_0] + [\mathbf{g}_k] \\ [\mathbf{g}_{k+1}] &= \mathbf{A}_o^{k+1} [\mathbf{g}_0] + [\mathbf{g}_k] \end{aligned} \quad (4.52)$$

Note that, the observer gain \mathbf{L} is computed such that the matrix \mathbf{A}_o is stable i.e all the eigenvalues λ_i of the matrix \mathbf{A}_o satisfy the following condition:

$$|\lambda_i| < 1, \quad \forall i = 1, \dots, n \quad (4.53)$$

From the condition (4.53), we can conclude that

$$\lim_{k \rightarrow +\infty} [\mathbf{e}_{k+1}] = \lim_{k \rightarrow +\infty} \mathbf{A}_o^{k+1} [\mathbf{e}_0] + \lim_{k \rightarrow +\infty} [\mathbf{g}_k] = [\mathbf{g}] \quad (4.54)$$

which proves that the box of the estimated error is bounded at the steady state.

4.6.3 Illustrative example

Let's consider the system described by the following dynamics:

$$\begin{cases} \mathbf{x}_{k+1} &= \mathbf{A}\mathbf{x}_k + \mathbf{h}(\delta, \mathbf{x}_k) + \mathbf{B}\mathbf{u}_k \\ \mathbf{y}_k &= \mathbf{C}\mathbf{x}_k + \mathbf{Z}\mathbf{v}_k \end{cases} \quad (4.55)$$

where

$$\mathbf{A} = \begin{pmatrix} 0.3 & -0.7 \\ 0.6 & -0.5 \end{pmatrix}, \quad \mathbf{B} = \begin{pmatrix} 1 & 0 \\ 0 & 1 \end{pmatrix}, \quad \mathbf{C} = (1 \ 0), \quad \mathbf{Z} = 1$$

and

$$\mathbf{h}(\delta, \mathbf{x}) = \delta \begin{pmatrix} \sin(0.5kx_2(k)) \\ \sin(0.3k) \end{pmatrix}, \quad \mathbf{u}_k = \begin{pmatrix} \sin(0.1k) \\ \cos(0.2k) \end{pmatrix}$$

δ is unknown but belongs to a bounded interval $[-0.8, 0.8]$. The unknown initial box of the state is taken sufficiently large in order to include the initial real state of the system, i.e $\mathbf{x}_0 \in [-3, 3] \times [-3, 3]$. The measurement noise v_k is unknown but bounded i.e $v_k \in [-0.2, 0.2]$, and it can be deterministic or random.

In the equation (4.55), The uncertain non linear term $\mathbf{h}(\delta, \mathbf{x}_k, k)$ is bounded:

$$\forall k \geq 0, \forall \mathbf{x}_k, \forall \delta : \mathbf{h}(\delta, \mathbf{x}_k, k) \in \begin{pmatrix} [-0.8, 0.8] \\ [-0.8, 0.8] \end{pmatrix}$$

The observer gain is computed by resolving the LMI (4.46) and it's numerical value is:

$$\mathbf{L} = \begin{pmatrix} 0.0074 \\ 0.3312 \end{pmatrix}$$

For this simulation the initial state of the system is taken $\mathbf{x}_0 = (2, -2)^T$ and that of the punctual Luenberger-like observer is set to $\mathbf{x}_0 = (-2, 2)^T$. The additive output noise v_k is randomly generated.

The interval observer described by (4.41), (4.42), (4.43) and (4.44) is applied to compute on-line an outer-approximation of the real state of the uncertain system. The Figure (4.12) shows an estimation of the state trajectory plotted in dashed blue line and an guaranteed enclosure of the real state of the system depicted by the green thick curves. In this figure the real state of the system is presented with the continuous red lines.

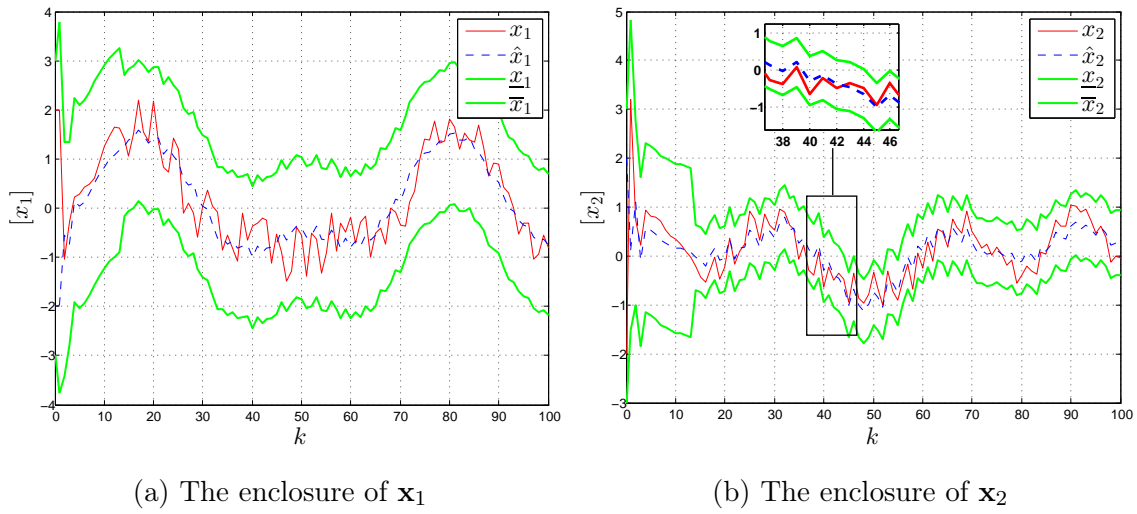


Figure 4.12: The estimated states enclosure

Figure (4.13) shows the enclosure of the estimation error over the whole simulation period.

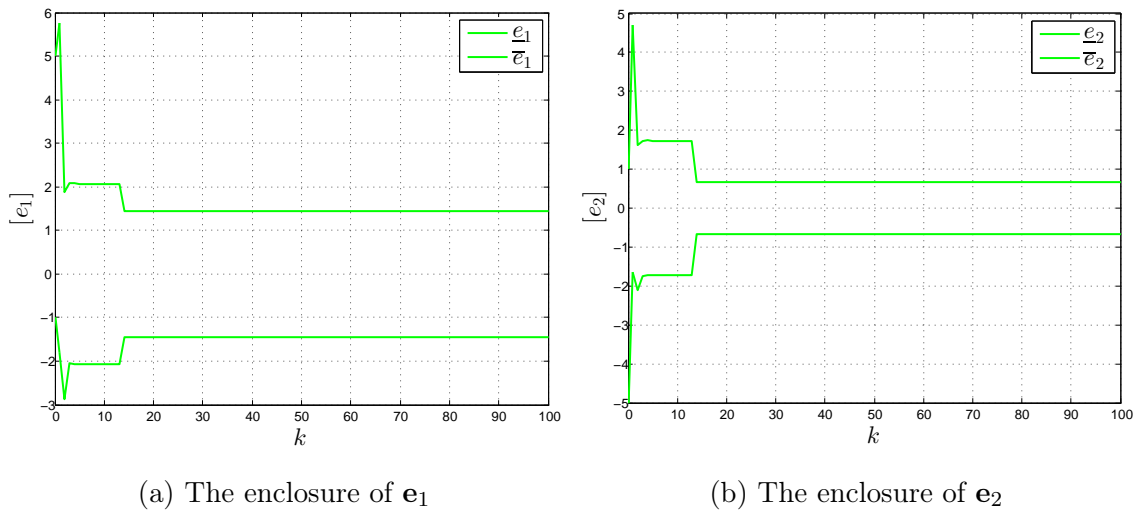


Figure 4.13: The enclosures of the estimation errors

4.7 Conclusion

In this chapter an interval observer for uncertain discrete-time systems has been proposed. The set-membership state estimation problem has been considered as classical punctual state estimation issue combined with a rigorous characterization of all the possible propagation of the estimation error, a non pessimistic numerical scheme to compute a rigorous enclosure of

the estimation error has been proposed. Then, based in the set invariance theory we have shown that a guaranteed bound of the estimation error can be off-line computed. Moreover, we have proposed an H_∞ observer gain design method to reduce the effect of the uncertainties on the size of the estimated state enclosure at the steady state. An extension of the interval observer for a class of uncertain nonlinear discrete-time system has been proposed in this chapter.

General conclusion and perspectives

This chapter recapitulates the contributions of this thesis and gives remarks for the future works. First, the main contributions and conclusions of this thesis will be summarized. Second, future work of this topic will be addressed.

4.8 Main conclusions

The main objective of this dissertation is to propose set-membership state estimation approaches for linear uncertain discrete-time systems with bounded perturbations and bounded measurement noises with explicit characterization of the estimation error bounds. These approaches can be seen as the combination between a punctual observer and a set-membership characterization of the observation error.

The contributions of this thesis can be listed into two main parts:

- The first main contribution is a set-membership observer based on ellipsoidal invariant sets for linear discrete-time systems and also Linear Parameter Varying systems. The proposed approach provides a deterministic state interval that is build as the sum of the estimated system states and its corresponding estimation errors bounds;
- The second main contribution is an interval version of the Luenberger state observer for uncertain discrete-time linear systems based on interval and invariant set computation. The set-membership state estimation problem is considered as a punctual state estimation issue coupled with an interval characterization of the estimation error.

In the first contribution, the proposed set-membership observer provides a deterministic state bounds that are build as the sum of the punctual estimated system states and its corresponding estimation error bounds. The design of the proposed observer is based on the solutions of a few number of Linear Matrix Inequalities that are suitable modified to provide both observer gain and ellipsoidal RPI sets. The obtained RPI sets are used to frame the estimation error in a very simple and accurate way. The observer synthesis process can includes an *a posteriori* steady-state covariance matrix for the estimation errors. This covariance matrix is used to enhance the precision on the computation of the estimation error bounds and to obtain less conservative dissipation inequality used in the Bounded real lemma formulation. Some of the most important advantages of the proposed observer is the fact that this is based on an explicit solution of the estimation-bounding problem. This allows to reduce the on-line computation costs. The proposed observer is very simple and easy to implement compared to set-membership observers available in the literature.

In the second contribution, we have proposed a new approach to design an interval observer for uncertain linear discrete-time systems, simple to implement, with less computation time

and reduced complexity. The set-membership state estimation problem is considered as a punctual state estimation issue coupled with an interval characterization of the estimation error. A non pessimistic numerical scheme to compute a rigorous enclosure of the estimation error is proposed. The advantage of such approaches is to reduce the complexity of the on-line implementation and the on-line computation time and to improve the precision of the estimated state enclosure. An extension for a class of uncertain non-linear systems is also proposed.

4.9 Future works

Several mid-term and long term future works are proposed for future developments of this thesis:

- Extend the proposed approaches to the case of systems with parametric uncertainty. In practice, some parameters of the real systems are poorly-known. So, it is of great interest to be able to design set-membership state estimator where the system's matrices are uncertain and modeled by interval matrices.
- Adapt these approaches to deal with the state and parameters estimation problems in the same time. In fact, based on the Kalman filtering principle, this extension is possible.
- Deal with the case of switched linear discrete-time systems. Based in this approaches we do not need to use similarity transformations to design a positive interval observer for each subsystem. So, the impulsive behavior induced by these similarity transformations can be avoided.
- Based on these approaches a guaranteed threshold on the estimation error can be computed. This threshold avoids generating false alarm linked to the modeling errors and the inaccuracy of the available measurements.
- Combine these robust state estimation methods with the methods dedicated to solve the fault detection issues and fault tolerant control problems. This will allow designing robust and guaranteed new methods.
- Apply these approaches to real-world applications. In fact, since the proposed estimation approaches are simple to implement and do not demand a huge on-line time computation, its application to industrial systems is possible.

Bibliography

- [ABC05] T. Alamo, J. M. Bravo, and E. F. Camacho. “Guaranteed state Estimation by Zonotopes.” In: *Automatica* 41 (2005), pp. 1035–1043 (cit. on pp. 3, 8).
- [AGB95] Pierre Apkarian, Pascal Gahinet, and Greg Becker. “Self-scheduled H control of linear parameter-varying systems: a design example.” In: *Automatica* 31.9 (1995), pp. 1251–1261 (cit. on p. 63).
- [AGV99] A. Tesi A. Garulli and A. Vicino. *Robustness in Identification and Control, Lecture Notes in Control and Information Sciences*. Vol. no. 245. Springer-Verlag, 1999 (cit. on pp. 2, 7).
- [AK06] Bilal M Ayyub and George J Klir. *Uncertainty modeling and analysis in engineering and the sciences*. CRC Press, 2006 (cit. on p. 14).
- [Ale+07] Alessandro Alessio et al. “Squaring the circle: An algorithm for generating polyhedral invariant sets from ellipsoidal ones.” In: *Automatica* 43.12 (2007), pp. 2096–2103 (cit. on p. 34).
- [AP06] Jason Matthew Aughenbaugh and Chris Paredis. “Why are intervals and imprecision important in engineering design.” In: (2006) (cit. on p. 14).
- [Bat08] Amitrajeet A Batabyal. *Dynamic and stochastic approaches to the environment and economic development*. World Scientific, 2008 (cit. on pp. 1, 7).
- [BC98] Mark L Brockman and Martin Corless. “Quadratic boundedness of nominally linear systems.” In: *International Journal of Control* 71.6 (1998), pp. 1105–1117 (cit. on p. 28).
- [Bla95] Franco Blanchini. “Nonquadratic Lyapunov functions for robust control.” In: *Automatica* 31.3 (1995), pp. 451–461 (cit. on p. 28).
- [Bla99] F. Blanchini. “Set invariance in control.” In: *Automatica* 35(11) (1999), pp. 1747–1767 (cit. on pp. 28, 31, 32).
- [BM08] Franco Blanchini and Stefano Miani. *Set-theoretic methods in control*. Springer, 2008 (cit. on p. 31).
- [Boy+94] Stephen Boyd et al. *Linear matrix inequalities in system and control theory*. SIAM, 1994 (cit. on p. 33).
- [BSL07] Corentin Briat, Olivier Sename, and Jean-Francois Lafay. “A LFT state feedback design for linear parameter varying time delay systems.” In: *Control Conference (ECC), 2007 European*. IEEE. 2007, pp. 4882–4888 (cit. on p. 59).
- [CAGZ98] L. Chisci, A. Vicino A. Garulli, and G. Zappa. “lock recursive parallelotopic bounding in set membership identification.” In: *Automatica* 34 (1998), pp. 15–22 (cit. on pp. 2, 8).

- [CDD08] Mohammed Chadli, Mohamed Darouach, and Jamal Daafouz. “Static output stabilisation of singular LPV systems: LMI formulation.” In: *Decision and Control, 2008. CDC 2008. 47th IEEE Conference on*. IEEE. 2008, pp. 4793–4796 (cit. on p. 60).
- [CGZ96] L. Chisci, A. Garulli, and G. Zappa. “Recursive state bounding by parallelotopes.” In: *Automatica* 32 (1996), pp. 1049–1055 (cit. on pp. 2, 8).
- [Che+13] Stanislav Chebotarev et al. “On interval observer design for a class of continuous-time lpv systems.” In: *IFAC Proceedings Volumes* 46.23 (2013), pp. 68–73 (cit. on pp. 3, 9, 58, 73, 75).
- [Com] C. Combastel. “Stable Interval Observers in C for Linear Systems with Time-Varying Input Bounds.” In: *IEEE Transactions on Automatic Control, year=2013, volume=58, pages=481-487*, (cit. on pp. 3, 9).
- [Com03] C. Combastel. “A State Bounding Observer Based on Zonotopes.” In: *Proc. of European Control Conference*. Cambridge, UK, 2003 (cit. on pp. 2, 3, 8).
- [DK12] A. N. Daryin and A. B. Kurzhanski. “Estimation of Reachability Sets for Large-Scale Uncertain Systems: from Theory to Computation.” In: *In Proc. of 51st IEEE Conference on Decision and Control, Maui, Hawaii, USA* (2012), pp. 7401–7406 (cit. on pp. 2, 8).
- [DKV06] A. N. Daryin, A. B. Kurzhanski, and I. V. Vostrikov. “Reachability Approaches and Ellipsoidal Techniques for Closed-Loop Control of Oscillating Systems under Uncertainty.” In: *In Proc. of 51st IEEE Conference on Decision and Control, San Diego, CA, USA* (2006), pp. 6390–6395 (cit. on pp. 2, 8).
- [DP05] Carlos ET Dórea and Antonio Carlos C Pimenta. “Set-invariant estimators for linear systems subject to disturbances and measurement noise.” In: *IFAC Proceedings Volumes* 38.1 (2005), pp. 590–595 (cit. on p. 39).
- [DPBO03] A. Nedić D. P. Bertsekas and A. E. Ozdaglar. *Convex analysis and optimization*. Athena Scientific, 2003 (cit. on pp. 1, 2, 7, 8).
- [DWP01] C. Durieu, E. Walter, and B. Polyak. “Multi-Input Multi-Output Ellipsoidal State Bounding.” In: *Journal of Optimization Theory and Applications* 111(2) (2001), pp. 273–303 (cit. on pp. 2, 8, 28).
- [Fog79] E. Fogel. “System identification via membership set constraints with energy constrained noise.” In: *IEEE Transaction on Automatic Control* AC-24 (1979), p. 752 (cit. on pp. 1, 7).
- [Hin06] Haitham Hindi. “A tutorial on convex optimization : duality and interior point methods.” In: *American Control Conference, 2006*. IEEE. 2006, 11–pp (cit. on p. 68).
- [HMD13] Meriem Halimi, Gilles Millerioux, and Jamal Daafouz. “Polytopic observers for lpv discrete-time systems.” In: *Robust Control and Linear Parameter Varying Approaches*. Springer, 2013, pp. 97–124 (cit. on p. 75).

- [Jau+01] L. Jaulin et al. *Applied interval analysis: with examples in parameter and state estimation, robust control and robotics*. London: Springer-Verlag, 2001 (cit. on pp. 2, 8, 14, 26, 83).
- [JLGHS00] A. Rapport J. L. Gouzé and Z. Hadj-Sadok. “Interval observers for uncertain biological systems.” In: *Ecological modelling* 133 (2000), pp. 45–56 (cit. on pp. 3, 9).
- [Kal60] R.E. Kalman. “A New Approach to Linear Filtering and Prediction Problems.” In: *Transactions of the ASME Journal of Basic Engineering* 82.Series D (1960), pp. 35–45 (cit. on pp. 1, 7, 14).
- [KDS12] E. Kofman, J.A. De Dona, and M. M. Seron. “Probabilistic set invariance and ultimate boundedness.” In: *Automatica* 48.10 (2012), pp. 2670–2676 (cit. on p. 48).
- [KV96] A. B. Kurzhanski and I. Vályi. *Ellipsoidal calculus for estimation and control*. Birkhäuser Boston, 1996 (cit. on pp. 2, 8, 28, 29).
- [KW02] M. Kieffer and E. Walter. “Guaranteed nonlinear state estimator for cooperative systems.” In: *Numerical algorithms* 37(1) (2002), pp. 187–198 (cit. on pp. 3, 9).
- [LA03] Hai Lin and Panos J Antsaklis. “Disturbance attenuation properties for discrete-time uncertain switched linear systems.” In: *Decision and Control, 2003. Proceedings. 42nd IEEE Conference on*. Vol. 5. IEEE. 2003, pp. 5289–5294 (cit. on p. 28).
- [Le+12] V. T. H. Le et al. “Guaranteed state estimation by zonotopes for systems with interval uncertainties.” In: *submitted to Automatica*. 2012 (cit. on pp. 2, 8).
- [Le+13] V. T. H. Le et al. “Zonotopic guaranteed state estimation for uncertain systems.” In: *Automatica* 49(1) (2013), pp. 3418–3424 (cit. on pp. 2, 8).
- [Lue71] D. Luenberger. “An introduction to observers.” In: *IEEE Transactions on Automatic Control* 16.6 (1971), pp. 596–602 (cit. on pp. 1, 7, 14).
- [MAB05] G. Millerioux, F. Anstett, and G. Bloch. “Considering the attractor structure of chaotic maps for observer-based synchronization problems.” In: *Mathematics and Computers in Simulation* 68.1 (2005), pp. 67–85 (cit. on pp. 59, 60).
- [Mar15] J. J. Martinez. “Minimal RPI sets computation for polytopic systems using the Bounded-real lemma and a new shrinking procedure.” In: *1st IFAC Symposium Workshop on Linear Parameter Varying Systems*. Grenoble, France, 2015 (cit. on pp. 14, 32).
- [May82] Peter S Maybeck. *Stochastic models, estimation, and control*. Vol. 3. Academic press, 1982 (cit. on pp. 1, 7, 14).
- [MDN13] Frédéric Mazenc, Thach Ngoc Dinh, and Silviu-Iulian Niculescu. “Robust interval observers and stabilization design for discrete-time systems with input and output.” In: *Automatica* 49.11 (2013), pp. 3490–3497 (cit. on pp. 3, 9).
- [MMW96] H. Piet-Lahanier M. Milanese J. Norton and E. Walter. *Bounding Approaches to System Identification*. Plenum Publishers, 1996 (cit. on pp. 2, 7).

- [Mon89] H. Montgomery. “Computing the volume of a zonotope.” In: *The American Mathematical Monthly* 97 (1989), p. 431 (cit. on pp. 2, 8).
- [Moo66] R. E. Moore. *Interval analysis*. Englewood Cliff, New Jersey: Prentice-Hall, 1966 (cit. on pp. 2, 8, 14, 23, 83).
- [MR11] N. Meslem and N. Ramdani. “Interval observer design based on nonlinear hybridization and practical stability analysis.” In: *International Journal of Adaptive Control and Signal Processing* 25(3) (2011), pp. 228–248 (cit. on pp. 3, 9).
- [MRC10] N. Meslem, N. Ramdani, and Y. Candau. “Using hybrid automata for set-membership state estimation with uncertain nonlinear continuous-time systems.” In: *Journal of Process Control* 20(4) (2010), pp. 481–489 (cit. on pp. 3, 9).
- [Neu90] Arnold Neumaier. *Interval methods for systems of equations*. Vol. 37. Cambridge university press, 1990 (cit. on p. 26).
- [Ola+09] Sorin Olaru et al. “Necessary and sufficient conditions for sensor recovery in a multisensor control scheme.” In: *IFAC Proceedings Volumes* 42.8 (2009), pp. 977–982 (cit. on p. 32).
- [Ola+10] Sorin Olaru et al. “Positive invariant sets for fault tolerant multisensor control schemes.” In: *International Journal of Control* 83.12 (2010), pp. 2622–2640 (cit. on p. 32).
- [Par74] Beresford N Parlett. “The Rayleigh quotient iteration and some generalizations for nonnormal matrices.” In: *Mathematics of Computation* 28.127 (1974), pp. 679–693 (cit. on p. 47).
- [Pol+04] Polyak et al. “Ellipsoidal Parameter or State Estimation under Model Uncertainty.” In: *Automatica* 40 (2004), pp. 1171–1179 (cit. on pp. 2, 8, 28).
- [PQE02] V. Puig, J. Quevedo, and T. Escobet. “Robust fault detection approaches using interval models.” In: *Proc. on IFAC World Congress*. Spain, 2002 (cit. on pp. 3, 8).
- [RRC04] T. Raissi, N. Ramdani, and Y. Candau. “Set membership state and parameter estimation for systems described by nonlinear differential equations.” In: *Automatica* 40(10) (2004), pp. 1771–1777 (cit. on pp. 3, 9).
- [Rug81] Wilson John Rugh. *Nonlinear system theory*. Johns Hopkins University Press Baltimore, 1981 (cit. on p. 59).
- [Sch68] F. C. Schweppe. “Recursive State Estimation: Unknown but Bounded Errors and System Inputs.” In: *IEEE Transactions on Automatic Control* 13(1) (1968), pp. 22–28 (cit. on pp. 1, 2, 7, 8, 14).
- [SG05] Zhendong Sun and Shuzhi Sam Ge. “Analysis and synthesis of switched linear control systems.” In: *Automatica* 41.2 (2005), pp. 181–195 (cit. on p. 28).
- [She74] G. Shephard. “Combinatorial properties of associated zonotopes.” In: *Canadian Journal of Mathematics* 26 (1974), pp. 302–321 (cit. on pp. 2, 8).
- [Sun58] Teruo Sunaga. “A Basic Theory of Communication.” In: *Memoirs* 2 (1958), pp. 426–443 (cit. on p. 14).

- [TLW17] Junbo Tan, Bin Liang, and Xueqian Wang. “Robust actuator fault estimation combining unknown input observer and invariant set approach.” In: *Control And Decision Conference (CCDC), 2017 29th Chinese*. IEEE. 2017, pp. 7360–7365 (cit. on p. 39).
- [TRZ12] D. Efimov T. Raissi and A. Zolghadri. “Interval state estimation for a class of nonlinear systems.” In: *IEEE Conference on Automatic Control, Maui, Hawaii, USA* 57(1) (2012), pp. 260–265 (cit. on pp. 3, 9).
- [UW11] Mukhtar Ullah and Olaf Wolkenhauer. *Stochastic approaches for systems biology*. Springer Science & Business Media, 2011 (cit. on pp. 1, 7, 14).
- [WBR15] Yan Wang, David M. Bevly, and Rajesh Rajamani. “Interval observer design for LPV systems with parametric uncertainty.” In: *Automatica* 60.01 (2015), pp. 79–85 (cit. on p. 58).
- [Wis68] H. S. Wistenhausen. “Sets of possible states of linear systems given perturbed observations.” In: *IEEE Transaction on Automatic Control* 13(5) (1968), pp. 556–558 (cit. on pp. 1, 2, 7, 8).
- [Ben+14a] S. Ben Chabane et al. “A new approach for guaranteed state estimation.” In: *Proc. on IFAC World Congress*. Cape town, South africa. 2014, pp. 6533–6537 (cit. on pp. 2, 8).
- [Ben+14b] S. Ben Chabane et al. “Improved set-membership estimation approach based on zonotopes and ellipsoids.” In: *Proc. of the IEEE European Control Conference*. Strasbourg, France. 2014, pp. 993–998 (cit. on pp. 3, 9).

Abstract — In This work, we propose two main new approaches for the set-membership state estimation problem based on explicit characterization of the estimation error bounds. These approaches can be seen as a combination between a punctual observer and a set-membership characterization of the observation error. The objective is to reduce the complexity of the on-line implementation, reduce the on-line computation time and improve the accuracy of the estimated state enclosure.

The first approach is a set-membership observer based on ellipsoidal invariant sets for linear discrete-time systems and also for Linear Parameter Varying systems. The proposed approach provides a deterministic state interval that is build as the sum of the estimated system states and its corresponding estimation error bounds. The important feature of the proposed approach is that the proposed approach does not require propagation of sets.

The second approach is an interval version of the Luenberger state observer for uncertain discrete-time linear systems based on interval and invariant set computation. The set-membership state estimation problem is considered as a punctual state estimation issue coupled with an interval characterization of the estimation error.

Key words : Set-membership state estimation, ellipsoidal sets, invariant sets, interval analysis, discrete-time, discrete-time LPV systems, State estimation in bounded error context, unknown-but-bounded uncertainties.

Abstract — Dans ce travail, nous proposons deux nouvelles approches ensemblistes pour l'estimation d'état basées sur la caractérisation explicite des bornes d'erreur d'estimation. Ces approches peuvent être vues comme la combinaison entre un observateur ponctuel et une caractérisation ensembliste de l'erreur d'estimation. L'objectif est de réduire la complexité de leur implémentation, de réduire le temps de calcul en temps réel et d'améliorer la précision et des encadrements des vecteurs d'état.

La première approche propose un observateur ensembliste basé sur des ensembles invariants ellipsoïdaux pour des systèmes linéaires à temps-discret et aussi des systèmes à paramètres variables. L'approche proposée fournit un intervalle d'état déterministe qui est construit comme une somme entre le vecteur état estimé du système et les bornes de l'erreur d'estimation. L'avantage de cette approche est qu'elle ne nécessite pas la propagation des ensemble d'état dans le temps.

La deuxième approche est une version intervalle de l'observateur d'état de Luenberger, pour les systèmes linéaires incertains à temps-discret, basés sur le calcul d'intervalle et les ensembles invariants. Ici, le problème d'estimation ensembliste est considéré comme un problème d'estimation d'état ponctuel couplé à une caractérisation intervalle de l'erreur d'estimation.

Mots clés: Estimation d'état ensembliste, ensembles ellipsoïdaux, ensembles invariants, analyse pas intervalle, systèmes linears à temps-discret, systèmes LPV à temps-discret , estimation dans un contexte à erreur bornée, incertitudes inconnues mais bornées.
